Karlsruhe Institute of Technology

# Short-term Risk Management for Electricity Retailers Under Rising Shares of Decentralized Solar Generation

**Marianna Russo**, Norwegian University of Science and Technology (NTNU), Trondheim, Norway
**Emil Kraft**, IIP, KIT
**Valentin Bertsch**, Ruhr-University Bochum, Bochum, Germany
**Dogan Keles**, Technical University of Denmark (DTU), Lyngby, Denmark

No. 57 | June 2021

WORKING PAPER SERIES IN PRODUCTION AND ENERGY

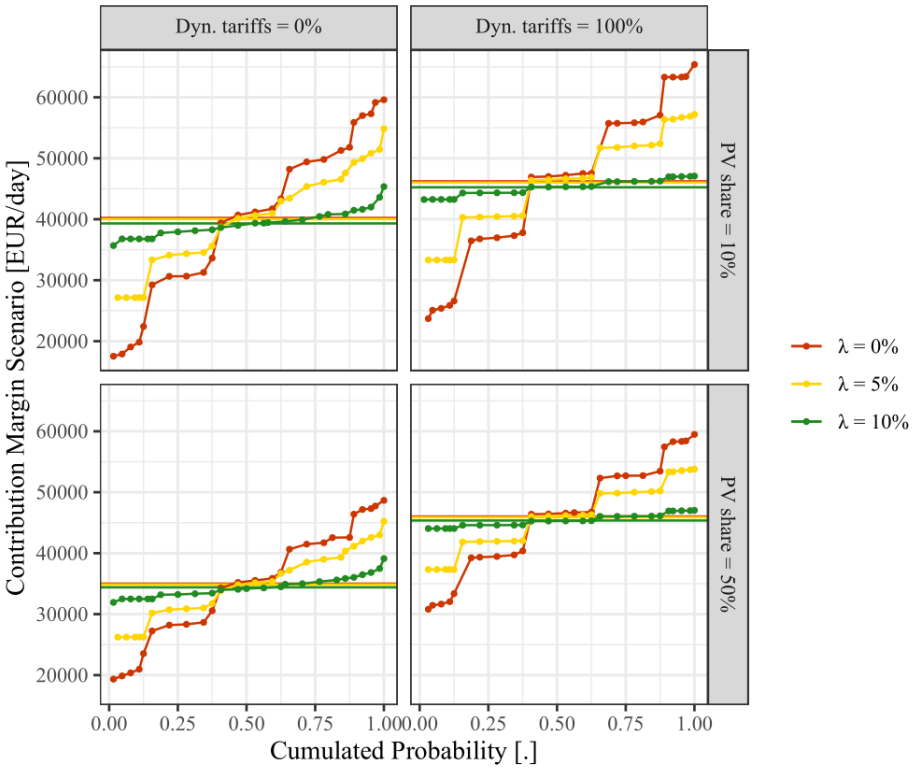

# Short-term Risk Management for Electricity Retailers Under Rising Shares of Decentralized Solar Generation

Marianna Russo[1], Emil Kraft[2], Valentin Bertsch, and Dogan Keles

[1]Corresponding author. E-mail: marianna.russo@ntnu.no

[2]Chair of Energy Economics, Institute for Industrial Production (IIP) at the Karlsruhe Institute of Technology (KIT),
Hertzstr. 16, Geb. 06.33, 76187 Karlsruhe,
emil.kraft@kit.edu; +49 721 608 44562

**Abstract**

Electricity retailers face increasing uncertainty due to the ongoing expansion of unpredictable, distributed generation in the residential sector. We analyze how increasing levels of households' solar PV self-generation affect the short-term decision-making and associated risk exposure of electricity retailers in day-ahead and intraday markets. First, we develop a stochastic model accounting for correlations between solar load, residual load and price in sequentially nested wholesale spot markets across seasons and type of day. Second, we develop a computationally tractable two-stage stochastic mixed-integer optimization model to investigate the trading portfolio and risk optimization problem faced by retailers. Through conditional value-at-risk we assess retailers' profitability and risk exposure to different levels of PV self-generation by assuming different retail tariff schemes. We find risk-hedging trading strategies and tariffs to have greater impact in Summer and with low levels of residual load in the system, i.e. when the solar generation uncertainty affect more the households demand to be served and the wholesale spot prices. The study is innovative in unveiling the potential of dynamic electricity tariffs, which are indexed to spot prices, to sustain a high penetration of renewable energy source while promoting risk sharing between customer and retailer. Our findings have implications for electricity retailers facing load and revenue risks in wholesale spot markets, likewise for regulators and policy-makers interested in electricity market design.

# Short-term Risk Management of Electricity Retailers Under Rising Shares of Decentralized Solar Generation

Marianna Russo[*,a], Emil Kraft[b], Valentin Bertsch[c], and Dogan Keles[d]

[a]*NTNU Business School, Norwegian University of Science and Technology, 7491, Trondheim, Norway*
[b]*Chair of Energy Economics, Karlsruhe Institute of Technology (KIT), Institute for Industrial Production (IIP), Karlsruhe, Germany*
[c]*Chair of Energy Systems and Energy Economics, Ruhr University Bochum, Germany*
[d]*Technical University of Denmark (DTU), Department of Technology, Management and Economics, Lyngby, Denmark*

**Abstract**

Electricity retailers face increasing uncertainty due to the ongoing expansion of unpredictable, distributed generation in the residential sector. We analyze how increasing levels of households' solar PV self-generation affect the short-term decision-making and associated risk exposure of electricity retailers in day-ahead and intraday markets. First, we develop a stochastic model accounting for correlations between solar load, residual load and price in sequentially nested wholesale spot markets across seasons and type of day. Second, we develop a computationally tractable two-stage stochastic mixed-integer optimization model to investigate the trading portfolio and risk optimization problem faced by retailers. Through conditional value-at-risk we assess retailers' profitability and risk exposure to different levels of PV self-generation by assuming different retail tariff schemes. We find risk-hedging trading strategies and tariffs to have greater impact in Summer and with low levels of residual load in the system, i.e. when the solar generation uncertainty affect more the households demand to be served and the wholesale spot prices. The study is innovative in unveiling the potential of dynamic electricity tariffs, which are indexed to spot prices, to sustain a high penetration of renewable energy source while promoting risk sharing between customer and retailer. Our findings have implications for electricity retailers facing load and revenue risks in wholesale spot markets, likewise for regulators and policy-makers interested in electricity market design.

[*]Corresponding author. E-mail: marianna.russo@ntnu.no.

Acknowledgments. We thank GET AG for kindly providing us with the retail tariff data for Germany used in this study. We thank Dr. Kai Sander (Netze BW GmbH) for the fruitful discussions and practical insights on uncertainties and associated risk exposure. This work has emanated from Marianna Russo's research time at the Economic and Social Research Institute, Dublin. Marianna Russo acknowledges funding from the ESRI's Energy Policy Research Center and the SFI Energy Systems Integration Partnership Programme (ESIPP) number SFI/15/SPP/E3125. Marianna Russo also acknowledges research support by COST Action "Fintech and Artificial Intelligence in Finance - Towards a transparent financial industry" (FinAI) CA19130. The authors acknowledge the financial support of the German Federal Ministry of Education and Research under grant number 03SFK1F0-2 (ENSURE – Neue Energienetzstrukturen für die Energiewende). The opinions, findings and conclusions or recommendations expressed in this material are those of the authors and do not necessarily reflect the views of the Energy Policy Research Center and Science Foundation Ireland. All errors remain our own.

**Keywords**: Electricity markets, Stochastic model, Stochastic programming, Retailer uncertainty modeling, Risk management

**JEL classification**: C10, C50, G10, Q42, Q48

# 1 Introduction

Increasing levels of distributed and large-scale variable renewable generation have different effects on short-term wholesale power markets. The uncertainty and intermittency introduced by weather-dependent generation translate into both volume and price risks, which affect the profitability and decision-making of retailers and generators. With large-scale renewable generation, day-ahead predictions on high levels of renewable energy increase the risk-related hedging pressure of generators. Furthermore, with distributed renewable generation, growing renewable power production raises the hedging needs of retailers (Koolen et al., 2021), particularly when considering rooftop solar PV installations (Russo and Bertsch, 2020). The deployment of rooftop solar PV systems has significantly expanded in recent years, mostly by virtue of supporting policies, such as net metering and fiscal incentives. In some markets, incentive schemes for households lead to an economic preference for solar PV self-consumption compared to buying electricity from the grid (IRENA, 2019). The competitiveness of distributed solar PV systems is apparent from their deployment in large markets, such as Brazil, China, Germany and Mexico. At a global level, around 40% of total solar PV capacity in 2050 would be distributed (rooftop), with the remaining 60% utility scale (IRENA, 2019). Yet, as far as rising solar PV self-generation increases the need of retailers for forecast adjustments, large adjustment volumes influence subsequent spot (day-ahead and intraday) prices and the retailers' risk exposure in short-term wholesale power markets, thus exacerbating the already-existing optimization issues faced by the electricity retailer to manage uncertainty in power markets. In the light of market efficiency considerations, increasing attention is to be paid thus on the short-term risk of electricity retailers, following a surge in the decentralized variable renewable generation and consumers' engagement as prosumers.

In this paper we have chosen to investigate the risk optimization problem faced by the electricity

retailer acting in the day-ahead and intraday markets, while considering volume risk induced by the households' solar PV self-generation. The retailer's decision-making problem with intermittent renewables has been explored in the literature (e.g. Conejo et al., 2010; Yang et al., 2017). Whereas the potential for risk transfer through derivative products can rise significantly for wind power, hedging solar risk is likely to remain difficult (Hain et al., 2018), mainly for retailers increasingly exposed to the volume risk driven by growing levels of solar PV self-generation on the demand side (Russo and Bertsch, 2020; Koolen et al., 2021). The variability of the electricity demand, its short-term inelasticity, and the supply rigidity expose retailers to a real-time volume risk, which is more complex to hedge within the day-ahead market, since high differences can emerge between predictions in the day-ahead and intraday market. Engaging in risk management strategies in the intraday market, which is closer to the actual realization, has proved to offer higher efficiency compared to the day-ahead and therefore weekly, monthly and yearly forward market (Boroumand et al., 2015, 2019). Nonetheless, pre-positioning in the day-ahead market and adjusting in the intraday market can result in a complex task for the retailer, mainly when risk management strategies fail to transfer the real-time unpredictability of self-generation to the consumer. The role of the intraday adjustment trading, and the extent to which this trading may foster risk sharing between electricity retailers and prosumers have been less explored in literature and are the focus of this paper. In addressing the short-term risk optimization problem faced by electricity retailers with households' self-generation, this study engages with practitioners and policy makers interested in the power market dynamics following increasing penetration of distributed renewable energy sources, and in the adequacy of price signals for investments and market design.

The contribution of this paper is threefold: First, we explicitly model the stochastic process of prices and solar generation in the day-ahead and intraday market, likewise inter-dependencies within and between the two markets. Simulations are thus carried to account for uncertainty in the ensuing stochastic optimization problem. We consider the German market since it is at the forefront of decentralized solar PV installations worldwide. Furthermore Germany shares a similar intraday continuous trading design with other electricity markets, such as in France and the Scandinavian

countries. Therefore, lessons learned from the German case should provide others with valuable insights concerning managing renewable energy risk in modern liberalized electricity markets. Second, we model the multistage trading problem faced by the retailer in the day-ahead and intraday market. We assume a computationally tractable two-stage stochastic optimization problem where day-ahead trading decisions for one single day are modeled in the first-stage, and the intraday balancing decisions under uncertainty are modeled in the second stage. Since we explicitly assume that the retailer faces the uncertainty of fluctuating rooftop solar PV generation until delivery, this approach aims to accurately model the underlying information flow between day-ahead and intraday market, thus reducing biases and often over-optimistic decisions (Wozabal and Rameseder, 2020). Third, we explore different retail pricing schemes with progressive levels of indexation to the wholesale spot prices. Since the retailer faces the risks caused by volatile customer demand and spot market prices, we investigate the potential for spot-indexed retail tariffs to represent a risk-sharing tool for retailers exposed to rising shares of decentralized solar PV self-generation.

The rest of the paper is organized as follows. In Section 2 we review related work on the retailer short-term decision-making process and the pertaining uncertainties requiring the solution of a complex optimization problem involving several uncertain quantities. The input variables are describe in Section 3. In Section 4, we describe our methodological approach. We present the stochastic model developed to jointly capture load and price uncertainties in the day-ahead and intraday markets, and elaborate on a set of simulations to represent the retailer's uncertainty in wholesale spot markets. Therefore, we define the retailer trading optimization problem under uncertainty, and extend it to the short-term risk management problem, subject to increasing levels of solar PV self-generation. In Section 5, we present our results in relation to the retailer's optimization problem and their short-term risk management. Results and implications are discussed in Section 6, while Section 7 offers concluding remarks and directions for future research.

# 2 Literature on The Retailer's Short-Term Decision-Making Process

Electricity markets are organized as a sequence of nested forward energy markets, allowing participants to trade different contracts (from yearly to quarter-hourly) at different points in time (Ela et al., 2018; Cretì and Fontini, 2019). This market design is thought to provide participants with the opportunity to adjust their positions up to a few minutes before the delivery, thus accommodating the inherent uncertainties of electricity markets. Since electricity for the same delivery period is traded in multiple markets, the retailer trading problem on these nested markets is interdependent. As intermediaries in competitive electricity markets, retailers need to procure the electricity required by their customers (i.e. load) in wholesale markets through different sources, like futures and bilateral contracts, or on the spot markets. While in wholesale markets the load uncertainty is adjusted in the spot markets through spot prices, in retail markets prices are based on tariffs, generally fixed for a longer period (Boroumand and Zachmann, 2012; Batlle, 2013). Therefore, serving the electricity demand of the residential sector at pre-specified tariffs and partially for pre-specified volumes is an obligation posed to the retailers (Newbery et al., 2018).

By procuring electricity for resale to final consumers, retailers are exposed to the volume risk, mostly over short-term horizons, i.e. from a few days or hours to real-time. While intraday markets allow for a finer adjustment of the day-ahead positions up to 15-minute resolution, the electricity generated by the renewable energy facilities has to be traded day-ahead to be adjusted intra-daily (Kiesel and Paraschiv, 2017). Furthermore, significant differences can emerge between day-ahead and intraday prices depending upon substitution effects between thermal and renewable energy generation (i.e. merit order effect), with intraday prices decreasing relatively to the day-ahead prices for increasing levels of renewable generation, or vice versa (Karanfil and Li, 2017; Kiesel and Paraschiv, 2017). Due to the surge in the distributed variable renewable generation, and the resulting greater requirement for close to real-time adjustments (e.g. Di Cosmo and Malaguzzi Valeri, 2018; Goodarzi et al., 2019), increasing attention is to be paid on the retailer's short-term re-

balancing in the intraday market and implications for market efficiency. The empirically observed positive correlation between price and load in wholesale electricity markets (e.g. Deng and Oren, 2006; Weron, 2007; Gelabert et al., 2011) implies an increasing short-term risk exposure for the retailers, depending on the difference between spot and retail prices (Willems and Morbee, 2010; Aïd et al., 2011; Dagoumas et al., 2017; Russo and Bertsch, 2020). With increasing penetration of rooftop solar PV systems and greater intraday uncertainties, imbalance costs are expected to raise for retailers, thus leading to potential financial distress for retailers who fail to hedge properly.

The importance of assessing the short-term effects of variable renewable energy generation on electricity markets is highlighted by the growing interest in the impact of wind and solar power forecast errors on intraday electricity prices (e.g. Garnier and Madlener, 2015; Bunn et al., 2018; Kath and Ziel, 2018; Kulakov and Ziel, 2019; Maciejowska et al., 2019; Uniejewski et al., 2019; Gianfreda et al., 2020; Kremer et al., 2020; Messner et al., 2020; Narajewski and Ziel, 2020a,b; Li and Paraschiv, 2021). Specularly to generators (Garnier and Madlener, 2015; Bunn et al., 2018; Maciejowska et al., 2019), retailers are confronted with the optimal decision of where to buy the electricity required to satisfy the customers' demand. This decision-making process depends upon the load uncertainty and the relation between prices in the day-ahead and intraday markets. Some previous research addresses the short-term trading problem faced by the electricity retailer in spot markets (Nojavan et al., 2019; Dadashi et al., 2020; Deng et al., 2020, and references therein). Yet, there is a paucity of studies addressing the optimal trading problem faced by electricity retailers in wholesale spot markets following increasing levels of solar PV self-generation, and consequently greater load uncertainty in the residential sector.

Various methods have been explored in the literature to model the optimal procurement problem in electricity markets. These methods include stochastic approaches (Ruszczyński and Shapiro, 2003; Wallace and Fleten, 2003) and robust optimization (Ben-Tal et al., 2009; Bertsimas et al., 2011). By considering a finite batch of possible realizations, stochastic approaches are adopted by practitioners and researchers due to their suitability in capturing uncertainty (e.g. Van Der Weijde and Hobbs, 2012; Morales et al., 2014; Mohan et al., 2015; Abbaspourtorbati et al., 2016; Boffino

et al., 2019; Dadashi et al., 2020; Deng et al., 2020; Laur et al., 2020). In contrast, in robust optimization models uncertainty is represented through uncertainty sets, often derived from the historical data, thus resulting in flexible and computationally tractable models (Parisio et al., 2012; Zugno and Conejo, 2015; Nojavan et al., 2017; Nazari-Heris and Mohammadi-Ivatloo, 2018; Nojavan et al., 2019). Nonetheless, as argued by Wozabal and Rameseder (2020), research involving trading strategies in electricity markets often models price or renewable generation as stochastic but fails to model the multi-settlement structure of the power markets. Similarly, in optimization problems some research often treats all the variables as deterministic.

In dealing with the optimal trading problem of the electricity retailer, who faces load and price uncertainties in wholesale spot markets while maximizing their revenue stream, we follow the approach in Conejo et al. (2010) and Wozabal and Rameseder (2020). We propose a two-stage stochastic optimization model for the German short-term electricity market where the first stage models the retailer's decision-making process on the day-ahead market; the second stage models their decision-making process in the intraday market. Uncertainty enters the problem via stochastic solar PV generation and short-term electricity prices. Yet, compared to previous research, in our optimization problem, we consider the impact of such stochasticity on prices through econometric modeling the inter-dependencies between load and prices in wholesale spot markets. With the increasing penetration of distributed renewable energy sources in worldwide power markets still only a recent phenomenon, to the best of our knowledge the research in this paper is the first to combine all the mentioned uncertainties via joint stochastic modeling, portfolio optimization and empirical validation to analyze the implications of distributed renewable technologies, such as rooftop solar PV systems on the short-term risk management problem of the retailer in wholesale spot power markets.

# 3 Input Variables: Definition and Data Sources

The German electricity market has been subject to a high renewable energy sources (RES) penetration, in particular rooftop solar PV systems in the residential sector, making this market a suitable case study to investigate retailers' risk exposure to increasing self-generation. The period under investigation runs from the $1^{st}$ July 2019 to the $29^{th}$ February 2020. This sample period is chosen to account for some major changes in the German market design, occurred during 2018 until July 2019, including the split of the Austrian market from the German market in October 2018. As the market split changed both the demand and the supply structure, price formation on both the day-ahead and the intraday market was affected. We use data until February 2020 to overcome the implications of COVID-19 and consequent lockdown on electricity markets starting from March 2020. Therefore, the period July 2019- February 2020 results as the most recent period where no structural market changes and economic downturns happen, which may have affected both the demand and supply of electricity in the German market. To study this risk exposure we consider three different seasons: a Transition season (September-November), Summer (July-August) and Winter (December-February). For each season, we consider a typical (i.e. average) working day and a typical weekend day.

In this study, both the day-ahead and the intraday market are considered. The day-ahead market is operated through a sealed-bid auction which takes place once a day, all year round. All hours of the following day are traded in this auction. The buy and sell volume-price bids are submitted by the market participants before the closure of the gate, at 12 pm. Aggregated demand and supply curves are thus recovered based on respectively the buy-bids and sell-bids for each hour of the following day. The hourly uniform market clearing price, namely the day-ahead price, lies at the intersection of both curves. Therefore, to recover the structure of the day-ahead market, data on the day-ahead forecast of the total, solar and wind loads at quarter-hourly frequency were collected from the ENTSO-E Transparency Platform (in MW)[1]. The German hourly day-ahead auction price

[1] `https://transparency.entsoe.eu/`

(DE-LU, EUR/MWh) was retrieved through the EPEX-Spot[2].

The intraday set of information consists of a further forecast update of the wind and solar load (and consequently for the total load) at 8:00 am of the actual delivery day, wherein however forecast is conditional on the day-ahead forecasts[3]. Consequently, intraday forecast and actual (realized) total, solar and wind loads were also recovered from the ENTSO-E platform at quarter-hourly frequency. Finally, the actual, day-ahead and intraday residual load were computed by subtracting the wind and solar loads from the corresponding total load, likewise a thermal generation must-run requirement of 23 GW[4].

On the continuous intraday market, trade is executed as soon as a buy- and sell-order match and electricity can be traded up to five minutes before delivery. The ID3 price index for the continuous intraday market is the volume-weighted average of the price of all trades taking place in the time window starting from three hours before the delivery and up to thirty minutes before the delivery. So, for example the ID3-price for the delivery in the quarter from 12 pm to 12:15 pm is the volume-weighted average of all transactions with time stamp between 9 am and 11:30 am. Hence, market participants use the intraday market to make last minute adjustments and to balance their positions closer to real-time. Similarly to the day-ahead auction price, the continuous intraday ID3 price index was obtained from EPEX-Spot[5].

To fit the electricity demand of the residential sector the households' standard load profile (SLP) is used. This profile is based on historical data for households with an annual consumption of 3,500 kWh at quarter-hourly resolution (BDEW, 2021). While the load profile of individual households can deviate from the SLP, the SLP is a suitable indicator for the electricity demand of larger groups of households(Hayn et al., 2018), thus representing a standard tool for retailers. Table 1 provides an overview of the variables used in the empirical analysis, along with their frequencies and sources.

[2] http://www.epexspot.com/en/market-data/dayaheadauction

[3] ENTSO-E also admits current forecast, where wind and solar forecast is the last update of the current forecast, which shall be regularly updated and published during intraday trading. The forecast published at 8 am of the delivery day is published twice, as "current forecast" and "intraday forecast at 8.00".

[4] The must-run capacity also includes technical restrictions and market commitments. Source: Bundesnetzagentur (2019)

[5] ibid.

Table 1: Overview of the variables used in the empirical analysis

| Variable (unit) | Frequency | Description | Data source |
|---|---|---|---|
| Solar PV load (MW), DA | Quarter-hourly | Day-ahead forecast solar PV load | European Network of Transmission System Operators (ENTSO-E) https://transparency.entsoe.eu/ |
| Solar PV load (MW), ID | Quarter-hourly | Intraday forecast solar PV load | ibid. |
| Solar PV load (MW), Actual (MW) | Quarter-hourly | Realized solar PV load | ibid. |
| Wind load (MW), DA | Quarter-hourly | Day-ahead forecast wind load | ibid. |
| Wind load (MW), ID | Quarter-hourly | Intraday forecast wind load | ibid. |
| Wind load (MW), Actual | Quarter-hourly | Realized wind load | ibid. |
| Total load (MW), DA | Quarter-hourly | Day-ahead forecast total electricity demand | ibid. |
| Total load (MW), Actual | Quarter-hourly | Realized total electricity demand | ibid. |
| Household standard load profile (MW) | Quarter-hourly | Standardized electricity demand in the residential sector | German Association of Energy and Water Industries (BDEW) https://www.bdew.de/ |
| Price (EUR/MWh), DA | Hourly | Market clearing price in the day-ahead auctions (DE-LU) | European Power Exchange (EPEX) https://www.epexspot.com/en |
| ID3 price (EUR/MWh), ID | Quarter-hourly | Intraday electricity prices in the continuous trading | European Energy Exchange Transparency Platform http://www.eex-transparency.com/de |

# 4 Overview of the Methodological Approach

To model uncertainties in day-ahead and intraday markets, while preserving the sequential market setting, and the key characteristics of each market, we develop a two-step procedure. In the first step, we jointly model and simulate load and price uncertainties in the day-ahead market at hourly resolution, while accounting for season and type of day specificities as detailed in Section 4.1. Based on these simulated series, different scenarios are generated. In the second step, uncertainties in the intraday marker are jointly modelled at quarter-hourly resolution. For each day-ahead scenario, coherent intraday realizations are generated, thus resulting in distinct scenario trees that capture the retailer's uncertainties in the day-ahead and intraday markets, as outlined in Section 4.2. In a third stage, the scenario trees are used to evaluate the retailer's trading decisions under uncertainty. More detailed, we consider the trading portfolio optimization of the electricity retailer via a two-stage stochastic mixed-integer linear program, as described in Section 4.3. The scenarios and stochastic programming approach are used to investigate the decision-making problem of the retailer wishing to optimize their contribution margins and the associated risk exposure in the day-ahead and intraday markets with increasing levels of solar PV self-generation in the residential sector, as described in Section 4.4. An overview of the whole methodological approach is given in Fig.1.

## 4.1 Modeling uncertainty in the day-ahead market

In modeling uncertainty in the day-ahead market, the dynamic relationships between solar infeed, residual load and prices are considered in a stepwise procedure. First, we account for negative values and outliers in the residual load and price time series. The time series of the day-ahead and intraday residual load are shifted up so to reach the smallest recorded positive value over the full sample period and the two markets, which however does not occur in the sample. This permits a correct recoding of the series in the simulation process (Keles et al., 2012). Hence, the series are logarithmized to reach variance stabilization. A similar procedure is applied to the day-ahead

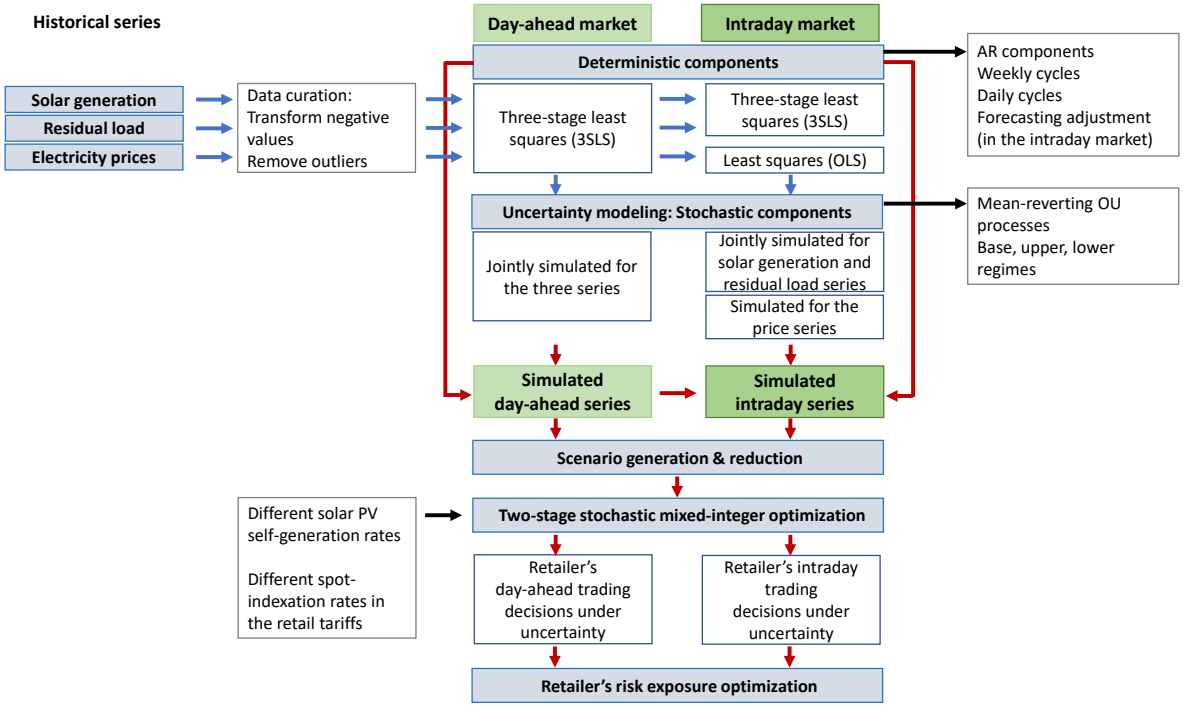


Figure 1: Overview of the whole methodological approach

and intraday price series. Outliers, i.e. observations above and below the upper and lower 2.5% percentiles of the empirical distribution in the season and in the market are also removed and replaced with the corresponding percentile (e.g. Janczura et al., 2013).

### 4.1.1 Solar PV generation

In this study, we assume that the rooftop solar PV generation of the retailer's households is perfectly correlated with the system-wide solar generation published by the TSOs. This complies with an evenly distributed customer portfolio. Therefore, we model the system-wide solar PV profile, likewise the seasonal and daily features of the deviations of the solar PV generation from its theoretical profile. As in Lingohr and Müller (2019), the solar PV generation process is described by a continuous-time process $S_t$, $t \geq 0$:

$$S_t = IC_t \times \Lambda_t \times V_t, \tag{1}$$

where $S_t \geq 0$; $IC_t \geq S_t \geq 0$ is the installed capacity; $\Lambda_t \geq 0$ is a deterministic function describing seasonal variations; and $V_t \geq 0$ denotes any irregular influence. $\Lambda_t$ can be regarded as the normalized theoretically possible maximum solar PV generation profile and represents the 'clear sky' solar radiation (Bacher et al., 2009). As in Russo and Bertsch (2020), it is computed as the average of the clear sky solar radiation of thirty-nine locations in Germany, weighted for the installed solar PV capacity in the area around selected locations. Therefore, $IC_t \times \Lambda_t$ represents the normalized theoretically possible maximum solar PV generation profile, while $V_t$ assumes the physical interpretation of cloud component. This component causes deviations of the actual solar generation from its theoretically possible maximum profile and is explicitly modelled to account for its impact on the residual load and prices.

After logarithmizing the data in Eq.1, the discretized hourly cloud component $v_t$ is assumed to be characterized by an autoregressive component, as in Benth and Ibrahim (2017), and by an hourly seasonal component, as in Keles et al. (2013) for the wind capacity utilization. To account for this hourly seasonal component of the cloudiness, the average value $\bar{v}_h^{DA}$ of the cloud component $v_t^{DA}$ is determined for each hour $h$=0,...,23, of the day throughout each season over the sample period (Summer, Transition season, Winter). Therefore, the following dynamic for the cloud component is assumed:

$$v_t^{DA} = \sum_{p=1}^{P} v_{t-p}^{DA} + \sum_{h=0}^{23} \bar{v}_h^{DA} * 1(h|h = t \; mod \; 24) + X_t^{DA}, \tag{2}$$

where the resulting residual component $X_t^{DA}$ contains neither seasonal or intraday regularities and is thus suitable for stochastic simulations.

### 4.1.2 Residual load

The hourly residual load $l_t^{DA}$ is assumed to be a function of the cloud component $v_t^{DA}$ and defined in an additive way:

$$l_t^{DA} = f(v_t^{DA}) + \sum_{h=0}^{23} \bar{l}_h^{DA} * 1(h|h = t \; mod \; 24) + Weekends + Y_t^{DA}, \tag{3}$$

where $f(v_t^{DA})$ is a deterministic function of $v_t^{DA}$, capturing the relationship between cloudiness and residual load; $\bar{l}_h^{DA}$ is a hourly cycle, which similar to the cloud component is defined as the hourly average of the residual load in the season. Public holiday effects and weekend effects (*Weekends*) are also considered, which account for differences in the load of a typical business day with respect to a weekend/holiday. The residual component $Y_t^{DA}$ represents thus the deseasonalized and stochastic component of the residual load. A polynomial function is used to approximate the deterministic function $f(v_t^{DA})$ of the cloud component in Eq.2, as implied by Fig.2.

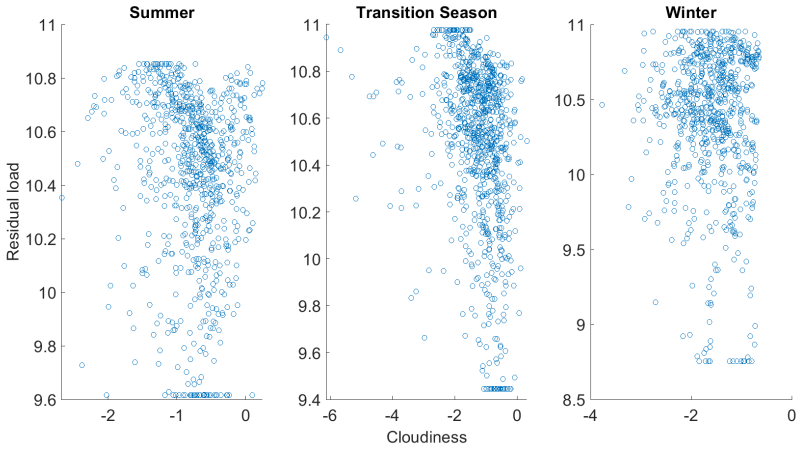


Figure 2: Relationship between the log residual load and cloudiness in the day-ahead market

### 4.1.3 Day-ahead prices

Following Burger et al. (2004), Schermeyer et al. (2018), and Benth and Ibrahim (2017) the hourly day-ahead price $p_t^{DA}$ is modeled as a function of the residual load and an autoregressive component as follows:

$$p_t^{DA} = \sum_{k=1}^{K} l_{t-k}^{DA} + \sum_{q=1}^{Q} p_{t-q}^{DA} + \sum_{h=0}^{23} \bar{p}_h^{DA} * 1(h|h = t \; mod \; 24) + Weekends + Z_t^{DA}, \qquad (4)$$

where $\bar{p}_h^{DA}$ is an hourly cycle, defined as the residual load and cloudiness cycles while (*Weekends*) account for public holiday and weekend effects. Finally, $Z_t^{DA}$ represents the residual and stochastic component of the day-ahead prices. Following the visual inspection of the scatter plot in Fig.3, the

relationship between residual load and price in the day-ahead market is assumed to be linear. Eq.2 -

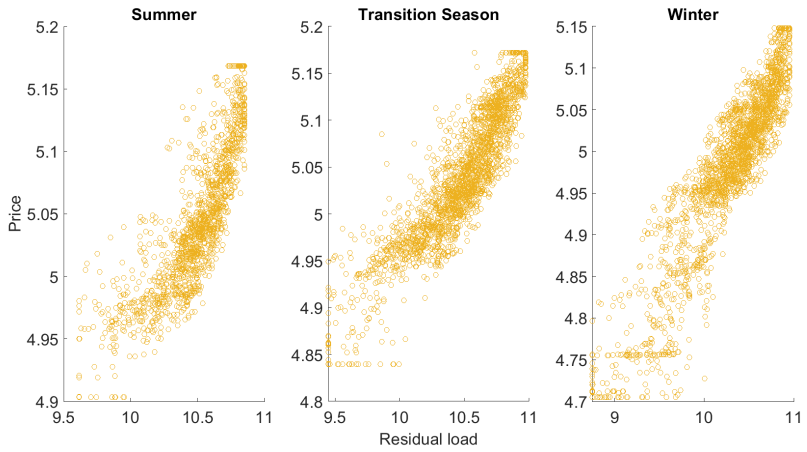


Figure 3: Relationship between log prices and residual load in the day-ahead market

Eq.4 result in a system of three equations, which for each season is jointly estimated through three-stage least squares (3SLS) (Zellner and Theil, 1992) to reflect the daily blind auction mechanism of the German market described above. The 3SLS estimation method is adopted since it allows to obtain efficient estimates in the presence of contemporaneously correlated residuals, which would be expected since the day-ahead forecast of solar PV generation, residual load and price are jointly determined.

#### 4.1.4 Modeling and simulating the stochasticity of the solar PV generation, residual load, and day-ahead price processes

Similar to Keles et al. (2012) and Coulon et al. (2013), the remaining stochastic components of the day-ahead solar PV generation, residual load and price variables, i.e. $X_t^{DA}, Y_t^{DA}, Z_t^{DA}$ respectively, are assumed to be mean-zero Ornstein–Uhlenbeck (OU) processes, since their mean levels are incorporated in the deterministic/seasonal functions in Eq.2 - Eq.4. Because logarithms of the variables are modeled, a multivariate OU process can be formulated for their changes through stochastic differential equations (SDEs) via Itô's lemma. Yet the relationship between the three variables can be dimmed by the consequences of outages, transmission problems and other constraints. Consequently, jumps in the series can occur, even at periods of low or average demand

(Christensen et al., 2009; de Lagarde and Lantz, 2018). Furthermore, similarly to wind, the volatility of solar generation has been observed to increase the electricity price volatility, due to the high day-to-day variability of the solar generation (Ballester and Furió, 2015; Rintamäki et al., 2017). Therefore, as in Keles et al. (2012) and Coulon et al. (2013), jump processes are added to the OU process to mimic this additional stochastic variability.

To accommodate the features above, and in the spirit of Keles et al. (2012), solar generation, residual load and prices are assumed to mainly remain at a base level, defined "base regime" and then to simultaneously jump into a higher (or lower) "jump regime", where they are assumed to remain for some hours according to their mean reverting dynamics, before jumping back to their base regime. Higher and lower jump regimes are defined as values that are above and below $3\sigma$, respectively (after assuming a mean-zero OU process, as mentioned above). Base, higher jump and lower jump regimes are separately computed for the summer, transition and winter seasons. Consequently, the base regime corresponds to values in the interval $[-3\sigma; +3\sigma]$.

A regime-switching approach, with a different model for the base, higher jump, and lower jump regime is thus introduced. The base regime is modeled through a system of SDE as follows:

$$d\mathbf{U}_t^{DA,Base} = -\boldsymbol{\beta}^{DA,Base}\mathbf{U}_t^{DA,Base}dt + \Sigma^{DA,Base}d\mathbf{W}_t^{DA,Base}, \tag{5}$$

where $\mathbf{U}_t^{DA,Base}$ is the $3 \times 1$ vector of the stochastic processes $X_t^{DA}, Y_t^{DA}, Z_t^{DA}$ in the base regime; $\boldsymbol{\beta}^{DA,Base}$ is the $3 \times 3$ drift matrix, which determines the "reversion speed" of the stochastic components towards their long-term mean zero. The stochastic component $\Sigma^{DA,Base}d\mathbf{W}_t^{DA,Base}$ corresponds to a multivariate Brownian motion: $\Sigma^{DA,Base}$ is the $3 \times 3$ covariance matrix, and $\mathbf{W}_t^{DA,Base}$ is a 3-dimensional vector of independent Wiener processes. Hence, $d\mathbf{W}_t^{DA,Base} = \boldsymbol{\varepsilon}_t dt^{1/2}$ follows a multivariate normal distribution where each Wiener process has mean zero and variance $dt$. By applying the Itô's lemma and following Meucci (2009), the solution to the system of SDE in Eq.5 is:

$$\mathbf{U}_{t+\delta} = e^{-\boldsymbol{\beta}\delta}\mathbf{U}_t + \boldsymbol{v}_{t+\delta}, \tag{6}$$

where $\boldsymbol{\upsilon}_{t+\delta} \equiv \int_t^{t+\delta} e^{\boldsymbol{\beta}(s-\delta)} \Sigma d\mathbf{W}_s \sim \mathcal{N}(0, \Omega)$. (Note that in Eq.6 we dropped the superscripts $DA, Base$ to ease the notation.) $\delta$ is the time difference of the day-ahead series between t and t+1, i.e. one hour. The solution in Eq.6 is a vector autoregressive process of order one, i.e. VAR(1), which reads $\mathbf{U}_{t+1} = A\mathbf{U}_t + \boldsymbol{\upsilon}_{t+1}$ where $A$ is a suitable $3 \times 3$ matrix, such that $A = e^{-\boldsymbol{\beta}\delta}$ while is $\Omega \equiv \Sigma\Sigma'$ (Meucci, 2009). The Maximum Likelihood (ML) estimator is used to recover the parameter matrices $A$ and $\Omega$ from the historical stochastic components $X_t^{DA}, Y_t^{DA}, Z_t^{DA}$. The substitution of $A$ and $\Omega$ delivers the original parameter matrices $-\boldsymbol{\beta}$ and $\Sigma$ of the exact solution in Eq.6, which are used to generate the simulated paths of the three stochastic components in the base regime.

The jump regimes are defined as extended versions of the base regime. Upward and downward jumps in the stochastic components of the day-ahead solar generation, residual load and prices are replaced by their mean values in the estimation of the mean reversion parameters in Eq.5, so to preserve the sample length. The added or subtracted "jump height" to the base regime process corresponds to the deviation of the jump value from the mean. A multivariate normal distribution is thus used to model the jump heights of the three stochastic processes $X_t^{DA}, Y_t^{DA}, Z_t^{DA}$. The distribution is based on the means and covariance matrix estimated from the historical deviations of the jump values from their corresponding mean. Accordingly, the upper and lower regimes are defined as:

$$\begin{aligned} \mathbf{U}_t^{DA,uJ} &= \mathbf{U}_t^{DA,Base} + \boldsymbol{\epsilon}_t^{DA,uJ}, \quad \boldsymbol{\epsilon}_t^{DA,uJ} \sim \mathcal{N}(\boldsymbol{\mu}^{DA,uJ}, \boldsymbol{\Sigma}^{DA,uJ}), \\ \mathbf{U}_t^{DA,lJ} &= \mathbf{U}_t^{DA,Base} - \boldsymbol{\epsilon}_t^{DA,lJ}, \quad \boldsymbol{\epsilon}_t^{DA,lJ} \sim \mathcal{N}(\boldsymbol{\mu}^{DA,lJ}, \boldsymbol{\Sigma}^{DA,lJ}), \end{aligned} \tag{7}$$

where $\boldsymbol{\epsilon}_t^{DA,uJ}$ ($\boldsymbol{\epsilon}_t^{DA,lJ}$) represents the upward (downward) jump height; $\boldsymbol{\mu}_t^{DA,uJ}$ ($\boldsymbol{\mu}_t^{DA,lJ}$) is the 3-dimensional mean vector of the upward (downward) jump heights; and $\boldsymbol{\Sigma}^{DA,uJ}$ ($\boldsymbol{\Sigma}^{DA,lJ}$) is the $3 \times 3$ covariance matrix of the upward (downward) heights. It is noteworthy that this approach is separately applied for the summer, transition and winter season series. Transition probabilities for the upward and downward jumps of the three stochastic components $X_t^{DA}, Y_t^{DA}, Z_t^{DA}$ are thus separately computed for the three seasons. The probabilities of switching from the base regime to

the upper regime and backwards are defined by:

$$
\begin{aligned}
P_{BB} &= \frac{\text{card}\left\{U_t \in [\mu - 3\sigma, \mu + 3\sigma] \wedge U_{t+1} \in [\mu - 3\sigma, \mu + 3\sigma]\right\}}{\text{card}\left\{U_t \in [\mu - 3\sigma, \mu + 3\sigma]\right\}}; \\
P_{BU} &= \frac{\text{card}\left\{U_t \in [\mu - 3\sigma, \mu + 3\sigma] \wedge U_{t+1} \in [\mu + 3\sigma, max\,(U)]\right\}}{\text{card}\left\{U_t \in [\mu - 3\sigma, \mu + 3\sigma]\right\}}; \\
P_{UB} &= \frac{\text{card}\left\{U_t \in [\mu + 3\sigma, max\,(U)] \wedge U_{t+1} \in [\mu - 3\sigma, \mu + 3\sigma]\right\}}{\text{card}\left\{U_t \in [\mu + 3\sigma, max\,(U)]\right\}}; \\
P_{UU} &= \frac{\text{card}\left\{U_t \in [\mu + 3\sigma, max\,(U)] \wedge U_{t+1} \in [\mu + 3\sigma, max\,(U)]\right\}}{\text{card}\left\{U_t \in [\mu + 3\sigma, max\,(U)]\right\}}.
\end{aligned}
\tag{8}
$$

where the superscript $DA$ is dropped to ease notation. $P_{BB}$ is the probability of remaining in the base regime; $P_{UU}$ is the probability of remaining in the upper jump regime; $P_{BU}$ and $P_{UB}$ are the probabilities to move from the base to the upper jump regime, and vice versa respectively. The probabilities of switching from the base to the lower jump regime and backwards ($P_{BL}$, $P_{LB}$, $P_{LL}$) are computed analogue to Eq.8, whereas the corresponding interval for downward jumps is defined as $[min(U), \mu - 3\sigma]$. These probabilities are thus combined to define the transition probabilities matrix $T_t$:

$$
T = \begin{bmatrix} P_{BB} & P_{BU} & P_{BL} \\ P_{UB} & P_{UU} & P_{UL} \\ P_{LB} & P_{LU} & P_{LL} \end{bmatrix}, \tag{9}
$$

where $P_{UL} = P_{LU}$=0, i.e. no transition from the upper jump to the lower jump regime, and vice versa, as suggested by empirical evidence. Based on their computed transition matrices, the hourly regime switching of three stochastic processes $X_t^{DA}, Y_t^{DA}, Z_t^{DA}$ are simulated for each season following the approach in Keles et al. (2013). A state parameter $\delta$ is used to identify the regime. For $\delta$=0, a base regime is identified and thus used in the simulation process. If $\delta$=1 ($\delta$=-1), an upper (lower) jump regime is instead identified and a upper (lower) jump is thus added (subtracted) from

the simulated, i.e.:

$$U_{t,s}^{DA,Sim} = \begin{cases} U_{t,s}^{DA,Base} + \epsilon_{t,s}^{DA,uJ}, \quad \epsilon_{t,s}^{DA,uJ} \sim \mathcal{N}(\mu^{DA,uJ}, \Sigma^{DA,uJ}) & \text{if } \delta = 1 \\ U_{t,s}^{DA,Base} & \text{if } \delta = 0 \\ U_{t,s}^{DA,Base} - \epsilon_{t,s}^{DA,lJ}, \quad \epsilon_{t,s}^{DA,lJ} \sim \mathcal{N}(\mu^{DA,lJ}, \Sigma^{DA,lJ}) & \text{if } \delta = -1 \end{cases} \tag{10}$$

For $s = 1, 2, ..., S$, $U_{t,s}^{DA,Base}$, $\epsilon_{t,s}^{DA,uJ}$, and $\epsilon_{t,s}^{DA,lJ}$ represent the $s^{th}$ simulated processes obtained from Monte Carlo simulations of the multivariate processes in Eq.5 and Eq.7.

To capture and describe the uncertainty in the day-ahead market, Monte Carlo simulations are conducted for each season by considering $S$=1,000 trials. After assuming for each trial a burn-in period of 28 days or 672 hours, 24 hours from 12 am to 11 pm are extracted from each simulated series. These series correspond to 1,000 simulations of the stochastic components of the day-ahead cloudiness, residual load and price for one day. Therefore, the deterministic components in Eq.2 - Eq.4 are added to the simulated stochastic components. These log series are thus transformed to retrieve their levels, while the residual load and price series are also shifted down to recover their original levels. This procedure allows to obtain 1,000 hourly cloudiness, residual load and price series of one typical working day (Monday-Friday) and 1,000 hourly cloudiness, residual load and price series of one typical weekend day (Saturday-Sunday) for each of the three seasons. Therefore, distinct and seasonal paths are recovered for working and weekend (and holidays) days, which account for the historically observed differences in the load and price values between working days and weekends/holidays across the seasons. In contrast, while cloudiness paths are differentiated across seasons, they are assumed to be the same in working and weekend days. The 1,000 series resulting from the Monte Carlo simulation are "reduced" to a recombining stochastic tree. This scenario generation-and-reduction is carried out by implementing the k-means clustering algorithm (MacQueen et al., 1967). This algorithm aims to partition a set of simulations $s_1, ..., s_n$ into $m$ clusters $C_1, ..., C_m$ such that an intra-cluster distance is minimized. The k-means algorithm used in this study employs the city block distance. Therefore, for each cluster, the absolute distance is computed with respect to the median of the points in that cluster. The number of clusters is identified by us-

ing silhouette plots and values to analyze the results of different k-means clustering solutions. The k-means algorithm is a mainstay clustering approach in many application domains, e.g. biology, market segmentation, internet search, digital imaging, power network allocation (Likas et al., 2003; Jain, 2010). It has been extensively used in the literature on energy systems for trading off computing time and precision (Green et al., 2014; Osório et al., 2015; Zhang et al., 2021, and references therein). A similar scenario generation-and-reduction approach is adopted by Gröwe-Kuska et al. (2000) and Heitsch and Römisch (2009). Fleten and Kristoffersen (2007) apply the approach in a similar way to stochastic programming of trading strategies for hydro-power in electricity markets. For scenario reduction, the authors use Lagrangian relaxation of a optimization problem instead of k-means clustering, as used in this study. Nonetheless, both the Lagrangian relaxation and k-means clustering follow the same goal of preserving the variety and uncertainty of the simulations and reducing the number of scenarios to be considered.

By following the k-means clustering approach above, three clusters are identified for each typical day (working day and weekend) and season (Summer, Winter, Transition season), which correspond to a high, medium, and low scenario of the solar PV generation. For each scenario, numerous consistent nodes can be derived by symmetrically defining deviation ranges. We use the following approach. For each scenario, simulations in the cluster are grouped and averaged in five nodes, based on their distance from a reference point, assumed to be the mean of the simulated residual load series in the cluster, as computed at 12 pm. Starting from this first node, four nodes are identified by averaging simulations in the range up to one standard deviation above and below the mean of the cluster, and simulations above and below one standard deviation from the mean of the cluster. Therefore, the three nodes in the range up to one standard deviation from the mean are assumed to be equally probable, with a probability of 25%. Equal probability is also assumed for the nodes above and below one standard deviation from the mean (12.5%). In all, these probabilities resemble probabilities drawn from a normal distribution. Finally, a spline interpolation method is used to obtain cloudiness and residual load series at quarter-hourly resolution. The quarter-hourly day-ahead price series are obtained by assuming the hourly day-ahead price constant in the quarter-of-hour

segments of the specific hour. The resulting fifteen nodes of the three series, i.e. five nodes for each of the three scenarios (high, medium and low) are used to design the intraday realizations and scenario trees, as described below.

## 4.2 Modeling uncertainty in the intraday market

In the intraday market, series at quarter-hourly resolution are taken. The updated forecast of the load and solar generation is used to model the uncertainty towards real-time. Since intraday solar and residual load forecasts follow their respective day-ahead forecasts, we use the same econometric approach adopted for the day-ahead market. Yet, since the ID3 price index is determined in the continuous market and up to thirty minutes before the delivery, the stochastic process of the intraday prices is modeled separately from the solar and residual load stochastic processes.

### 4.2.1 Solar PV generation

Similar to the day-ahead market, we model the intraday cloud component, that is the deviation of the intraday solar PV generation from its theoretical (seasonal and intraday) profile, and from the day-ahead profile, i.e.:

$$v_{\tau}^{ID} = v_{\tau}^{DA} + \sum_{p=1}^{P} v_{\tau-p}^{ID} + \sum_{q=0}^{95} \bar{v}_{q}^{ID} * 1(q|q = \tau \; mod \; 96) + X_{\tau}^{ID}, \tag{11}$$

where the intraday cloud component $v_{\tau}^{ID}$ is assumed to be a function of the day-ahead cloud component, likewise of an autoregressive component and a seasonal component. Similar to the day-ahead process, the seasonal component is obtained as the average value $\bar{v}_{q}^{ID}$ of the cloud component $v_{\tau}^{ID}$ for each quarter-of-hour in the day ($q$=0,...,95) and for each season in the sample period (Summer, Transition season, Winter). The resulting residual component $X_{\tau}^{ID}$ is thus used for stochastic simulations.

### 4.2.2 Residual load

Following updates in the intraday forecasts of the solar PV and wind generation, forecasts of the residual load $l_\tau^{ID}$ are also updated at quarter-hourly resolution, and assumed to be a linear function of the day-ahead forecasts and of the intraday cloud component. An autoregressive component is also considered in the process:

$$l_\tau^{ID} = l_\tau^{DA} + v_\tau^{ID} + \sum_{p=1}^{P} l_{\tau-p}^{ID} + \sum_{q=0}^{95} \bar{l}_q^{ID} * 1(q|q = \tau \; mod \; 96) + Weekends + Y_\tau^{ID}, \tag{12}$$

where $\bar{l}_q^{ID}$ is a quarter-of-hour cycle is defined as the quarterly hour average of the intraday residual load in the season. Public holiday effects and weekend effects (*Weekends*) are also considered. The residual component $Y_\tau^{ID}$ represents thus the deseasonalized and stochastic component of the residual load factor in the intraday market. Parameter estimates in Eq.11-12 are obtained through the 3SLS estimation method to account for contemporaneous correlations between the jointly determined intraday solar PV generation and residual load forecasts.

### 4.2.3 Intraday prices

Following Kiesel and Paraschiv (2017), the intraday ID3 price process is described in terms of its distance from the day-ahead price, i.e. $p_\tau^{ID} - p_\tau^{DA} = \Delta p_\tau$. The day-ahead price $p_\tau^{DA}$, at quarter-hourly resolution, is obtained from the hourly series $p_t^{DA}$ via spline interpolation (Lahmiri, 2015; Steinert and Ziel, 2019). The model specification reads as follows:

$$\begin{aligned}\Delta p_\tau = &\sum_{j=1}^{J} \Delta p_{\tau-j} + p_{\tau-1}^{DA} + \Delta p_{\tau-1}^{ID} + \sum_{k=3}^{K} \Delta l_{\tau-k} + \sum_{r=3}^{R} \Delta v_{\tau-r} + \sum_{q=0}^{95} \bar{\Delta} p_\tau * 1(q|q = \tau \; mod \; 96) + \\ &+ Weekends + Z_\tau^{ID},\end{aligned} \tag{13}$$

where $p_{\tau-1}^{DA}$ is the first-order lag of the day-ahead price at quarter-hourly resolution; $\Delta p_{\tau-1}^{ID}$ represents increments in the intraday price series. As in Kiesel and Paraschiv (2017), these increments account for the price formation process in the intraday market, which is based on continuous trades

of several quarter-hourly products. Therefore, the increment captures the change in the price of a certain quarter of an hour when new information on solar forecasts becomes available. $\Delta l_\tau$ is the distance of the actual (realized) residual load from its intraday forecast $l_\tau^{ID}$; likewise $\Delta v_\tau$ is the distance of the actual solar generation from its intraday forecast $v_\tau^{ID}$, thus representing the solar forecast error. Here the actual residual load and solar generation are assumed to be exogenous and corresponding to the 15-minute average of the historical actual observations for the season in the sample period. Parameters in Eq.13 are estimated through least-square error.

#### 4.2.4 Modeling and simulating the stochasticity of the solar PV, residual load and intraday price processes

Similar to the day-ahead market, the remaining stochastic components of the intraday solar PV generation and residual load, i.e. $X_\tau^{ID}$ and $Y_\tau^{ID}$ respectively, are assumed to follow a multivariate mean-zero OU process. Jump processes are thus added to account for the uncertainty. Base, higher and lower jump regimes are identified following the approach described in Section 4.1 and by taking as upwards and downwards the values of $X_\tau^{ID}$ and $Y_\tau^{ID}$ that are above and below $3\sigma$ their corresponding mean values in the season. The base regime is thus modeled through SDE as follows:

$$d\boldsymbol{U}_\tau^{ID,Base} = -\boldsymbol{\beta}^{ID,Base}\boldsymbol{U}_\tau^{ID,Base}d\tau + \Sigma^{ID,Base}d\mathbf{W}_\tau^{ID,Base}, \tag{14}$$

where $\boldsymbol{U}_\tau^{DA,Base}$ is the $2 \times 1$ vector of the stochastic processes $X_\tau^{ID}, Y_\tau^{ID}$ in the base regime; $\boldsymbol{\beta}^{ID,Base}$ is the $2 \times 2$ positive definite symmetric drift matrix; $\Sigma^{ID,Base}$ is the $2 \times 2$ constant diffusion matrix and $\mathbf{W}_\tau^{ID,Base}$ is a 2-dimensional Wiener process. The jump regimes are thus defined as extended versions of the base regime like for the day-ahead market:

$$\begin{aligned}
\mathbf{U}_\tau^{ID,uJ} &= \mathbf{U}_\tau^{ID,Base} + \boldsymbol{\epsilon}_\tau^{ID,uJ}, \quad \boldsymbol{\epsilon}_\tau^{ID,uJ} \sim \mathcal{N}(\boldsymbol{\mu}^{ID,uJ}, \boldsymbol{\Sigma}^{ID,uJ}), \\
\mathbf{U}_\tau^{ID,lJ} &= \mathbf{U}_\tau^{ID,Base} - \boldsymbol{\epsilon}_\tau^{ID,lJ}, \quad \boldsymbol{\epsilon}_\tau^{ID,lJ} \sim \mathcal{N}(\boldsymbol{\mu}^{ID,lJ}, \boldsymbol{\Sigma}^{ID,lJ}),
\end{aligned} \tag{15}$$

where $\boldsymbol{\epsilon}_\tau^{ID,uJ}$ ($\boldsymbol{\epsilon}_\tau^{ID,lJ}$) represents the upward (downward) jump height; $\boldsymbol{\mu}_\tau^{ID,uJ}$ ($\boldsymbol{\mu}_\tau^{ID,lJ}$) is the 2-dimensional mean vector of the upward (downward) jump heights; and $\boldsymbol{\Sigma}^{ID,uJ}$ ($\boldsymbol{\Sigma}^{ID,lJ}$) is the $2 \times 2$ variance-covariance matrix of the upward (downward) heights. Finally, the probabilities for $X_\tau^{ID}$ and $Y_\tau^{ID}$ to switch from the base regime to the upper regime and backwards are computed as in Eq.8 and used to define the transition probabilities matrix as in Eq.9.

Similarly to the day-ahead series, the stochastic component of the intraday ID3 price $Z_\tau^{ID}$ is assumed to follow an univariate mean-reverting OU process with a base, upper jump and lower jump regimes, i.e.:

$$\begin{aligned} dZ_\tau^{ID,Base} &= -\beta^{ID,Base} Z_\tau^{ID,Base} d\tau + \sigma^{ID,Base} dW_\tau^{ID,Base}, \\ Z_\tau^{ID,uJ} &= Z_\tau^{ID,Base} + \epsilon_\tau^{ID,uJ}, \quad \epsilon_\tau^{ID,uJ} \sim \mathcal{N}(\mu^{ID,uJ},\, \sigma^{ID,uJ}), \\ Z_\tau^{ID,lJ} &= Z_\tau^{ID,Base} - \epsilon_\tau^{ID,lJ}, \quad \epsilon_\tau^{ID,lJ} \sim \mathcal{N}(\mu^{ID,lJ},\, \sigma^{ID,lJ}). \end{aligned} \tag{16}$$

The parameter estimates in Eq.11-Eq.13 and the simulated day-ahead scenarios are thus used to obtain intraday scenarios. For each of the five nodes of the high, medium and low day-ahead scenarios, the corresponding intraday node is retrieved for the cloudiness, residual load and ID3 price index, thus generating high, medium and low intraday scenarios coherent with the day-ahead scenarios. Yet still the intraday nodes represent the deterministic and predictable component of the intraday series, to which a stochastic component is added as obtained from Monte Carlo simulations of the processes in Eq.14-Eq.16 with 1,000 trials. Similar to the day-ahead market, for each scenario, numerous consistent nodes can be derived by symmetrically defining deviation ranges. We assume the average of the simulated processes as the representative node for the intraday cloudiness, residual load and price. Therefore, for each of these nodes, we assume a range of possible realizations, which are obtained by adding (subtracting) to the node one and two standard deviations of the historical differences between intraday and day-ahead series, as computed for each quarter-of-hour in the season. For each day-ahead node, five possible realizations are assumed in the intraday market, resulting in $5 \times 5$ nodes. Intraday nodes in the range up to one standard deviation from the mean are assumed to be equally probable, with probability of 25%. Equal probability is also assumed

for the nodes above and below one standard deviation from the mean (12.5%), thus resembling probabilities drawn from a normal distribution.

In all, for a typical working/weekend day, we obtain a scenario tree of $3 \times 5 \times 5$ possible states. It follows that to obtain the ID3 price index realizations, the corresponding realizations for the intraday cloudiness and residual load series are used. The resulting scenario tree, which is depicted in Fig.4, permits to characterize the uncertainty surrounding the forecasting process in liberalized electricity wholesale spot markets through a discrete representation of its realizations in a probability space.

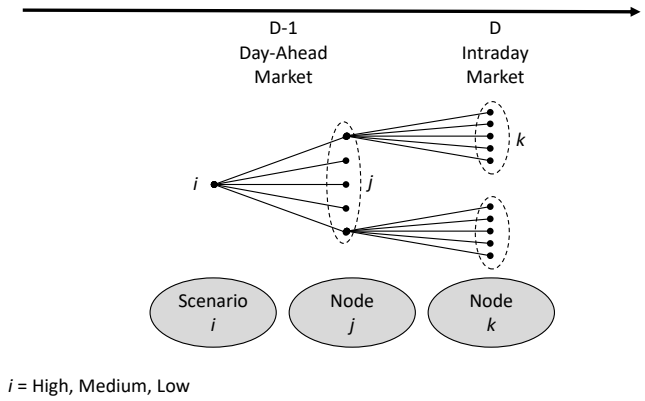


Figure 4: Scenario tree with different nodes in the day-ahead and intraday markets

## 4.3 Retailers' trading portfolio optimization problem

When an electricity retailer faces volume and price risks in purchasing load to be served from the wholesale market, conventional risk management optimization methods are observed to be quite inefficient due to the difficulty of formulating a multi-period optimization that incorporates correlated price and demand risks (Kettunen et al., 2010). In this context, we develop a two-stage stochastic optimization approach, which accounts for correlated uncertainties of both electricity prices and loads, and which permits the consideration of the conditional value-at-risk (CVaR) as

risk metric to optimize risk hedging across intermediate stages in the planning horizons. Hereby, the retailer procures electricity on the spot markets (day-ahead spot market and continuous intraday trading) in order to resell it via predefined tariff schemes to household customers according to their residual demand, i.e. according to the standard load profile net of the solar PV generation in case the household has a solar installation. It is worth noting that we do not consider the potential impact of battery storage systems on temporal shifts in residual demand, or smart metering and intelligent electric devices for demand side management. Therefore, in this study, the hypothesis that the retailer can participate in short-term demand response programs to adjust the uncertainty brought by the self-sufficiency is not considered[6].

We consider input data for the German market area and a hypothetical retailer with 100,000 household customers, that are spatially distributed such that the German PV generation is representative for the portfolio PV generation. For customers without PV generation, the load to be served by the retailer in a typical working/weekend day of the season corresponds to the standard load profile $q_{qh}$, where $qh$ represents the quarter-of-hour of the day. For customers with PV generation, the residual demand $q_{qh}^{\mathrm{RD}}$ to be served by the retailer is calculated as $q_{qh}$ minus the solar PV self-generation. This self-generation is determined under uncertainty in the intraday cloudiness $v_{qh}^{\mathrm{ID}}$, as described in Section 4.2. For each scenario $j$ of the day-ahead market, and corresponding realization $k$ in the intraday market, the residual demand to be served after accounting for the PV self-generation is defined as follows:

$$q_{j,k,qh}^{\mathrm{RD}} = \max\left\{q_{qh} - (1 - v_{j,k,qh}^{\mathrm{ID}}) \cdot P^{\mathrm{inst.}}, 0\right\}, \tag{17}$$

where $P^{\mathrm{inst.}}$ represents the rooftop solar PV installed capacity. Therefore, in the absence of cloudiness, i.e. $v_{j,k,qh}$=0, the solar PV self-generation reaches its theoretical maximum, given a certain amount of installed capacity. Following the approach in Ruppert et al. (2016) and Russo and Bertsch (2020), rooftop solar PV systems with capacity up to 12 kW are considered, i.e. in-

[6]We refer to Fett et al. (2021) who investigate potential impacts of household PV battery storage systems on day-ahead electricity markets on a system level.

stallations for residential buildings up to 80 $m^2$, and with a median size of 7 kW[7]. Therefore, in our empirical analysis, $P^{\text{inst.}}$ in Eq.17 is assumed to be 7 kW.

According to the last published statistics, the number of residential buildings in Germany amounted to 19.2 million at the end of 2019[8], while almost 2 million rooftop solar PV systems were installed in Germany, thus representing an installation rate $\phi$ of PV systems in the residential sector of 10% [9]. Due to the lack of granular data on generation from solar PV systems, the solar system load and capacity factor is used indeed to infer the profile of self-generation at quarter-hourly basis. On average, a solar PV capacity factor of 10% was observed in Germany during the sample period, as recovered from the historical data. This factor is used to compute the total amount of solar PV self-generation. For each season, the quarter-hourly self-generation profile in a typical day is obtained by assuming the same quarter-hourly profile of the system solar load on an average day of the season in the sample[10].

We frame the retailer's trading strategy problem and risk investigation by assuming metering of deviations from the standard load profile on a quarter-hourly basis, as supposed after completion of the smart meter roll-out program[11]. In this case, the participation of the retailer in the wholesale spot markets to balance all the potential profit and loss is mandatory. We also rule out the hypothesis that the retailer has self-consumption, or storage and generation facilities to cope with deviations of the actual load from the standard load profile, as led by solar PV self-generation. Consequently, the amount of self-generation exceeding households' demand is not accounted for, since this excess

[7]Source: Core Energy Market Data Register Ordinance, MaStRV. https://www.bundesnetzagentur.de/EN/Areas/Energy/Companies/CoreEnergyMarketDataRegister/CoreDataReg_node.html.

[8]Source: Statista Research Department. https://de.statista.com/statistik/daten/studie/70094/umfrage/wohngebaeude-bestand-in-deutschland-seit-1994/. Access on 31.05.2021.

[9]Source: Strom-Report: Photovoltaik in Deutschland. https://strom-report.de/photovoltaik/. Access on 31.05.2021.

[10]While this approach represents a simplification, it is reasonable for retailers with a national customer portfolio, as assumed in this study, the aggregated PV load profile of which largely follows the same pattern of the system solar PV load profile.

[11]Currently, the majority of households are metered on a semi-annual or annual basis. This metering system makes it hard for the retailer to identify and account for deviations from the standard load profile in the short term. In Germany, dedicated distribution system operators actively manage so-called difference balancing groups on the spot markets to balance expected deviations from the standard load profile. The costs of these deviations are thus rolled over to the involved retailers via an excess/shortage price, determined on a monthly basis. Accordingly, the developed methodology can be easily applied to manage different balancing groups in the current German market design.

is fed into the grid either based on a remuneration scheme or sold by the household itself. We finally assume that the household electricity demand is inelastic to wholesale spot prices due to the prevalence of fix components (i.e. taxes, grid fees and renewables support levy) in the retail tariffs, which represent a distortion to the price signals coming from the market.

A risk-neutral retailer maximizes the expected value of contribution margins $\mathbb{E}_{(j,k)\in\Omega}(\pi_{j,k})$ over all scenarios $(j,k)$ in the discrete probability space $\Omega$, which contains the tariff revenues from the customers $\mathbb{E}_{(j,k)\in\Omega}(\rho^{\text{tariff}}_{j,k})$, the procurement costs on the day-ahead and intraday markets, i.e $\mathbb{E}_{(j,k)\in\Omega}(\kappa^{\text{DA}}_{j,k})$ and $\mathbb{E}_{(j,k)\in\Omega}(\kappa^{\text{ID}}_{j,k})$, and the potential imbalance costs $\mathbb{E}_{(j,k)\in\Omega}(\kappa^{\text{Imb}}_{j,k})$[12], that is:

$$\mathbb{E}_{(j,k)\in\Omega}(\pi_{j,k}) = \mathbb{E}_{(j,k)\in\Omega}(\rho^{\text{tariff}}_{j,k}) - \mathbb{E}_{(j,k)\in\Omega}(\kappa^{\text{DA}}_{j,k}) - \mathbb{E}_{(j,k)\in\Omega}(\kappa^{\text{ID}}_{j,k}) - \mathbb{E}_{(j,k)\in\Omega}(\kappa^{\text{Imb}}_{j,k}). \tag{18}$$

The tariff revenues are determined by fixed and dynamic base rates, namely $\tau^{\text{base,fix}}$ and $\tau^{\text{base,dyn}}$, which represent the fix components of the retail prices. The tariff revenues are also determined by fixed and dynamic energy rates, i.e. $\tau^{\text{energy,fix}}$ and $\tau^{j,qh\text{energy,dyn}}$, which are energy-based and thus proportional to the served load. As mentioned above, we distinguish between retailer's customers with and without PV self-generation ($q^{\text{RD}}_{j,k,qh}$ and $q_{qh}$ in Eq.17, respectively). By assuming $n$ to be the number of households, $\phi \in [0,1]$ the share of customers with rooftop solar PV systems, and $\delta \in [0,1]$ the share of customers with dynamic tariffs. Hence, the tariff revenues from the costumers are given by:

$$\mathbb{E}_{(j,k)\in\Omega}(\rho^{\text{tariff}}_{j,k}) = \sum_{j=1}^{J} pr_j \sum_{k=1}^{K} pr_k \Big( (1-\delta)\cdot(\tau^{\text{base,fix}} + ((1-\phi)\cdot q_{qh} + \phi \cdot q^{\text{RD}}_{j,k,qh})\cdot \tau^{\text{energy,fix}}) + (\delta\cdot(\tau^{\text{base,dyn}} + ((1-\phi)\cdot q_{qh} + \phi\cdot q^{\text{RD}}_{j,k,qh})\cdot \tau^{\text{energy,dyn}}_{qh})\Big)\cdot n. \tag{19}$$

Procurement costs on day-ahead market and intraday market are based on the day-ahead sce-

[12]The contract of German balancing responsible parties explicitly forbids intentional imbalances while forcing to close positions with market operations. To cope with this rule, in this study we assume an imbalance price sufficiently high and equal to 10,000 EUR/MWh to ensure imbalance volumes and costs to be zero.

narios $j$ and corresponding intraday realizations $k$, as described Sections 4.1 and 4.2. The scenario-based prices $lda$ and $lid$ represent the price levels at which the retailer can place volumes as selling and buying bids, i.e. $x^{\mathrm{DA,bid,buy/sell}}_{lda,j,h}$ and $x^{\mathrm{ID,bid,buy/sell}}_{lid,j,k,qh}$ in the day-ahead market and in intraday market, respectively. Price-volume bids lead to demand and supply curves, which are submitted on at hourly time step $h$ in the day-ahead market, and at quarter-hourly time step $qh$ in the intraday market.

By using binary acceptance parameters $\beta^{\mathrm{DA}}_{lda,j,h}$ and $\beta^{\mathrm{ID}}_{lid,j,k,qh}$, trades are determined from the submitted bids, thus allowing for modeling the retailer's non-anticipative trading strategies and scenario-based contribution margins[13]. As bids are possible in both buying and selling direction, the retailer might intentionally take either a short or a long position to profit from potential price spreads between the day-ahead and intraday market. Procurement costs on the intraday market are defined as:

$$\mathbb{E}_{(j,k)\in\Omega}(\kappa^{\mathrm{ID}}_{j,k}) = \sum_{j=1}^{J} pr_j \sum_{k=1}^{K} pr_k \Big( \sum_{qh}^{QH} \sum_{lid}^{LID} \big((1-\beta^{\mathrm{ID}}_{lid,j,k,qh}) \cdot x^{\mathrm{ID,bid,buy}}_{lid,j,k,qh} \cdot p^{\mathrm{ID}}_{j,k,qh} + \beta^{\mathrm{ID}}_{lid,j,k,qh} \cdot x^{\mathrm{ID,bid,sell}}_{lid,j,k,qh} \cdot (-p^{\mathrm{ID}}_{j,k,qh})\big) \cdot \triangle t \Big), \tag{20}$$

where the term $\triangle t$ adapts for the 15 minutes resolution of the intraday market (i.e., $\triangle t$ = 0.25). Following Ottesen et al. (2018) and Laur et al. (2018), and using the approach in Kraft et al. (2021), we model the continuous intraday market as one hypothetical auction, with the intraday ID3 index price $p^{\mathrm{ID3}}_{\tau}$ in Section 4.2.3 as the price for each quarter hour $qh$. In doing so, we consider the hypothetical auction as a uniform pricing auction, thus limiting the potentially greater price volatility and risk exposure due to the arrival process towards gate closure time in the continuous intraday. It is worth noting that if the retailer is short in one market segment, the term of the costs can potentially become negative indicating revenues. Procurement costs in the day-ahead market

[13] In Kraft et al. (2021), a bidding framework is developed that allows for both selling and buying bids. To remain consistent, $\beta$ denotes the acceptance of selling bids. To evaluate the buying bids predominant in this study, the opposite of the binary parameter, i.e. $(1-\beta)$, is applied.

are defined analogously to Eq. 20.

Based on the current contract for balancing responsible parties in Germany, the volume of a short or long position on the spot markets is limited to a certain percentage $q^{\max,\text{short/long}}$ of the maximum schedule volume of the day[14]. As the retailer does not trade any generation, storage, or demand apart from the load to be served, the maximum short position on the day-ahead market is defined as follows:[15]

$$-\max_{qh\in QH}\left((1-\phi)\cdot q_{qh}+\phi\cdot\max_{k\in K}q^{\text{RD}}_{j,k,qh}\right)\cdot n\cdot q^{\max,\text{short}}\leq x^{\text{DA,trade}}_{j,h}\quad\forall j\in J,h\in H. \tag{21}$$

(The short position constraints for the intraday market are defined analogously.)

Since the market design requires closed positions, any imbalances $x^{\text{imb}}_{j,k,qh}$ in the day-ahead and intraday positions ($x^{\text{DA,trade}}_{j,h}$ and $x^{\text{ID,trade}}_{j,k,qh}$, respectively) need to be balanced by the TSO, i.e.:

$$x^{\text{DA,trade}}_{j,h}+x^{\text{ID,trade}}_{j,k,qh}+x^{\text{imb}}_{j,k,qh}=x^{\text{DA,trade}}_{j,h}+x^{\text{ID,trade}}_{i,j,k,qh}\quad\forall(j,k)\in\Omega,h\in H,qh(h)\in QH(H), \tag{22}$$

where $x^{\text{DA,trade}}_{j,h}$ and $x^{\text{ID,trade}}_{i,j,k,qh}$ represent all trades in the day-ahead and the intraday markets, respectively. The notation $qh(h)$ indicates a mapping of quarter hours to the respective hour, that is $qh1$, $qh2$, $qh3$, and $qh4$ represent the four quarters of hour $h1$ of the day, and so on. To ensure the non-anticipativity of the trading strategy, the retailer submits the same bids under the same set of information. For the bids submitted to the day-ahead market, this constraint translates into:

$$x^{\text{DA,bid}}_{lda,j,h}=x^{\text{DA,bid}}_{lda,j+1,h}\quad\forall lda\in LDA,\{j\in J\mid Ord(j)<|J|\},h\in H, \tag{23}$$

with $Ord(j)$ representing the ordinal number of the scenario $j$ in the set $J$ and $|J|$ the cardinality of set $J$. The intraday market constraints on the realizations $k$ are defined in analogous way.

One major shortfall of determining trading strategies in a risk-neutral way and with the associ-

[14] In the current contract, a strategic position of 10% is allowed, which is thus used in this study.

[15] Note, that considering the maximum scenario value $\max_{k\in K}q^{\text{RD}}_{j,k,qh}$ of residual load over all $k$ in Eq. 21 is a rather relaxed interpretation of the strategic position constraints. However, the peak demand of the standard load profile is observed in the evening. At that time, the uncertainty in solar generation is low and the scenarios differ only slightly.

ated uncertainty is that the probability distribution of potential scenario outcomes is reduced to one single figure, i.e. the expected value. Yet, the expected value is affected by abnormal values in the distribution, thus driven by a few scenario leaves with extreme values but low probabilities. Furthermore, the risk-neutral determination of trading strategies does not take into account outcome uncertainty, which is of particular relevance for a retailer under competitive pressure. Therefore, the hypothesis of risk-neutrality may lead to trading strategies overestimating the retailer's risk exposure in terms of low contribution margins and thus profitability. With increasing volumes of variable renewable generation in the energy system, and consequent impact on electricity prices, it becomes paramount for the retailer to assess the distribution of contribution margins by including risk considerations within the probability space $\Omega$.

We use the approach of Conejo et al. (2010) as reformulated by Kraft et al. (2021), and include into the retailer's trading problem the conditional value-at-risk (CVaR) risk metric with a level $\alpha$=95% (see e.g. Alexander, 2008; Conejo et al., 2010, for the mathematical definition)[16]. By including the expected value and the CVaR, the target function is extended to a multi-objective optimization where $\lambda \in [0, 1]$ denotes the weight allocated to the risk metric: $\lambda$=0% is equivalent to the risk-neutral problem above; increasing values of $\lambda$ correspond to a growing risk-aversion. We also include into the target function two additional constraints: the first, $\eta$, represents the value-at-risk, i.e. the quantile value at (1-$\alpha$%); the second, $s$, represents the (positive) difference between $\eta$ and the contribution margin $\pi$ in a single scenario. Hence, the retailer's decision-making problem under uncertainty is reformulated as follows (see Conejo et al., 2010; Kraft et al., 2021, for further details):

$$\max \quad (1-\lambda) \cdot \mathbb{E}_{(j,k)\in\Omega}(\pi_{j,k}) + \lambda \cdot \left(\eta - \frac{1}{1-\alpha} \sum_{j=1}^{J} pr_j \sum_{k=1}^{K} pr_k \cdot s_{j,k}\right) \tag{24}$$

[16] As a coherent risk metric, the CVaR has the properties of monotonicity, sub-additivity, homogeneity, and translational invariance. With regard to portfolio problems, the sub-additivity is a particularly desirable property as it allows to scale or combine portfolios, and thereby ensures the validity of the decision calculus in terms of risk exposure. The level of $\alpha$ denotes the quantile of the loss distribution assumed to assess the risk exposure. In this study, we consider $\alpha = 95\%$ as suitable level in the determination of bids, thereby capturing the expected value of the 5% greatest losses for the retailer.

$$\eta - \pi_{j,k} \leq s_{j,k} \quad \forall (j,k) \in \Omega \tag{25}$$

$$s_{j,k} \geq 0 \quad \forall (j,k) \in \Omega \tag{26}$$

In the next section, the developed approach is used to solve the retailer's trading optimization problem and investigate the retailer's risk exposure and trading adjustment to increasing levels of PV self-sufficiency.

## 4.4 Retailer's risk-management problem with increasing solar PV self- generation: A case study with fixed and dynamic energy tariffs

The retailer's risk-management problem, and their risk exposure to increasing levels of solar PV self-generation are investigated by assuming different installation rates of PV systems in the residential sector, i.e. different shares of residential houses with installed rooftop solar PV systems. An installation rate $\phi$=10% is assumed, which is the *status quo* in Germany (Section 4.3). We also assume installation rates $\phi$=30% and $\phi$=50%, which are in line with the solar photovoltaic expansion targets in Germany (from 54 to 150 GW by 2030, and 25% of electricity needs powered with solar energy by 2050 (Bundesministerium für Wirtschaft und Energie, 2021). By maintaining the solar PV capacity factor constant at 10%, the levels of PV self-generation corresponding to the different penetration rates are computed for a typical day in the season, as described in Section 4.3. Hence, the computed self-generation levels are subtracted from the standard load profile to obtain the residual demand of the residential sector, as in Eq.17.

We notice that a lower demand from customers with PV systems implies lower revenues for the retailer, as generated by the energy rates (Eq.19). To evaluate the impact that more dynamic retail tariffs may have on the risk exposure and management of the retailer, we consider two different retail tariff schemes. In the first scheme, we assume a fixed retail tariff, i.e. the most common and currently applied tariff structure in Germany. This tariff is composed of a fixed base rate and

a fixed energy rate. The fixed base rate is valued in EUR per time interval (e.g. EUR/a), while the fixed energy rate is valued in EUR per unit of energy demanded (e.g. EUR-ct/kWh). We collect from GET AG[17] the ten most competitive retail tariffs from the 39 locations considered in the stochastic modeling of solar generation and subtract the fixed rate (i.e. taxes, grid fees and renewables support levies) to isolate energy rate used to evaluate the retailer's net revenues. Fig. 5 depicts the collected fixed base rates and fixed energy rates. For the purpose of our study, we use the median value as representative of the sample in the empirical analysis. The median fixed base rate is 6.87 EUR/month or 0.23 EUR/day; after removing levies, taxes and grid fees as provided by GET AG, the median fixed energy rate is 0.058 EUR/kWh (i.e. 58.24 EUR/MWh). In the

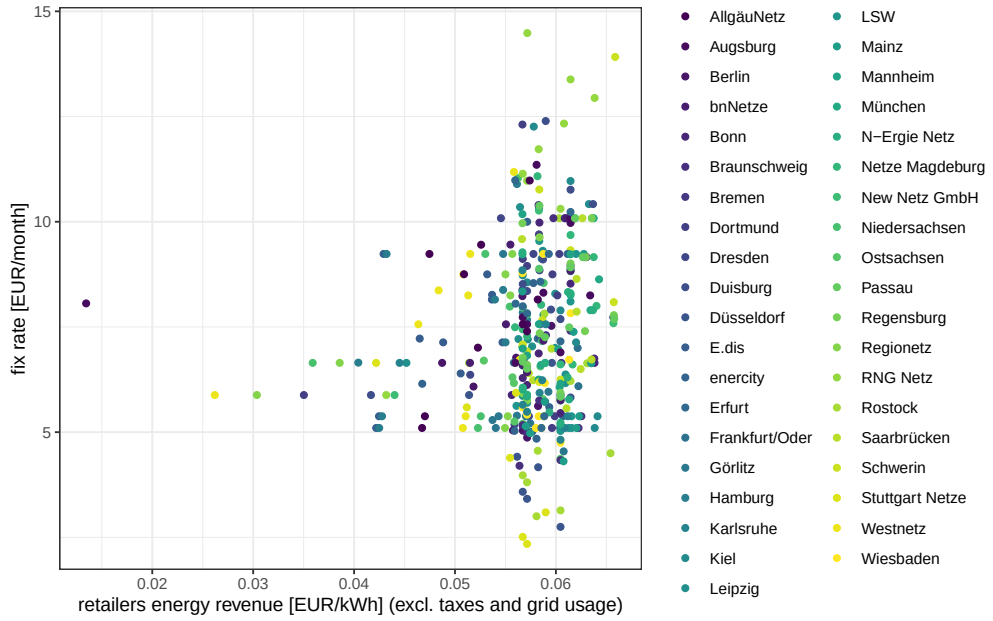


Figure 5: Fixed base rates and energy rates in Germany for 39 different locations, net (Source: GET AG)

second tariff scheme, we consider a dynamic tariff with a fixed base rate and a time-varying energy rate. The time-varying energy rate is assumed to be indexed to day-ahead electricity prices. In this second scheme, the fixed base rate is calibrated so as to obtain the same contribution margin of the fixed tariff scheme in the sample. This guarantees the reliability of our analysis on the impact of increasing self-sufficiency and dynamic tariffs on the retailer's net revenues and risk exposure.

[17] https://www.get-ag.com/

For the second tariff scheme, a fixed base rate of 0.453 EUR/day is computed. We maintain the assumption of price-inelasticity of electricity demand, likewise the assumption of no electricity storage allowing for adjustments to the PV feed-in and self-generation patterns in the retailer's portfolio.

We investigate the retailer's trading optimization problem with increasing levels of solar PV self-generation by assuming an increasing number of costumers with PV generation in the retailer portfolio, as defined in Eq.17, and consistent with installation rates $\phi$=30% and $\phi$=50%. We assume a hypothetical retailer with 100,000 household customers as in Section 4.3, and consider the implications of increasing self-sufficiency under the two tariff schemes described above by assuming that customers with and without PV self-generation and costumers with fixed and dynamic tariffs are equally distributed in the retailer portfolio[18]. $\phi$ denotes the share of customers with PV installations, i.e. the PV installation rate, while the share of customers with a dynamic tariff is denoted by $\delta$. In our case study, we consider $\delta$=0%, i.e. the *status quo* of the market with no indexation to the day-ahead prices in the energy rate, and $\delta$=50% and $\delta$=100%. This case study is of particular interest to assess the extent to which tariff schemes can affect risk sharing in electricity markets with increasing levels of distributed variable renewable generation. Results from the stochastic modeling and retailer's trading optimization are presented in the following section.

# 5 Results

Table 2 shows descriptive statistics of the time series for dependent variables used in the empirical analysis. We distinguish between Summer, Transition season and Winter, and observe that in Summer and Winter, the intraday solar PV generation and ID3 price are on average above their day-ahead values for the corresponding delivery period. The opposite holds during the Transition season. Not surprisingly, differences between the intraday and day-ahead solar PV are larger and

[18] Although a bias introduced by the self-selection of certain customers' group towards certain tariffs is possible, we consider this assumption to be legitimate as there is no technical flexibility to be exploited economically. However, extending the approach to customers with PV battery storage systems would require a investigation of individual economic incentives.

more volatile in Winter. Differences between intraday and day-ahead price are larger, in absolute value, during the Transition season but more volatile in Winter, is response to the greater uncertainty of the solar PV generation, and consequently of the residual load. Overall, skweness and kurtosis imply a departure from the assumption of a Gaussian distribution, as also suggested by the Jarque-Bera statistics and their p-values (JB and JB p-value in columns nine and ten of the table). The Augmented Dickey-Fuller tests reject the null hypothesis of non-stationarity.

## 5.1 Day-ahead and intraday stochastic modeling

Parameter estimates of deterministic components of the day-ahead and intraday series, as described in Eq.2-Eq.4 and Eq.11-Eq.13 are presented in Appendix A.1 and A.2, respectively. The OU parameter estimates for the day-ahead stochastic components $X_t$, $Y_t$, $Z_t$ in the base regime are shown in Tab.3. The mean-reverting parameters in the diagonal of the matrix $\boldsymbol{\beta}^{\boldsymbol{DA,Base}}$ point to a higher persistence of the residual load when compared to the cloudiness and price series across the system. In contrast, the prices series show the lowest persistence. Higher volatility is observed in the residual load and price series during the Transition season and in Winter, as indicates by the parameters in the diagonal of the matrix $\boldsymbol{\Sigma}^{\boldsymbol{DA,Base}}$. The opposite holds for the cloudiness component, which is more volatile in Summer. Overall, the out-of-diagonal parameters of the matrix validate the positive correlation linking cloudiness, residual load and price. Lower jump regime produce more spiked series compare to the upper jump regime, as implied by the parameters $\boldsymbol{\mu}$ in Tab.4. In all, the lower regime is also more volatile than the upper regime, as indicated by the estimated covariance matrices $\boldsymbol{\Sigma}$. Series in the lower regime are also more volatile than in the base regime, thus in line with findings in Coulon et al. (2013).

Parameter estimates of the stochastic component of the intraday cloudiness and residual load series (Tab. 5) are in line with the results observed in day-ahead market, thus suggesting the highest persistence of the cloudiness across seasons with respect to the residual load. Yet, residual load is found to be more volatile than cloudiness in the intraday market across the seasons. Furthermore, in contrast to the day-ahead market, more spiked series are observed in the upper rather than in

Table 2: Descriptive statistics

| Summer | Mean | Median | Min | Max | St.Dev. | Skew | Kurt | JB | JB p-value | ADF | ADF p-value | Obs. |
|---|---|---|---|---|---|---|---|---|---|---|---|---|
| Solar PV load (MW), DA | 11105 | 10914 | 1 | 29409 | 8296 | 0.197 | 1.797 | 263.5 | 0.001 | -16.21 | 0.001 | 5952 |
| Solar PV load (MW), ID | 11146 | 10851 | 1 | 29622 | 8317 | 0.202 | 1.812 | 258.4 | 0.001 | -16.44 | 0.001 | 5952 |
| Residual load (MW), DA | 14188 | 14758 | -20414 | 33539 | 9567 | -0.575 | 3.292 | 349.6 | 0.001 | -9.870 | 0.001 | 5952 |
| Residual load (MW), ID | 14284 | 14778 | -18415 | 33834 | 9413 | -0.539 | 3.173 | 295.5 | 0.001 | -10.05 | 0.001 | 5952 |
| Price (EUR/MWh), DA | 38.27 | 37.69 | -49.62 | 80.01 | 11.11 | -1.082 | 11.71 | 4993 | 0.001 | -5.120 | 0.001 | 1488 |
| ID3 Price (EUR/MWh), ID | 38.45 | 37.45 | -116.2 | 174.53 | 15.61 | -0.316 | 19.59 | 68329 | 0.001 | -13.31 | 0.001 | 5952 |
| Delta price (EUR/MWh), (ID-DA) | 0.179 | -0.225 | -100.8 | 115.17 | 10.97 | 0.863 | 16.20 | 43893 | 0.001 | -14.40 | 0.001 | 5952 |
| **Transition season** | **Mean** | **Median** | **Min** | **Max** | **St.Dev.** | **Skew** | **Kurt** | **JB** | **JB p-value** | **ADF** | **ADF p-value** | **Obs.** |
| Solar PV load (MW), DA | 7226 | 5936 | 1 | 26943 | 6115 | 0.845 | 3.049 | 490.4 | 0.001 | -9.77 | 0.001 | 8736 |
| Solar PV load (MW), ID | 7200 | 5788 | 1 | 27216 | 6189 | 0.874 | 3.094 | 526.3 | 0.001 | -9.56 | 0.001 | 8736 |
| Residual load (MW), DA | 14566 | 15015 | -19315 | 44328 | 11707 | -0.172 | 2.690 | 78.13 | 0.001 | -10.76 | 0.001 | 8736 |
| Residual load (MW), ID | 14489 | 14819 | -21842 | 44681 | 11879 | -0.170 | 2.654 | 85.7 | 0.001 | -10.82 | 0.001 | 8736 |
| Price (EUR/MWh), DA | 38.38 | 38.05 | -37.29 | 87.12 | 12.20 | -0.599 | 6.179 | 692.7 | 0.001 | -6.351 | 0.001 | 2184 |
| ID3 Price (EUR/MWh), ID | 36.69 | 37.51 | -94.3 | 200.3 | 18.78 | -1.368 | 13.13 | 40060 | 0.001 | -13.80 | 0.001 | 8736 |
| Delta price (EUR/MWh), (ID-DA) | -1.227 | -0.825 | -98.5 | 140.2 | 12.58 | -1.109 | 16.31 | 66183 | 0.001 | -15.84 | 0.001 | 8736 |
| **Winter** | **Mean** | **Median** | **Min** | **Max** | **St.Dev.** | **Skew** | **Kurt** | **JB** | **JB p-value** | **ADF** | **ADF p-value** | **Obs.** |
| Solar PV load (MW), DA | 4190 | 3404 | 1 | 15705 | 3597 | 0.911 | 3.206 | 482.2 | 0.001 | -9.194 | 0.001 | 8736 |
| Solar PV load (MW), ID | 4362 | 3488 | 1 | 16790 | 3777 | 0.889 | 3.105 | 455.2 | 0.001 | -9.85 | 0.001 | 8736 |
| Residual load (MW), DA | 10189 | 10512 | -22072 | 42688 | 13470 | -0.068 | 2.343 | 164.0 | 0.001 | -9.963 | 0.001 | 8736 |
| Residual load (MW), ID | 10230 | 10611.5 | -20394 | 42696 | 13328 | -0.042 | 2.318 | 171.8 | 0.001 | -9.97 | 0.001 | 8736 |
| Price (EUR/MWh), DA | 29.85 | 32.25 | -50.43 | 76.47 | 15.93 | -1.040 | 5.155 | 815.3 | 0.001 | -7.978 | 0.001 | 2184 |
| ID3 Price (EUR/MWh), ID | 30.79 | 33.46 | -80.6 | 438.8 | 20.66 | 0.678 | 29.25 | 25152 | 0.001 | -12.21 | 0.001 | 8736 |
| Delta price (EUR/MWh), (ID-DA) | 0.982 | 0.96 | -90.4 | 397.4 | 14.81 | 3.082 | 78.41 | 20831 | 0.001 | -16.24 | 0.001 | 8736 |

Table 3: Parameter estimates of the stochastic components in base regime: Day-ahead series

| Summer | $\beta^{DA,Base}$ | | | $\Sigma^{DA,Base}$ | | |
|---|---|---|---|---|---|---|
| | *X* | *Y* | *Z* | *X* | *Y* | *Z* |
| *X* | 0.3286 | -0.0311 | -0.1836 | 0.00614 | 0.00014 | 0.00006 |
| *Y* | -0.0016 | 0.2415 | 0.2695 | 0.00014 | 0.00207 | 0.00011 |
| *Z* | -0.0055 | 0.0022 | 1.9412 | 0.00006 | 0.00011 | 0.00056 |
| Transition season | $\beta^{DA,Base}$ | | | $\Sigma^{DA,Base}$ | | |
| | *X* | *Y* | *Z* | *X* | *Y* | *Z* |
| *X* | 0.612 | -0.143 | 0.462 | 0.00432 | 0.00039 | 0.00014 |
| *Y* | -0.004 | 0.343 | 1.473 | 0.00039 | 0.00476 | 0.00017 |
| *Z* | -0.003 | 0.030 | 2.198 | 0.00014 | 0.00017 | 0.00078 |
| Winter | $\beta^{DA,Base}$ | | | $\Sigma^{DA,Base}$ | | |
| | *X* | *Y* | *Z* | *X* | *Y* | *Z* |
| *X* | 0.641 | -0.019 | 0.022 | 0.00036 | -0.00002 | 0.00002 |
| *Y* | 0.050 | 0.437 | 0.930 | -0.00002 | 0.01019 | 0.00041 |
| *Z* | 0.037 | 0.019 | 2.270 | 0.00002 | 0.00041 | 0.00116 |

Table 4: Parameter estimates of the stochastic components in the upper jump and lower jump regimes: Day-ahead series

| Summer | $\varepsilon^{DA,uJ}$ | | | | $\varepsilon^{DA,lJ}$ | | | |
|---|---|---|---|---|---|---|---|---|
| | $\mu$ | $\Sigma$ | | | $\mu$ | $\Sigma$ | | |
| *X* | 0.018 | 0.008527 | 0.000028 | 0.000021 | 0.0310 | 0.0150021 | 0.0001185 | 0.0000143 |
| *Y* | 0.001 | 0.000028 | 0.000262 | 0.000001 | 0.0001 | 0.0001185 | 0.0000287 | 0.0000001 |
| *Z* | 0.001 | 0.000021 | 0.000001 | 0.000032 | 0.0005 | 0.0000143 | 0.0000001 | 0.0000226 |
| Transition season | $\varepsilon^{DA,uJ}$ | | | | $\varepsilon^{DA,lJ}$ | | | |
| | $\mu$ | $\Sigma$ | | | $\mu$ | $\Sigma$ | | |
| *X* | 0.050 | 0.031659 | 0.000078 | 0.000003 | 0.0631 | 0.040807 | 0.014639 | 0.000040 |
| *Y* | 0.001 | 0.000078 | 0.000290 | -0.000001 | 0.0168 | 0.014639 | 0.022301 | 0.000011 |
| *Z* | 0.001 | 0.000003 | -0.000001 | 0.000044 | 0.0006 | 0.000040 | 0.000011 | 0.000032 |
| Winter | $\varepsilon^{DA,uJ}$ | | | | $\varepsilon^{DA,lJ}$ | | | |
| | $\mu$ | $\Sigma$ | | | $\mu$ | $\Sigma$ | | |
| *X* | 0.058 | 0.02063 | 0.00019 | -0.00004 | 0.0623 | 0.039472 | 0.004743 | -0.000031 |
| *Y* | 0.004 | 0.00019 | 0.00168 | 0.00004 | 0.0101 | 0.004743 | 0.004888 | 0.000021 |
| *Z* | 0.001 | -0.00004 | 0.00004 | 0.00010 | 0.0014 | -0.000031 | 0.000021 | 0.000108 |

the lower regimes (Tab.6), thus implying more frequent upward adjustments in the cloudiness and residual load intraday forecasting process. High persistence and volatility are also observed in the intraday ID3 prices when compared to the day-ahead price series (Tab.7). Similar to the cloudiness and residual load series, ID3 prices are in all more spiked and volatile in the higher regime. Parameter estimates of these stochastic components are thus used to generate 1,000 path over one typical working and weekend day for each of the three seasons. The resulting scenario trees are presented in the next section.

Table 5: Parameter estimates of the stochastic components in the base regime: Intraday cloudiness and residual load series

| Summer | $\boldsymbol{\beta}^{ID,Base}$ | | $\boldsymbol{\Sigma}^{ID,Base}$ | |
|---|---|---|---|---|
| | X | Y | X | Y |
| X | 0.1665 | -0.0065 | 0.000022 | 0.000002 |
| Y | 0.0883 | 1.2913 | 0.000002 | 0.000167 |
| Transition season | $\boldsymbol{\beta}^{ID}$ | | $\boldsymbol{\Sigma}^{ID,Base}$ | |
| | X | Y | X | Y |
| X | 0.3221 | 0.0097 | 0.000002 | 0.000001 |
| Y | -0.4380 | 1.2956 | 0.000001 | 0.000171 |
| Winter | $\boldsymbol{\beta}^{ID,Base}$ | | $\boldsymbol{\Sigma}^{ID,Base}$ | |
| | X | Y | X | Y |
| X | 0.7539 | -0.0061 | 0.000007 | 0.000002 |
| Y | -0.3567 | 1.0473 | 0.000002 | 0.000417 |

Table 6: Parameter estimates of the stochastic components in the upper jump and lower jump regimes: Intraday cloudiness and residual load series

| Summer | $\boldsymbol{\epsilon}^{ID,uJ}$ | | | $\boldsymbol{\epsilon}^{ID,lJ}$ | | |
|---|---|---|---|---|---|---|
| | $\boldsymbol{\mu}$ | $\boldsymbol{\Sigma}$ | | $\boldsymbol{\mu}$ | $\boldsymbol{\Sigma}$ | |
| X | 0.0052 | 0.000292 | 0.000002 | 0.0060 | 0.000530 | 0.000002 |
| Y | 0.0006 | 0.000002 | 0.000023 | 0.0004 | 0.000002 | 0.000018 |
| Transition season | $\boldsymbol{\epsilon}^{ID,uJ}$ | | | $\boldsymbol{\epsilon}^{ID,lJ}$ | | |
| | $\boldsymbol{\mu}$ | $\boldsymbol{\Sigma}$ | | $\boldsymbol{\mu}$ | $\boldsymbol{\Sigma}$ | |
| X | 0.0096 | 0.000830 | 0.000009 | 0.0085 | 0.000858 | 0.000003 |
| Y | 0.0010 | 0.000009 | 0.000047 | 0.0007 | 0.000003 | 0.000038 |
| Winter | $\boldsymbol{\epsilon}^{ID,uJ}$ | | | $\boldsymbol{\epsilon}^{ID,lJ}$ | | |
| | $\boldsymbol{\mu}$ | $\boldsymbol{\Sigma}$ | | $\boldsymbol{\mu}$ | $\boldsymbol{\Sigma}$ | |
| X | 0.0126 | 0.001144 | -0.00002 | 0.0097 | 0.001139 | 0.000005 |
| Y | 0.0018 | -0.000018 | 0.00016 | 0.0018 | 0.000005 | 0.000162 |

Table 7: Parameter estimates of the stochastic component in base regime of the intraday ID3 price

| | $\boldsymbol{\beta}^{ID3,Base}$ | $\boldsymbol{\sigma}^{ID3,Base}$ |
|---|---|---|
| Summer | 1.744 | 0.0029 |
| Transition season | 2.064 | 0.0087 |
| Winter | 1.437 | 0.0047 |

Table 8: Parameter estimates of the stochastic component in the upper jump and lower jump regimes of the intraday ID3 prices

| | $\boldsymbol{\epsilon}^{ID3,uJ}$ | | $\boldsymbol{\epsilon}^{ID3,lJ}$ | |
|---|---|---|---|---|
| | $\boldsymbol{\mu}$ | $\boldsymbol{\sigma}$ | $\boldsymbol{\mu}$ | $\boldsymbol{\sigma}$ |
| Summer | 0.0010 | 0.0107 | 0.0007 | 0.0087 |
| Transition season | 0.0030 | 0.0245 | 0.0025 | 0.0218 |
| Winter | 0.0027 | 0.0212 | 0.0036 | 0.0255 |

## 5.2 Scenario trees

In all, the scenario generation-and-reduction procedure described in Section 4.1.4 and Section 5 results in totally 540 nodes, and 90 scenario trees across the three seasons (Summer, Transition

season, Winter) and the two typical days (working and weekend day), as depicted in Fig.4. For illustration purposes, we plot the scenario trees for the low, medium and high scenario obtained for one typical working day in Summer. These scenarios correspond to high, medium and low levels of solar PV generation respectively, i.e. low, medium and high levels of cloudiness, residual load and prices in the scenario generation-reduction, as filtered through the clustering algorithm. The choice of driving attention on a working day in Summer is motivated by the intuition that solar PV generation and self-generation should have a greater impact on the retailer's trading decisions and risk-exposure in Summer and during a business day, i.e. when the levels of solar generation and total load are expected to be higher.

Fig.6 shows the obtained nodes for the day-ahead solar PV generation, residual load and prices in the low (left charts), medium (mid) and high (right) scenarios. Solid black line show the historical values, i.e. the average working day in the sample season as computed from the hourly averages; solid blue lines represent the expected day-ahead profile $j_1$ obtained from the scenario-reduction procedure. Dashed lines represent day-ahead profiles $j_2$ and $j_3$, which are above and below one standard deviation from the expected profile. These nodes have 25% probability of realization; dotted lines correspond to more extreme day-ahead profiles $j_4$ and $j_5$, which are above and below one standard deviation from the expected profile and have 12.5% probability of realization. Despite the limited randomness of the solar PV generation (top charts), the simulated paths well capture the iconic *duck-curve* effect of the solar PV generation on the residual load, and the load-to-price relationship, while the three scenarios remain consistent with the historical values[19]. Fig. 7 provides distributional information of the historical and simulated day-ahead series through boxplots. On each blue box, the central red mark indicates the median, the bottom and top edges of the box indicate the $25^{th}$ and $75^{th}$ percentiles, respectively. The whiskers extend to the most extreme data points, which are not considered outliers. The simulated five nodes in the medium scenario (mid plots) well reproduce the distribution of the historical series, being this scenario obtained

[19] As solar PV generation increases during the day, it reduces the residual load. The residual load drops in the middle of the day (like a belly) and then raises as the solar generation reduces (like a neck), thus leading to the definition of a *duck-curve*

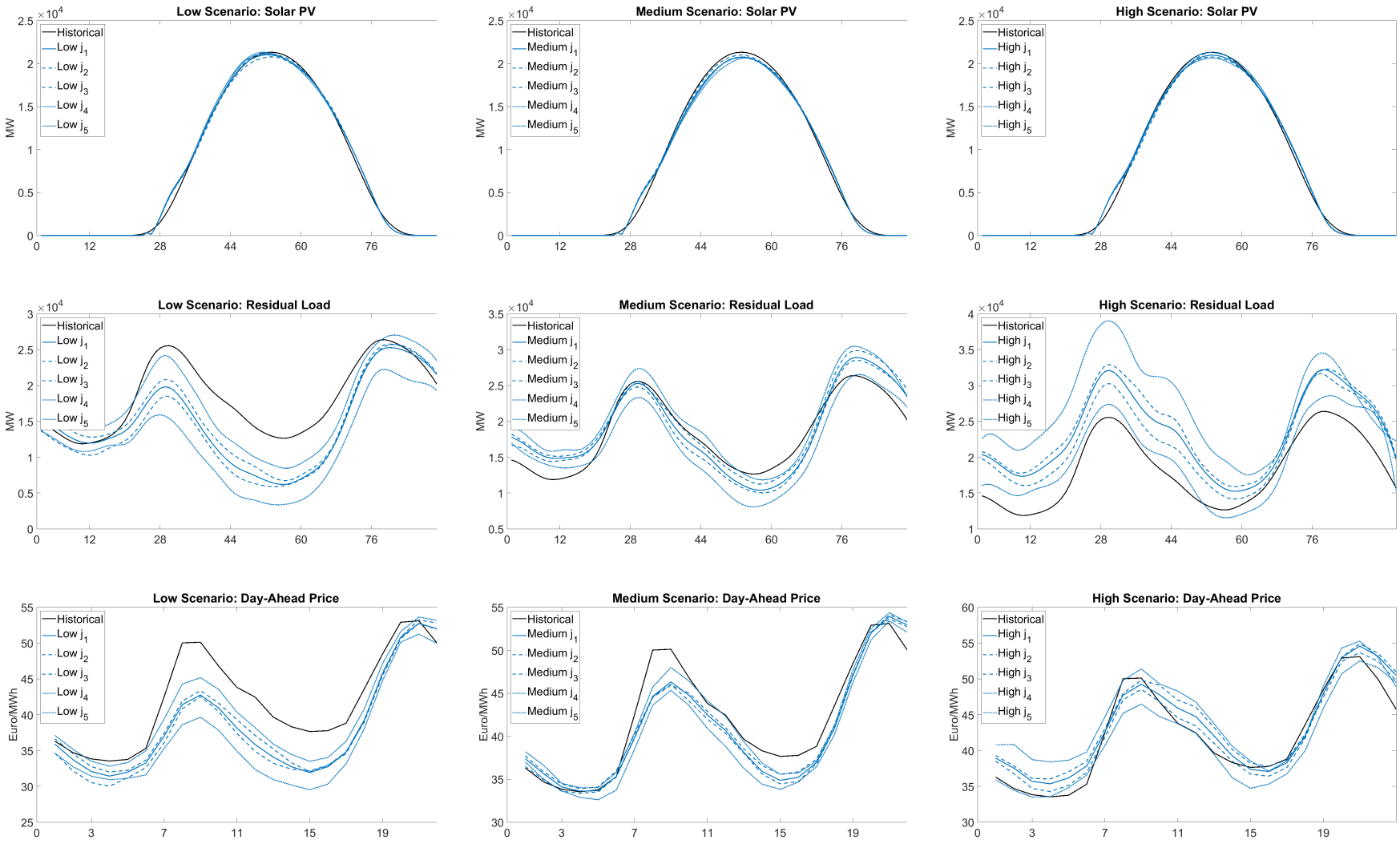


Figure 6: Historical and simulated day-ahead series: Summer working day

from the partition of simulated paths that are in the variance cluster closest to the median of all the simulated paths. Nodes in the high and low scenarios (left and right plots, respectively) represent the partitions of simulated paths in highest and lowest variance clusters respectively, and such that their median point is above and below the all-point median of the corresponding nodes in the medium scenario. Therefore, consistent with the identified three scenarios, boxplots indicate that the correlation structure between solar PV generation, residual load and price in the day-ahead market is well reproduced across nodes in the three scenarios. Results for the simulated series in transition and Winter seasons are reported in the Appendix. The scenario trees depicted in Fig.8 show the possible intraday realizations $\boldsymbol{k}$ of the day-ahead node $\boldsymbol{j_1}$ in the low, medium and high scenario in Fig.6. These scenario trees reflect the adjustment process occurring between day-ahead and intraday market, following the arrive of new information and consequent update of the solar forecasting error. The intraday realizations $\boldsymbol{k_1}$ represent expected intraday profiles minimizing the forecasting error, thus leading to intraday realizations close to the expected day-ahead profiles (blue solid lines in the plots). For growing forecasting errors, greater deviations are observed in the intraday residual load and price profiles, which are consistent with the duck-curve effect and the positive correlation between residual load and price, as also unveiled by the historical values (black solid lines). Furthermore, the intraday realizations well capture the empirically observed jagged pattern of the intraday prices, as noticed by comparing the historical observations (black solid lines) with the simulated values. This pattern is of particular interest when investigating trading strategies in the intraday market, and thus the retailer's trading and risk optimization problem with increasing levels of solar PV self-generation. Results from this analysis are presented below.

## 5.3 Retailer's trading optimization in the day-ahead and intraday market

In this section, the results of the retailer's trading optimization problem are presented. For illustration purposes and in line with the scenario trees presented in Section 5.2, the results for the day-ahead node $\boldsymbol{j_1}$ and all its possible intraday realizations $\boldsymbol{k}$ in the typical summer working day are shown, and for the low and high scenarios, i.e. for high (low) and low (high) levels of solar PV

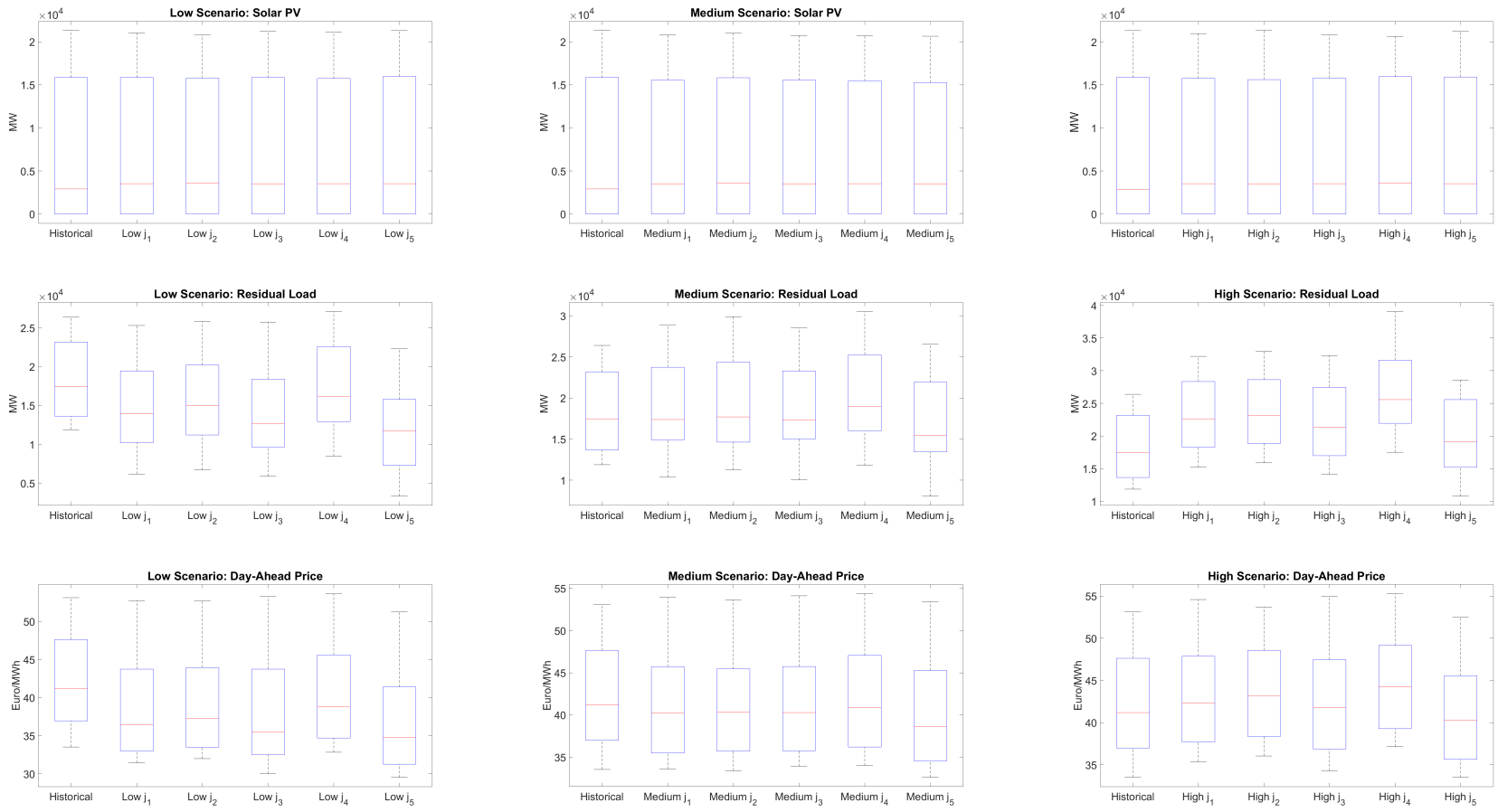


Figure 7: Distribution of the historical and simulated day-ahead series: Summer working day

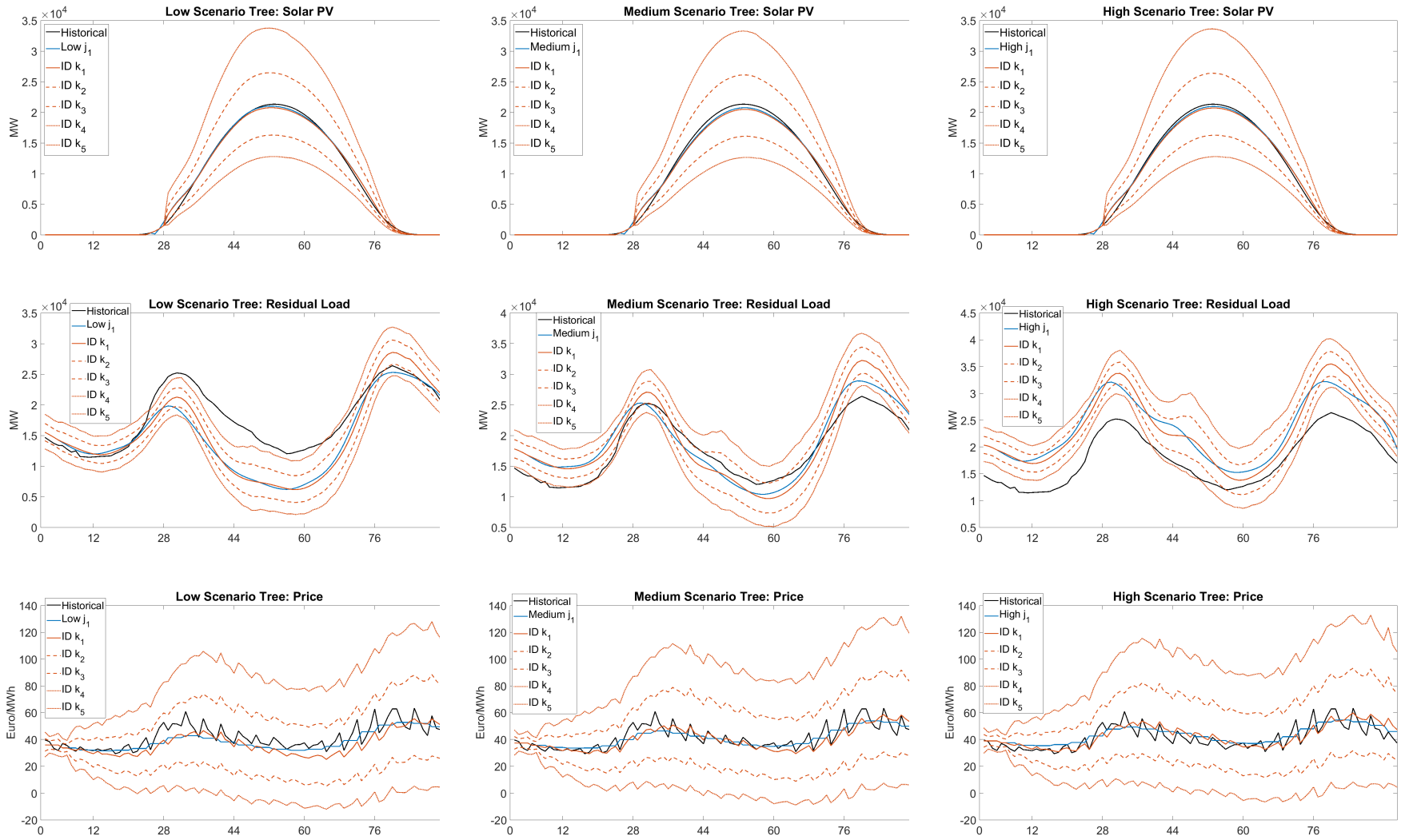


Figure 8: Scenario trees for the representative day-ahead node $\boldsymbol{j_1}$ and its intraday realizations $\boldsymbol{k}$: Summer working day

generation (residual load) since these scenarios can be expected to better represent the implications of high levels of self-sufficiency for a retailer serving customers with decentralized self-generation. Results concerning the retailer's trading strategies in the medium scenario, and for the transition and Winter seasons are reported in the Appendix.

Fig.9 and Fig.10 summarize the retailer's optimal trading strategies in the day-ahead and intraday markets in the low scenario. These figures show the buying and selling bids of the retailer in the two markets for different levels of their risk aversion, as indicated by the parameter $\boldsymbol{\lambda}$, with increasing levels of solar PV generation (corresponding to installation rates of 10% and 50%) and under the two different retail tariff schemes, i.e. for 0% and 100% indexation of the dynamic energy rate to the day-ahead price[20]. Buying/selling positions are denoted by the direction of the marker in the plots; the acceptance probability of the bids is denoted by the colour gradation while bidding volumes are indicated by the size of the marker. It should be noted that bids submitted on the day-ahead market do not anticipate realizations in the intraday market, and are thus consistent over the represented scenario tree.

In the low scenario, a risk-neutral retailer ($\boldsymbol{\lambda}$=0%) takes buying positions in the day-ahead market during the solar generation peak between 11 am and 3 pm (left column of Fig.9). This trading strategy is consistent across different levels of self-generation and tariff schemes, and implies the preference of a risk-neutral retailer to buy electricity in the day-ahead market for the solar-peak hours against the expectation of potentially higher prices in the intraday market, as driven by lower than expected levels of solar generation (Fig.10). Yet, in all the risk-neutral retailer is more prone to take buying positions in the intraday market, in particular in the evening, i.e. when the expected price benefit of the solar generation and the impact of self-generation are less evident.

Differently from a risk-neutral retailer, a more risk-averse retailer ($\boldsymbol{\lambda}$=10%) prefers to take buying positions in the day-ahead market, in particular for the hours starting from 7 pm onward

[20]The increasing solar PV penetration level is not considered to take place on a system level in the stochastic price model. For the results to remain comparable, we rather compare larger shares of households with rooftop solar PV systems in the retailer's portfolio by assuming unchanged market circumstances and solar system load. However, this assumption is likely to underestimate the importance of risk hedging under higher penetration of distributed renewable generation, since price volatility is likely to increase with increasing shares of variable generation.

and for low levels of self-generation. This trading behavior is more evident in the tariff scheme without indexation to the day-ahead price, thus in line with a strategy focused on reducing the risk exposure to the solar self-generation in the intraday market. This reasoning is supported by the observed selling positions in the intraday market for the morning and evening hours, i.e. when the impact of the solar generation (and self-generation) uncertainty on residual load and price is higher (Fig.8). The trading positions of a moderately risk-averse retailer are mixed and imply a propensity to take selling positions in the day-ahead market, mostly at the sunrise and sunset, and in the case of tariff with 0% indexation to the day-ahead prices. The mirroring buying positions in the intraday market suggest some trading adjustment to benefit of lower than expected intraday prices. Yet, the exposure of this retailer in the intraday market reduces for high levels of self-generation, when buying positions in the day-ahead market increase, mostly in the night hours and despite the presence of a more dynamic tariff (100% day-ahead price-indexation). In the high scenario, i.e. with lower levels of solar generation and high levels of residual load (Fig.11 and Fig.12), the risk-neutral retailer takes buying positions on the day-ahead market during the solar-peak hours and in the evening. This is more evident at 10% of self-sufficiency, regardless of the tariff scheme. Exposure in the intraday market increases for increasing levels of self-sufficiency thus under the expectation of potentially lower prices in the intraday market. Thus similar to the low scenario, arisk-neutral retailer in the high scenario is probably willing to take buying positions in the intraday market. The day-ahead buying positions of risk-averse retailers visibly increase in the high scenario, in response to lower levels of solar generation. Interestingly, buying positions in the day-ahead market are greater with the first retail tariff scheme, with 0% indexation to the day-ahead price. In contrast, the selling positions of a risk-averse retailer increase in the intraday market, mainly for high levels of self-generation and for the evening hours, i.e. after the sunset, thus implying some trading adjustment with respect to the day-ahead buying positions. Implications for the retailer's risk exposure of these trading strategies are discussed in the next section.

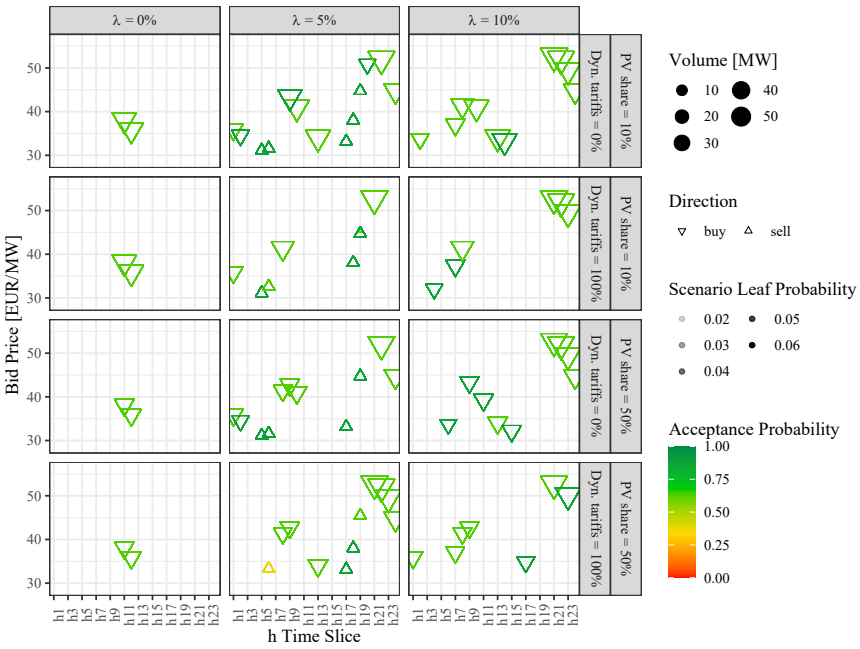


Figure 9: Retailer's day-ahead trading strategy in the summer working day: Low scenario

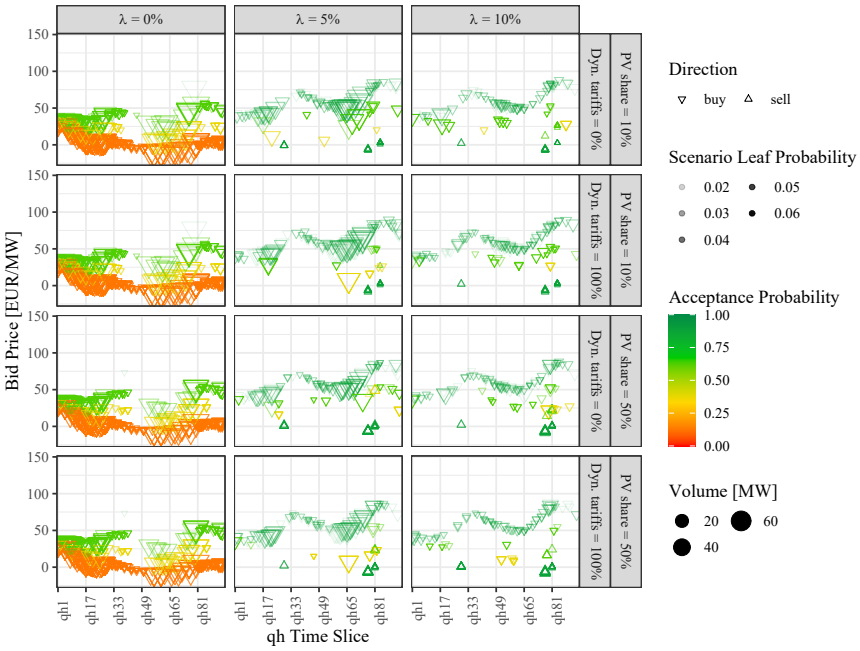


Figure 10: Retailer's intraday trading strategy in the summer working day: Low scenario

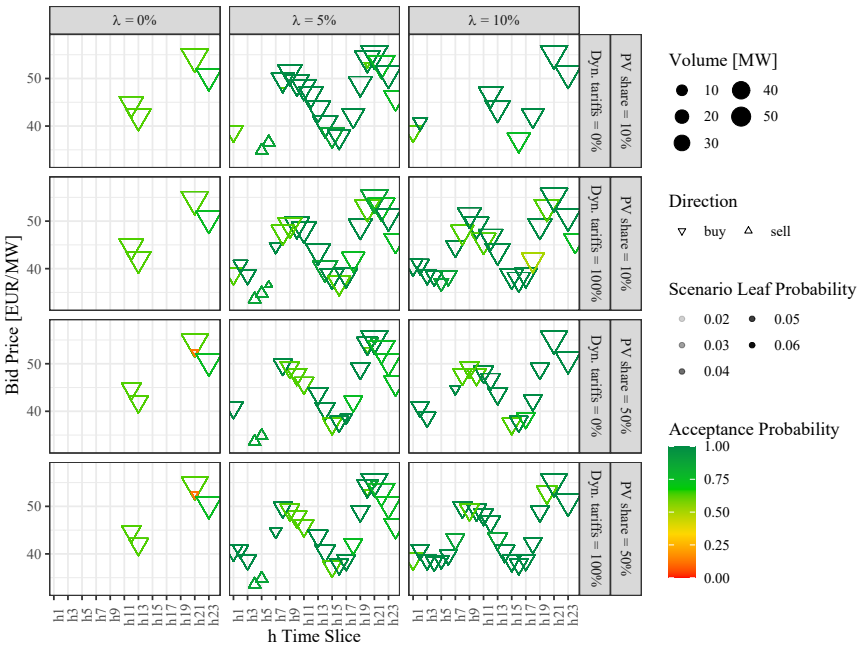


Figure 11: Retailer's day-ahead trading strategy in the summer working day: High scenario

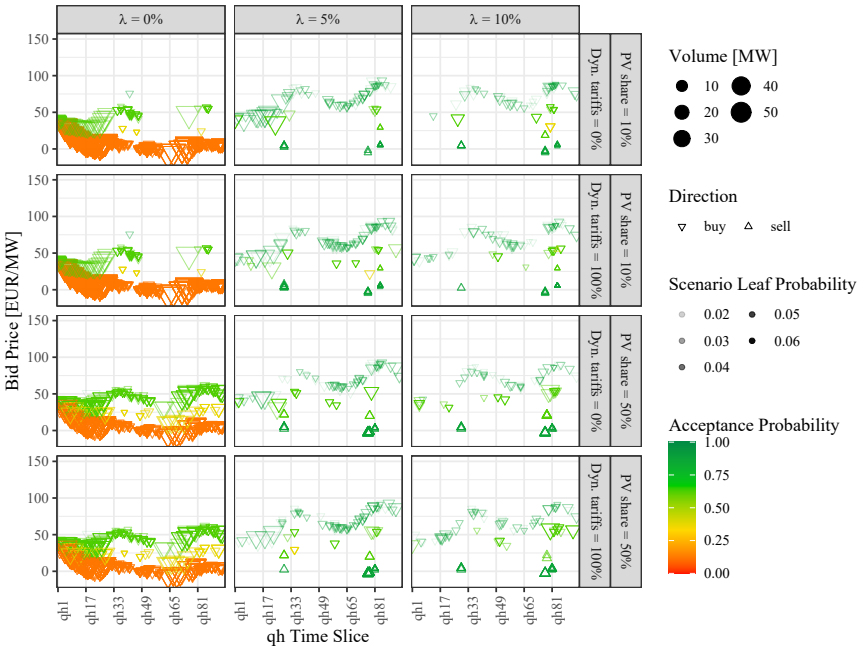


Figure 12: Retailer's intraday trading strategy in the summer working day: High scenario

## 5.4 Retailer's portfolio risk management with increasing solar PV self - generation

In this section, we present evidence of the retailer's risk exposure and management in the low and high scenarios presented in the previous section. Fig. 13 and Fig.14 show the empirical cumulative distribution functions (ECDFs) of the contribution margin of the retailer at 10% and 50% of solar PV self-generation and under the two retail tariff schemes (0% and 100% day-ahead price indexation of the retail energy tariff). The ECDFs are depicted for values of the risk preference $\boldsymbol{\lambda}$ in the target function in Eq.24: 0% (risk neutral, red line in the figures), 5% (low risk aversion, in yellow), and 10% (high risk aversion, green) and for a CVaR level at confidence level $\boldsymbol{\alpha = 95\%}$. The horizontal lines in the plots represent the expected contribution margins at each level of $\boldsymbol{\lambda}$.

In all, these figures point to a reduction of the retailer's expected contribution margin for increasing levels of self-generation without any indexation to the day-ahead price in the retail tariff. This reduction is higher in the low scenario, i.e. with higher solar PV generation (from around 40,000 EUR/day to 35,000 EUR/day, Fig.13) compared to the high scenario (from around 37,500 EUR/day to 32,000 EUR/day, Fig.14). Yet, under a highly dynamic tariff scheme with complete indexation to the day-ahead price ($\boldsymbol{\delta = 100\%}$), the expected contribution margin of the retailer remains almost unchanged for increasing levels of self-sufficiency and across scenarios (45,000 EUR/day). Interestingly, the ECDFs imply greater but more uncertain and dispersed contribution margins at lower levels of self-sufficiency for different risk preferences. For instance, in the low scenario (Fig.13), 10% of self-sufficiency implies a contribution margin for a risk-neutral retailer (red line) ranging from 17,000 EUR/day to 60,000 EUR/day with a 0%-indexed tariff, and from 24,000 EUR/day to 65,000 EUR/day with a 100%-indexed tariff. At 50% of self-sufficiency, these margins range from 20,000 EUR/day to 49,000 EUR/day with the 0%-indexed tariff, and from 30,000 EUR/day to 60,000 EUR/day with the 100%-indexed tariff. Same dynamics are observed in ECDFs under the high scenario (Fig.14), where however lower dispersion in the contribution margin is observed. Further evidence concerning the variability of the risk exposure of the retailer is provided in the bar plots in Fig.15 and Fig.16, which depict the contribution margin of the retailer

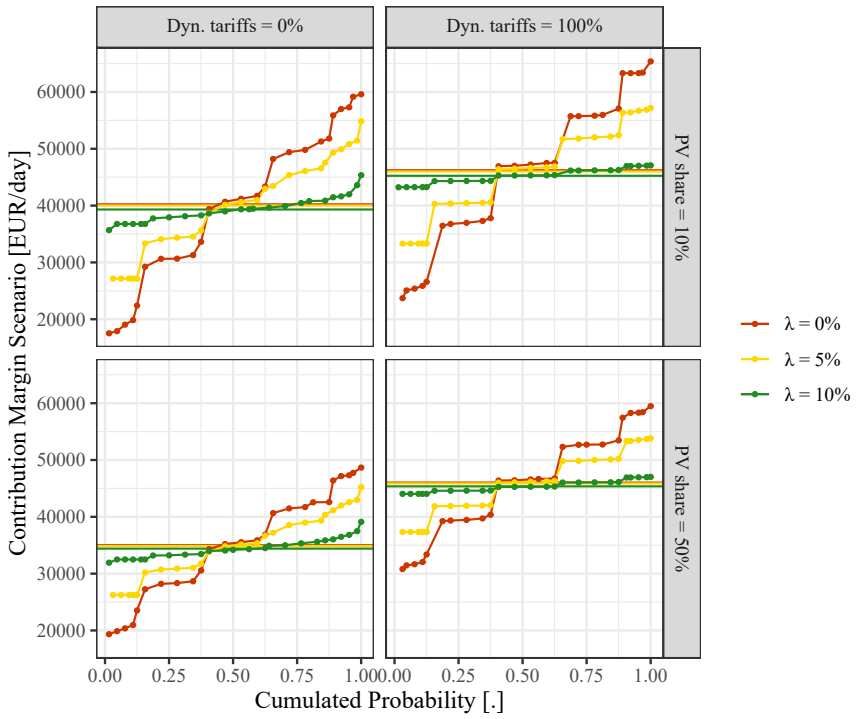


Figure 13: Empirical cumulative distribution functions of contribution margins for the summer working day: Low scenario

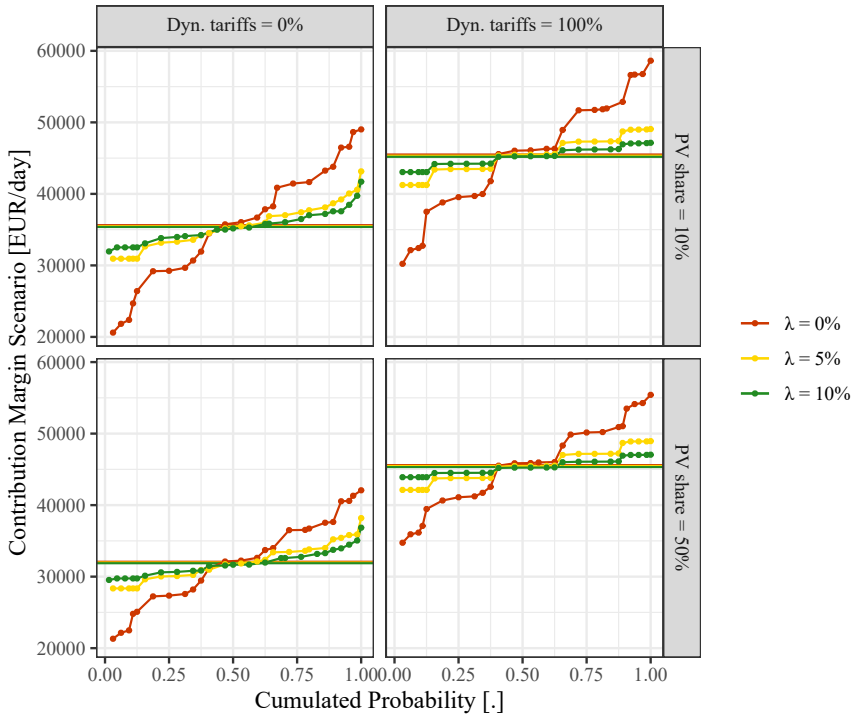


Figure 14: Empirical cumulative distribution functions of contribution margins for the summer working day: High scenario

across the five possible intraday realizations of the day-ahead node $j_1$ in the low and high scenarios, respectively. As mentioned above, the $j_1$ node represent the typical, i.e. expected summer working day in the low and high scenario. The charts point to a lower contribution margins across scenarios for 50% of solar PV self-generation when compared to 10% levels. Yet, variability across intraday realizations for a risk-neutral retailer ($\boldsymbol{\lambda = 0\%}$) and with a 10% self-generation. This variability is clearly reduced for risk-averse retailers ($\boldsymbol{\lambda = 5\%}$ and $\boldsymbol{\lambda = 10\%}$, respectively). Contribution margins in the intraday market are higher and more dispersed in the low scenario with high solar PV generation, and with fixed tariffs (0% indexation). In contrast, dynamic tariffs (100% indexation) contribute towards higher and less volatile margins, particularly at 50% of self-generation [21]. In all, these findings imply higher risk exposure in the intraday market for a risk-neutral retailer with static tariffs and increasing levels of solar PV generation and self-generation. Fig.17 depicts the retailer's efficient frontiers in the low (top charts) and high (bottom charts) scenarios for different levels of self-generation (10% and 50%) and with fixed (0% day-ahead price indexation) rather than highly dynamic (100% day-ahead price indexation) retail tariffs. These frontiers depict the highest expected contribution margin at each given level of risk (indicated by the corresponding CVaR), and risk preference $\boldsymbol{\lambda}$. From the perspective of the risk-neutral retailer, in the leftmost end of the curves, greater risk exposure is observed for increasing levels of self-generation. In the low scenario and with a static retail tariff (i.e. Dyn. tariff=0%), for comparable CVaR values ( 18,500-19,000 EUR/day) the retailer's expected contribution margin diminishes from around 40,000 EUR/day at 10% of self-generation to around 35,000 EUR/day at 50% of self-generation. In the high scenario, the expected lost contribution margin amount to around 11,000 EUR/day, i.e. from around 35,000 EUR/day at 10% of self-generation to roughly 26,000 EUR/day at 50% for CVaR values of approximately 19,000 EUR/day and 21,000 EUR/day. Yet, when considering more dynamic retail tariff, i.e. Dyn.Tariff=100%, the risk exposure of the risk-neutral appears to increase.

[21] It should be noted that due to lower levels of (residual) load, wholesale spot prices are typically below the yearly average in Summer. The dynamic indexation captures this seasonal variation. The fixed tariff scheme however is constant throughout the year, which implies higher specific contribution margins (EUR per served MWh) in Summer compared to Transition season and Winter. We refer to the Appendix for results on the transition and Winter season with higher wholesale spot prices.

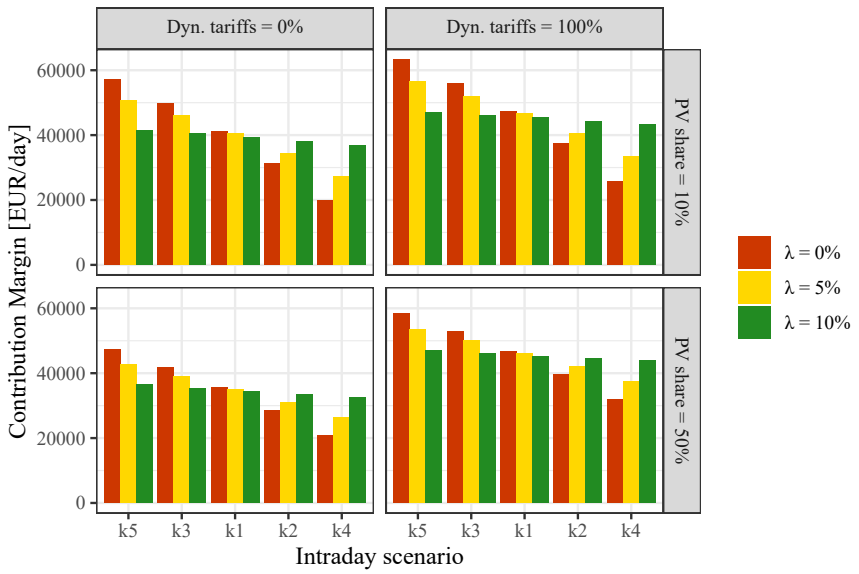


Figure 15: Retailer's contribution margin variability in the intraday market: Low scenario

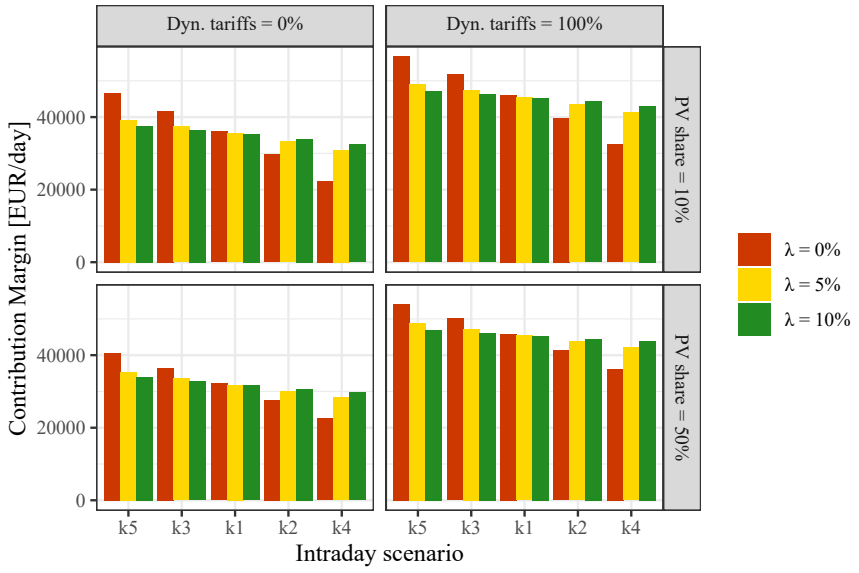


Figure 16: Retailer's contribution margin variability in the intraday market: High scenario

This finding is intuitive as the price uncertainty has an influence on both the tariff revenues and the procurement costs. In the low scenario, the expected contribution margin remains almost constant to roughly 46,500 EUR/day for increasing levels of self-generation against CVaR values increasing from 24,000 EUR/day at 10% to 31,000 EUR/day at 50% of PV self-generation. A comparable effect is observed in the high scenario.

From the perspective of the most risk-averse retailer ($\lambda$=10% in the rightmost end of the curves), an increase in the risk exposure is also noticeable when considering a static retail tariff in the low scenario, the retailer's expected contribution margin reduces from around 39,5000 EUR/day at 10% of self-generation to around 35,500 EUR/day at 50% of self-generation for CVaR values of approximately 36,500 and 37,500 EUR/day. In contrast, in the high scenario, thus for lower levels of solar PV generation, the expected contribution margin increases of around 2,500 EUR/day, i.e. from around 35,000 EUR/day at 10% of self-generation to roughly 37,500 EUR/day at 50%, against a decrease in the CVaR of approximately 3,000 EUR/day (from 32,000 EUR/day at 10% of self-sufficiency to 29,000 EUR/day at 50%). When considering more dynamic retail tariff, i.e. Dyn.Tariff=100%, an expected contribution margin of approximately 45,500 EUR/day is observed in the low scenario against a CVaR value of 43,500 EUR/day at both 10% and 50% of self-generation. Similar values are observed in the high scenario. Therefore, with highly dynamic retail tariff assuming 100%-indexation of the energy rate to the day-ahead price, the risk exposure of the risk-averse retailer remains unchanged for increasing levels of self-generation, and this is consistent across different scenarios of solar PV generation. The implications of the results presented in this section are discussed in the next section.

# 6 Discussion

The comprehensive investigation above provides interesting insights to evaluate the risk optimization problem faced by the retailer with increasing levels of solar PV self-generation in the residential sector. While a higher volume-risk has been observed in previous research with greater

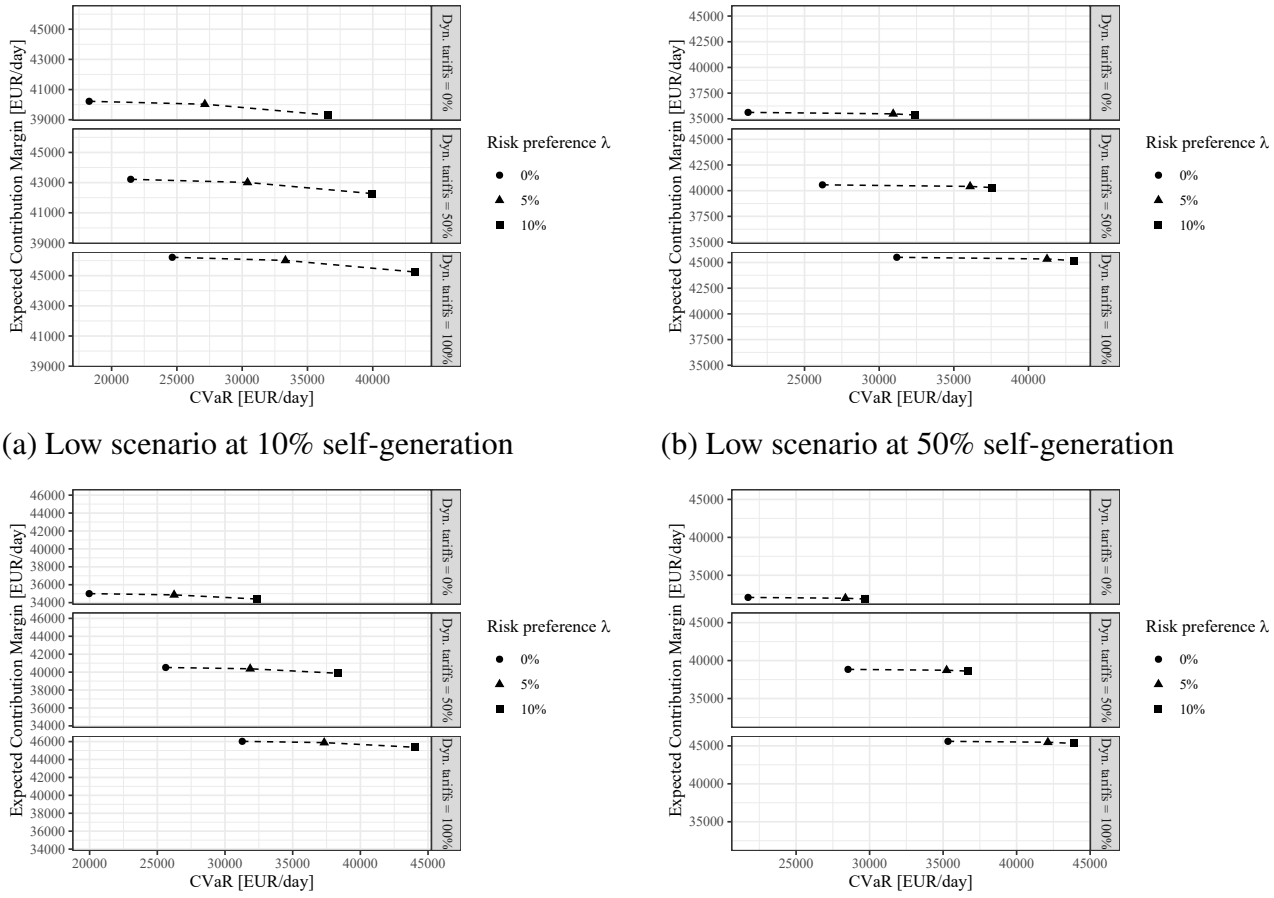


(a) Low scenario at 10% self-generation

(b) Low scenario at 50% self-generation

(c) High scenario at 10% self-generation

(d) High scenario at 50% self-generation

Figure 17: Efficient frontier of trading decisions for different risk preferences of the retailer

self-generation (Russo and Bertsch, 2020; Koolen et al., 2021), results in this study offer a broader understanding of the trading decision and risk optimization problem faced by the retailer in the day-ahead and intraday markets to adjust to this increasing short-term risk.

Results on the retailer's optimal trading strategy in Fig.9-Fig.12 imply that increasing PV self-generation, while affecting a risk-neutral retailer only marginally , has a significantly larger impact on a risk-averse retailer. The risk-neutral retailer remains exposed to the higher load uncertainty of the intraday market by preferring to take buying positions in the day-ahead market only for the solar-peak hours, i.e. when solar load uncertainty is greater and, in the high scenario, at the sunset, i.e. when the expected solar generation is lower and its expected uncertainty is also higher. This trading strategy remains unchanged despite changes in the retail tariff scheme and is consistent

with a risk-neutral retailer preferring to adjust the position on the intraday market, where prices are expected to be lower with high solar self-generation. Interestingly, we do not find evidence of selling positions in the day-ahead and intraday market, thus suggesting the preference of a risk-neutral retailer for adjusting the positions in the intraday market by buying at prices above the expected level rather than by selling at prices below the expected level. In contrast, we observe that the risk-averse retailer is more likely to increase the exposure in the day-ahead market to cope with the higher load uncertainty driven by the self-generation. In all, our results are in line with Kettunen et al. (2010) and Kraft et al. (2021). Yet, findings in this study also imply an increase in the day-ahead buying positions likewise in the intraday selling positions of the risk-averse retailer for higher levels of solar PV self-generation. We can therefore infer that a risk-averse retailer is more likely to accept buying in the day-ahead market and lower selling prices in the intraday market to reduce their load-risk exposure. We also highlight that trading strategies in the day-ahead and intraday markets are found to be driven by the retailer's risk preferences and by the levels of self-generation, which directly affect the retailer's load-risk exposure. Trading strategies are instead unaffected by the considered retail tariff schemes, and the presence or not of indexation to the day-ahead prices. However, such indexation is relevant when investigating the retailer revenue-risk exposure and their risk-management problem.

While the ECDFs in Fig.13 and Fig.14 unveil the adverse impact of increasing self-generation on the contribution margin of the retailer, they also point to the role of differently designed retail tariff schemes as hedging instrument for retailers exposed to increasing revenue-risk. While self-generation significantly reduces the expected contribution margin of the retailer, dynamic retail tariffs, with energy rates partially or fully indexed to the spot (day-ahead in this study) prices, may offset this reduction and potentially increase the expected margin of the retailer. The efficient frontiers in Fig.17, which are defined by the highest (i.e. non-dominated) expected contribution margins for 95%-CVaR for different risk attitudes, open the possibility for dynamic tariffs to allow a transfer of the load-risk from the retailer to the consumers thus preserving the expected contribution margin of the retailer. This is mostly evident for a risk-averse retailer by noticing that both

their expected contribution margin and 95%-CVaR remain unchanged for increasing levels of self-generation with a dynamic tariff fully indexed to the day-ahead price, while in the case a risk-neutral retailer this tariff contributes to maintain the expected contribution margin unchanged against an increase of the 95%-CVaR. With a 0%-indexed tariff and for increasing levels of self-generation, we observe both an increase in the 95%-CVaR and a reduction of the expected contribution margin of the risk-neutral retailer, thus implying a significant increase of their revenue-risk exposure with self-generation compared to a risk-averse retailer.

# 7 Conclusions and Outlook

This paper investigates the risk management problem faced by electricity retailers in day-ahead and intraday markets following the uncertainty driven by increasing levels of solar PV self-generation in the residential sector. Compared to previous studies, we jointly model the solar generation, load and price stochasticities in the nested day-ahead and intraday markets, thus capturing the inherently correlated price and quantity uncertainties. We consider these uncertainties to assess the retailers' trading problem in a two-stage stochastic optimization model, which thus accounts for the risks rising from both uncertain prices and quantities. We mark a contribution in considering the retailers' multi-stage trading optimization and decision-making in the day-ahead and intraday market while explicitly incorporating solar generation, load and price risks. These move stochastically in path-dependent and correlated processes, such that the risk optimization is effectively carried out along the considered short-term trading horizon. Therefore, the approach in this study allows to draw valuable insights on the risk exposure and optimization of retailers procurement strategy with increasing levels of solar PV self-generation.

In all, the results of the risk optimization unveil greater load-risk exposure for retailers in the day-ahead market with higher levels of self-generation, as implied by an increase of the buying positions in this market. The results also indicate a growth of the price-risk exposure in the intraday market, where an increase of selling positions is observed for lower and more volatile intraday

prices. These dynamics become even more evident when considering a risk-averse rather than a risk-neutral retailer, thus highlighting the importance of risk preferences when evaluating retailers' optimal trading strategies. Our findings imply a reduction of the retailer's expected contribution margin of 10% on a typical summer working day when assuming a increase of self-generation in the residential sector from 10% to 50%. Yet, findings also imply that this reduction can be offset when assuming more dynamic and spot-indexed retail tariffs, which allow a risk-averse retailer to transfer load and price risks to the consumers. While this outcome may rely on the assumed inelasticity of the households' electricity demand to wholesale spot prices, thus representing a limitation of this study, nonetheless our findings are of particular interest for practitioners, policymakers and regulators. First, they highlight the role of intraday trading to cope with the increasing short-term uncertainty driven by the penetration of distributed (variable) generation and consumers' engagement. Therefore, our findings contribute towards a better understanding of the importance of well-functioning and liquid intraday markets for the profitability and risk-mitigation costs of retailers. Second, in emphasizing the importance of intraday trading adjustment for retailers, findings in this study also point to the need for different hedging approaches to mitigate the greater risk-exposure implicit in more prosumer-oriented electricity markets. In particular, our results unveil the potential for electricity tariffs, which are indexed to the spot price, to induce retailer-consumer/prosumer risk sharing. Whereas this outcome relies on the German market considered in this study, and does not account for price (in)elasticities in retail markets and/or for the efficiency and costs of such spot-indexed tariffs, it represents a contribution in a still under-researched question concerning the optimal design of the retailer-prosumer relationship. This questions is relevant for practitioners, policymakers and regulators and further research is needed for considerations of risk exposure and sharing in evolving electricity markets.

# References


Abbaspourtorbati, F., Conejo, A. J., Wang, J., and Cherkaoui, R. (2016). Three-or two-stage stochastic market-clearing algorithm? *IEEE Transactions on Power Systems*, 32(4):3099–3110.

Aïd, R., Chemla, G., Porchet, A., and Touzi, N. (2011). Hedging and vertical integration in electricity markets. *Management Science*, 57(8): 1438–1452.

Alexander, C. (2008). *Value-at-risk models*. John Wiley & Sons.

Bacher, P., Madsen, H., and Nielsen, H. A. (2009). Online short-term solar power forecasting. *Solar energy*, 83(10):1772–1783.

Ballester, C. and Furió, D. (2015). Effects of renewables on the stylized facts of electricity prices. *Renewable and Sustainable Energy Reviews*, 52:1596–1609.

Batlle, C. (2013). *Electricity Retailing*. In: I. J. Pérez-Arriaga (ed.), Regulation of the Power Sector, Power Systems, Springer-Verlag London 2013, p. 443-499.

BDEW (2021). Standardlastprofile strom (standard load profile electricity).

Ben-Tal, A., El Ghaoui, L., and Nemirovski, A. (2009). *Robust optimization*. Princeton university press.

Benth, F. E. and Ibrahim, N. A. (2017). Stochastic modeling of photovoltaic power generation and electricity prices. *Journal of Energy Markets*, 10(3): 1–33.

Bertsimas, D., Brown, D. B., and Caramanis, C. (2011). Theory and applications of robust optimization. *SIAM review*, 53(3):464–501.

Boffino, L., Conejo, A. J., Sioshansi, R., and Oggioni, G. (2019). A two-stage stochastic optimization planning framework to decarbonize deeply electric power systems. *Energy Economics*, 84:104457.

Boroumand, R.-H., Goutte, S., Guesmi, K., and Porcher, T. (2019). Potential benefits of optimal intra-day electricity hedging for the environment: The perspective of electricity retailers. *Energy Policy*, 132:1120–1129.

Boroumand, R. H., Goutte, S., Porcher, S., and Porcher, T. (2015). Hedging strategies in energy markets: The case of electricity retailers. *Energy Economics*, 51: 503–509.

Boroumand, R. H. and Zachmann, G. (2012). Retailers' risk management and vertical arrangements in electricity markets. *Energy Policy*, 40: 465–472.

Bundesministerium für Wirtschaft und Energie (2021). Gesetz für den ausbau erneuerbarer energien. `http://www.bgbl.de/xaver/bgbl/start.xav?startbk=Bundesanzeiger_BGBl&jumpTo=bgbl120s3138.pdf`.

Bunn, D. W., Gianfreda, A., and Kermer, S. (2018). A trading-based evaluation of density forecasts in a real-time electricity market. *Energies*, 11(10):2658.

Burger, M., Klar, B., Müller, A., and Schindlmayr, G. (2004). A spot market model for pricing derivatives in electricity markets. *Quantitative Finance*, 4(1): 109–122.

Christensen, T., Hurn, S., and Lindsay, K. (2009). It never rains but it pours: modeling the persistence of spikes in electricity prices. *The Energy Journal*, 30(1).

Conejo, A. J., Carrión, M., Morales, J. M., et al. (2010). *Decision making under uncertainty in electricity markets*, volume 1. Springer.

Coulon, M., Powell, W. B., and Sircar, R. (2013). A model for hedging load and price risk in the Texas electricity market. *Energy Economics*, 40: 976–988.

Cretì, A. and Fontini, F. (2019). *Economics of electricity: Markets, competition and rules*. Cambridge University Press.

Dadashi, M., Haghifam, S., Zare, K., Haghifam, M.-R., and Abapour, M. (2020). Short-term scheduling of electricity retailers in the presence of demand response aggregators: A two-stage stochastic bi-level programming approach. *Energy*, 205:117926.

Dagoumas, A. S., Koltsaklis, N. E., and Panapakidis, I. P. (2017). An integrated model for risk management in electricity trade. *Energy*, 124: 350–363.

de Lagarde, C. M. and Lantz, F. (2018). How renewable production depresses electricity prices: Evidence from the german market. *Energy Policy*, 117:263–277.

Deng, S.-J. and Oren, S. S. (2006). Electricity derivatives and risk management. *Energy*, 31(6-7): 940–953.

Deng, T., Yan, W., Nojavan, S., and Jermsittiparsert, K. (2020). Risk evaluation and retail electricity pricing using downside risk constraints method. *Energy*, 192:116672.

Di Cosmo, V. and Malaguzzi Valeri, L. (2018). Wind, storage, interconnection and the cost of electricity generation. *Energy Economics*, 69: 1–18.

Ela, E., Milligan, M., Bloom, A., Cochran, J., Botterud, A., Townsend, A., and Levin, T. (2018). Overview of wholesale electricity markets. In *Electricity Markets with Increasing Levels of Renewable Generation: Structure, Operation, Agent-based Simulation, and Emerging Designs*, pages 3–21. Springer.

Fett, D., Fraunholz, C., and Keles, D. (2021). Diffusion and system impact of residential battery storage under different regulatory settings.

Fleten, S.-E. and Kristoffersen, T. K. (2007). Stochastic programming for optimizing bidding strategies of a nordic hydropower producer. *European Journal of Operational Research*, 181(2):916–928.

Garnier, E. and Madlener, R. (2015). Balancing forecast errors in continuous-trade intraday markets. *Energy Systems*, 6(3):361–388.

Gelabert, L., Labandeira, X., and Linares, P. (2011). An ex-post analysis of the effect of renewables and cogeneration on Spanish electricity prices. *Energy Economics*, 33: S59–S65.

Gianfreda, A., Ravazzolo, F., and Rossini, L. (2020). Comparing the forecasting performances of linear models for electricity prices with high res penetration. *International Journal of Forecasting*, 36(3):974–986.

Goodarzi, S., Perera, H. N., and Bunn, D. (2019). The impact of renewable energy forecast errors on imbalance volumes and electricity spot prices. *Energy Policy*, 134:110827.

Green, R., Staffell, I., and Vasilakos, N. (2014). Divide and conquer? $\boldsymbol{k}$-means clustering of demand data allows rapid and accurate simulations of the british electricity system. *IEEE Transactions on Engineering Management*, 61(2):251–260.

Gröwe-Kuska, N., Kiwiel, K., Nowak, M., Römisch, W., and Wegner, I. (2000). Power management under uncertainty by lagrangian relaxation. In *Proceedings of the 6th International Conference Probabilistic Methods Applied to Power Systems PMAPS*, volume 2.

Hain, M., Schermeyer, H., Uhrig-Homburg, M., and Fichtner, W. (2018). Managing renewable energy production risk. *Journal of banking & finance*, 97:1–19.

Hayn, M., Zander, A., Fichtner, W., Nickel, S., and Bertsch, V. (2018). The impact of electricity tariffs on residential demand side flexibility: results of bottom-up load profile modeling. *Energy Systems*, 9(3):759–792.

Heitsch, H. and Römisch, W. (2009). Scenario tree modeling for multistage stochastic programs. *Mathematical Programming*, 118(2):371–406.

IRENA (2019). Future of Solar Photovoltaic. International Renewable Energy Agency. November 2019.

Jain, A. K. (2010). Data clustering: 50 years beyond k-means. *Pattern recognition letters*, 31(8):651–666.

Janczura, J., Trück, S., Weron, R., and Wolff, R. (2013). Identifying spikes and seasonal components in electricity spot price data: A guide to robust modeling. *Energy Economics*, 38:96–110.

Karanfil, F. and Li, Y. (2017). The role of continuous intraday electricity markets: The integration of large-share wind power generation in Denmark. *The Energy Journal*, 38(2): 107–130.

Kath, C. and Ziel, F. (2018). The value of forecasts: Quantifying the economic gains of accurate quarter-hourly electricity price forecasts. *Energy Economics*, 76:411–423.

Keles, D., Genoese, M., Möst, D., and Fichtner, W. (2012). Comparison of extended mean-reversion and time series models for electricity spot price simulation considering negative prices. *Energy Economics*, 34(4): 1012–1032.

Keles, D., Genoese, M., Möst, D., Ortlieb, S., and Fichtner, W. (2013). A combined modeling approach for wind power feed-in and electricity spot prices. *Energy Policy*, 59: 213–225.

Kettunen, J., Salo, A., and Bunn, D. W. (2010). Optimization of electricity retailer's contract portfolio subject to risk preferences. *IEEE Transactions on Power Systems*, 25(1): 117–128.

Kiesel, R. and Paraschiv, F. (2017). Econometric analysis of 15-minute intraday electricity prices. *Energy Economics*, 64: 77–90.

Koolen, D., Bunn, D., and Ketter, W. (2021). Renewable energy technologies and electricity forward market risks. *The Energy Journal*, 42(4).

Kraft, E., Russo, M., Keles, D., and Bertsch, V. (2021). Stochastic optimization of trading strategies in sequential electrcity markets.

Kremer, M., Kiesel, R., and Paraschiv, F. (2020). An econometric model for intraday electricity trading. *Philosophical Transactions of the Royal Society A, Forthcoming*, page Available at `https://doi.org/10.2139/ssrn.3489214`.

Kulakov, S. and Ziel, F. (2019). The impact of renewable energy forecasts on intraday electricity prices. *Available at* `https://arxiv.org/pdf/1903.09641.pdf`.

Lahmiri, S. (2015). Comparing variational and empirical mode decomposition in forecasting day-ahead energy prices. *IEEE Systems Journal*, 11(3):1907–1910.

Laur, A., Nieto-Martin, J., Bunn, D. W., and Vicente-Pastor, A. (2018). Optimal procurement of flexibility services within electricity distribution networks. *European Journal of Operational Research*.

Laur, A., Nieto-Martin, J., Bunn, D. W., and Vicente-Pastor, A. (2020). Optimal procurement of flexibility services within electricity distribution networks. *European Journal of Operational Research*, 285(1):34–47.

Li, W. and Paraschiv, F. (2021). Modelling the evolution of wind and solar power infeed forecasts. *Journal of Commodity Markets*, page 100189.

Likas, A., Vlassis, N., and Verbeek, J. J. (2003). The global k-means clustering algorithm. *Pattern recognition*, 36(2):451–461.

Lingohr, D. and Müller, G. (2019). Stochastic modeling of intraday photovoltaic power generation. *Energy Economics*, 81: 175–186.

Maciejowska, K., Nitka, W., and Weron, T. (2019). Day-ahead vs. intraday—forecasting the price spread to maximize economic benefits. *Energies*, 12(4):631.

MacQueen, J. et al. (1967). Some methods for classification and analysis of multivariate observations. In *Proceedings of the fifth Berkeley symposium on mathematical statistics and probability*, volume 1, pages 281–297. Oakland, CA, USA.

Messner, J. W., Pinson, P., Browell, J., Bjerregård, M. B., and Schicker, I. (2020). Evaluation of wind power forecasts—an up-to-date view. *Wind Energy*, 23(6):1461–1481.

Meucci, A. (2009). Review of statistical arbitrage, cointegration, and multivariate ornstein-uhlenbeck. *Cointegration, and Multivariate Ornstein-Uhlenbeck (May 14, 2009)*.

Mohan, V., Singh, J. G., and Ongsakul, W. (2015). An efficient two stage stochastic optimal energy and reserve management in a microgrid. *Applied energy*, 160:28–38.

Morales, J. M., Zugno, M., Pineda, S., and Pinson, P. (2014). Electricity market clearing with improved scheduling of stochastic production. *European Journal of Operational Research*, 235(3):765–774.

Narajewski, M. and Ziel, F. (2020a). Econometric modelling and forecasting of intraday electricity prices. *Journal of Commodity Markets*, 19:100107.

Narajewski, M. and Ziel, F. (2020b). Ensemble forecasting for intraday electricity prices: Simulating trajectories. *Applied Energy*, 279:115801.

Nazari-Heris, M. and Mohammadi-Ivatloo, B. (2018). Application of robust optimization method to power system problems. *Classical and recent aspects of power system optimization*, pages 19–32.

Newbery, D., Pollitt, M., Ritz, R., and Strielkowski, W. (2018). Market design for a high-renewables European electricity system. *Renewable and Sustainable Energy Reviews*, 91: 695–707.

Nojavan, S., Nourollahi, R., Pashaei-Didani, H., and Zare, K. (2019). Uncertainty-based electricity procurement by retailer using robust optimization approach in the presence of demand response exchange. *International Journal of Electrical Power & Energy Systems*, 105:237–248.

Nojavan, S., Zare, K., and Mohammadi-Ivatloo, B. (2017). Robust bidding and offering strategies of electricity retailer under multi-tariff pricing. *Energy Economics*, 68:359–372.

Osório, G., Lujano-Rojas, J., Matias, J., and Catalão, J. (2015). A new scenario generation-based method to solve the unit commitment problem with high penetration of renewable energies. *International Journal of Electrical Power & Energy Systems*, 64:1063–1072.

Ottesen, S. Ø., Tomasgard, A., and Fleten, S.-E. (2018). Multi market bidding strategies for demand side flexibility aggregators in electricity markets. *Energy*, 149:120–134.

Parisio, A., Del Vecchio, C., and Vaccaro, A. (2012). A robust optimization approach to energy hub management. *International Journal of Electrical Power & Energy Systems*, 42(1):98–104.

Rintamäki, T., Siddiqui, A. S., and Salo, A. (2017). Does renewable energy generation decrease the volatility of electricity prices? an analysis of denmark and germany. *Energy Economics*, 62:270–282.

Ruppert, M., Hayn, M., Bertsch, V., and Fichtner, W. (2016). Impact of residential electricity tariffs with variable energy prices on low voltage grids with photovoltaic generation. *International Journal of Electrical Power & Energy Systems*, 79: 161–171.

Russo, M. and Bertsch, V. (2020). A looming revolution: Implications of self-generation for the risk exposure of retailers. *Energy Economics*, 92:104970.

Ruszczyński, A. and Shapiro, A. (2003). Stochastic programming models. *Handbooks in operations research and management science*, 10:1–64.

Schermeyer, H., Vergara, C., and Fichtner, W. (2018). Renewable energy curtailment: A case study on today's and tomorrow's congestion management. *Energy Policy*, 112: 427–436.

Steinert, R. and Ziel, F. (2019). Short-to mid-term day-ahead electricity price forecasting using futures. *The Energy Journal*, 40(1).

Uniejewski, B., Marcjasz, G., and Weron, R. (2019). Understanding intraday electricity markets: Variable selection and very short-term price forecasting using lasso. *International Journal of Forecasting*, 35(4):1533–1547.

Van Der Weijde, A. H. and Hobbs, B. F. (2012). The economics of planning electricity transmission to accommodate renewables: Using two-stage optimisation to evaluate flexibility and the cost of disregarding uncertainty. *Energy Economics*, 34(6):2089–2101.

Wallace, S. W. and Fleten, S.-E. (2003). Stochastic programming models in energy. *Handbooks in operations research and management science*, 10:637–677.

Weron, R. (2007). *Modeling and forecasting electricity loads and prices: A statistical approach*. Wiley Finance Series, John Wiley & Sons Ltd.

Willems, B. and Morbee, J. (2010). Market completeness: How options affect hedging and investments in the electricity sector. *Energy Economics*, 32(4): 786–795.

Wozabal, D. and Rameseder, G. (2020). Optimal bidding of a virtual power plant on the spanish day-ahead and intraday market for electricity. *European Journal of Operational Research*, 280(2):639–655.

Yang, J., Zhao, J., Luo, F., Wen, F., and Dong, Z. Y. (2017). Decision-making for electricity retailers: A brief survey. *IEEE Transactions on Smart Grid*, 9(5):4140–4153.

Zellner, A. and Theil, H. (1992). Three-stage least squares: simultaneous estimation of simultaneous equations. In *Henri Theil's Contributions to Economics and Econometrics*, pages 147–178. Springer.

Zhang, H., Hu, X., Cheng, H., Zhang, S., Hong, S., and Gu, Q. (2021). Coordinated scheduling of generators and tie lines in multi-area power systems under wind energy uncertainty. *Energy*, 222:119929.

Zugno, M. and Conejo, A. J. (2015). A robust optimization approach to energy and reserve dispatch in electricity markets. *European Journal of Operational Research*, 247(2):659–671.

# A Appendixes

## A.1 Parameter estimates for the deterministic component of the day-ahead series

Table 9: Summer season

| Summer | Cloudiness$^{DA}$ | | Residual load$^{DA}$ | | Price$^{DA}$ | |
|---|---|---|---|---|---|---|
| | Coeff. | Std.err. | Coeff. | Std.err. | Coeff. | Std.err. |
| Intercept | | | -0.623*** | 0.178 | | |
| Cloudiness$^{DA}_{t-1}$ | 0.160*** | 0.013 | | | | |
| Cloudiness$^{DA}_{t-24}$ | 0.601*** | 0.020 | | | | |
| Cloudiness$^{DA}_{t}$ | | | 0.107*** | 0.027 | | |
| (Cloudiness$^{DA}_{t}$)$^{2}$ | | | 0.114*** | 0.037 | | |
| (Cloudiness$^{DA}_{t}$)$^{3}$ | | | 0.021* | 0.012 | | |
| Residual load$^{DA}_{t}$ | | | | | 0.161*** | 0.007 |
| Residual load$^{DA}_{t-1}$ | | | 0.882*** | 0.009 | -0.138*** | 0.008 |
| Price$^{DA}_{t-1}$ | | | | | 1.009*** | 0.023 |
| Price$^{DA}_{t-2}$ | | | | | -0.189*** | 0.019 |
| Daily cycle$^{DA}$ | 0.255*** | 0.024 | 0.179*** | 0.018 | 0.132*** | 0.010 |
| Weekends | | | | | -0.002* | 0.001 |
| Daily cycle$^{DA}\times$ Weekends | | | -0.005*** | 0.001 | | |
| Adjusted R-squared | 0.873 | | 0.945 | | 0.942 | |
| S.E. of regression | 0.184 | | 0.067 | | 0.014 | |
| Durbin-Watson stat | 0.877 | | 0.407 | | 1.774 | |
| Mean dependent var | -0.405 | | 10.47 | | 5.041 | |
| S.D. dependent var | 0.517 | | 0.288 | | 0.059 | |
| Sum squared resid | 49.52 | | 6.628 | | 0.292 | |

Table 10: Transition season

| Transition season | Cloudiness$^{DA}$ | | Residual load$^{DA}$ | | Price$^{DA}$ | |
|---|---|---|---|---|---|---|
| | Coeff. | Std.err. | Coeff. | Std.err. | Coeff. | Std.err. |
| Intercept | | | | | 0.354*** | 0.049 |
| Cloudiness$^{DA}_{t-1}$ | 0.147*** | 0.009 | | | | |
| Cloudiness$^{DA}_{t-24}$ | 0.778*** | 0.013 | | | | |
| Cloudiness$^{DA}_{t}$ | | | 0.218*** | 0.019 | | |
| (Cloudiness$^{DA}_{t}$)$^2$ | | | 0.125*** | 0.009 | | |
| (Cloudiness$^{DA}_{t}$)$^3$ | | | | | | |
| Residual load$^{DA}_{t}$ | | | | | 0.197*** | 0.007 |
| Residual load$^{DA}_{t-1}$ | | | 0.935*** | 0.013 | -0.154*** | 0.008 |
| Price$^{DA}_{t-1}$ | | | | | 0.874*** | 0.019 |
| Price$^{DA}_{t-2}$ | | | | | -0.149*** | 0.019 |
| Daily cycle$^{DA}$ | 0.085*** | 0.014 | 0.013*** | 0.013 | 0.115*** | 0.010 |
| Weekends | | | | | -0.003** | 0.001 |
| Daily cycle$^{DA}\times$ Weekends | | | -0.002* | 0.001 | | |
| Adjusted R-squared | 0.871 | | 0.760 | | 0.952 | |
| S.E. of regression | 0.288 | | 0.175 | | 0.016 | |
| Durbin-Watson stat | 1.036 | | 1.623 | | 1.982 | |
| Mean dependent var | -0.514 | | 10.46 | | 5.037 | |
| S.D. dependent var | 0.800 | | 0.357 | | 0.073 | |
| Sum squared resid | 178.4 | | 65.76 | | 0.559 | |

Table 11: Winter season

| Winter | Cloudiness$^{DA}$ | | Residual load$^{DA}$ | | Price$^{DA}$ | |
|---|---|---|---|---|---|---|
| | Coeff. | Std.err. | Coeff. | Std.err. | Coeff. | Std.err. |
| Intercept | | | -0.580*** | 0.131 | 0.399205*** | 0.058 |
| Cloudiness$^{DA}_{t-1}$ | 0.100*** | 0.010 | | | | |
| Cloudiness$^{DA}_{t-24}$ | 0.759*** | 0.014 | | | | |
| Cloudiness$^{DA}_{t}$ | | | 0.268*** | 0.027 | | |
| (Cloudiness$^{DA}_{t}$)$^2$ | | | 0.1501*** | 0.015 | | |
| (Cloudiness$^{DA}_{t}$)$^3$ | | | | | | |
| Residual load$^{DA}_{t}$ | | | | | 0.176*** | 0.007 |
| Residual load$^{DA}_{t-1}$ | | | 0.938*** | 0.007 | -0.144*** | 0.007 |
| Price$^{DA}_{t-1}$ | | | | | 0.875*** | 0.021 |
| Price$^{DA}_{t-2}$ | | | | | -0.071*** | 0.020 |
| Daily cycle$^{DA}$ | 0.147*** | 0.017 | 0.118*** | 0.014 | 0.049*** | 0.010 |
| Weekends | | | | | | |
| Daily cycle$^{DA}\times$ Weekends | | | -0.005*** | 0.001 | -0.001*** | 0.000 |
| Adjusted R-squared | 0.899 | | 0.932 | | 0.958 | |
| S.E. of regression | 0.261 | | 0.135 | | 0.022 | |
| Durbin-Watson stat | 0.807 | | 0.739 | | 1.993 | |
| Mean dependent var | -0.538 | | 10.27 | | 4.979 | |
| S.D. dependent var | 0.819 | | 0.520 | | 0.106 | |
| Sum squared resid | 146.4 | | 39.49 | | 1.017 | |

## A.2 Parameter estimates for the deterministic component of the intraday Series

Table 12: Cloudiness and residual load: Summer season

| Summer | Cloudiness$^{ID}$ | | Residual load$^{ID}$ | |
|---|---|---|---|---|
| | Coeff. | Std.error | Coeff. | Std.error |
| Intercept | | | | |
| Cloudiness$_t^{DA}$ | 0.987*** | 0.002 | | |
| Cloudiness$_{t-1}^{ID}$ | 0.021*** | 0.002 | | |
| Cloudiness$_t^{ID}$ | | | 0.002*** | 0.0003 |
| Residual load$_t^{DA}$ | | | 0.181*** | 0.005 |
| Residual load$_{t-1}^{ID}$ | | | 1.188*** | 0.014 |
| Residual load$_{t-2}^{ID}$ | | | -0.096*** | 0.020 |
| Residual load$_{t-3}^{ID}$ | | | -0.194*** | 0.020 |
| Residual load$_{t-4}^{ID}$ | | | -0.089*** | 0.012 |
| Daily cycle$^{ID}$ | -0.001* | 0.001 | 0.010*** | 0.001 |
| Weekends | | | 0.172*** | 0.022 |
| Daily cycle$^{ID}\times$ Weekends | | | -0.017*** | 0.002 |
| Adjusted R-squared | 0.997 | | 0.999 | |
| S.E. of regression | 0.031 | | 0.010 | |
| Durbin-Watson stat | 0.166 | | 1.690 | |
| Mean dependent var | -0.398 | | 10.47 | |
| S.D. dependent var | 0.521 | | 0.284 | |
| Sum squared resid | 5.644 | | 0.635 | |

Table 13: Cloudiness and residual load: Transition season

| Transition season | Cloudiness$^{ID}$ | | Residual load$^{ID}$ | |
|---|---|---|---|---|
| | Coeff. | Std.error | Coeff. | Std.error |
| Intercept | | | | |
| Cloudiness$_t^{DA}$ | 0.996*** | 0.001 | | |
| Cloudiness$_{t-1}^{ID}$ | 0.021*** | 0.001 | | |
| Cloudiness$_t^{ID}$ | | | 0.001*** | 0.0002 |
| Residual load$_t^{DA}$ | | | 0.132*** | 0.004 |
| Residual load$_{t-1}^{ID}$ | | | 1.333*** | 0.011 |
| Residual load$_{t-2}^{ID}$ | | | -0.236*** | 0.018 |
| Residual load$_{t-3}^{ID}$ | | | -0.133*** | 0.018 |
| Residual load$_{t-4}^{ID}$ | | | -0.095*** | 0.010 |
| Daily cycle$^{ID}$ | -0.001* | 0.0004 | -0.001** | 0.0005 |
| Weekends | | | 0.110*** | 0.018 |
| Daily cycle$^{ID}\times$ Weekends | | | -0.011*** | 0.002 |
| Adjusted R-squared | 0.997 | | 0.999 | |
| S.E. of regression | 0.043 | | 0.012 | |
| Durbin-Watson stat | 0.605 | | 1.799 | |
| Mean dependent var | -0.524 | | 10.45 | |
| S.D. dependent var | 0.857 | | 0.365 | |
| Sum squared resid | 16.20 | | 1.336 | |

Table 14: Cloudiness and residual load: Winter season

| Winter | Cloudiness$^{ID}$ | | Residual load$^{ID}$ | |
|---|---|---|---|---|
| | Coeff. | Std.error | Coeff. | Std.error |
| Intercept | | | | |
| Cloudiness$_t^{DA}$ | 0.984*** | 0.001 | | |
| Cloudiness$_{t-1}^{ID}$ | 0.010*** | 0.002 | | |
| Cloudiness$_t^{ID}$ | | | | |
| Residual load$_t^{DA}$ | | | 0.148*** | 0.004 |
| Residual load$_{t-1}^{ID}$ | | | 1.059*** | 0.006 |
| Residual load$_{t-2}^{ID}$ | | | | |
| Residual load$_{t-3}^{ID}$ | | | -0.134*** | 0.013 |
| Residual load$_{t-4}^{ID}$ | | | -0.084*** | 0.010 |
| Daily cycle$^{ID}$ | -0.005*** | 0.001 | 0.010*** | 0.001 |
| Weekends | | | 0.120*** | 0.020 |
| Daily cycle$^{ID}\times$ Weekends | | | -0.012*** | 0.002 |
| Adjusted R-squared | 0.996 | | 0.998 | |
| S.E. of regression | 0.050 | | 0.023 | |
| Durbin-Watson stat | 0.240 | | 1.578 | |
| Mean dependent var | -0.538 | | 10.28 | |
| S.D. dependent var | 0.837 | | 0.504 | |
| Sum squared resid | 22.18 | | 4.586 | |

Table 15: $\boldsymbol{\Delta}$ price (ID3-DA)

| | Summer | | Transition season | | Winter | |
|---|---|---|---|---|---|---|
| | Coeff. | Std.error | Coeff. | Std.error | Coeff. | Std.error |
| Intercept | -0.793*** | 0.060 | 0.518*** | 0.089 | -0.692*** | 0.091 |
| $\boldsymbol{\Delta}$ Price$_{t-1}$ | -0.700*** | 0.039 | 0.551*** | 0.017 | 0.495*** | 0.039 |
| $\boldsymbol{\Delta}$ Price$_{t-2}$ | 0.0223** | 0.010 | 0.037*** | 0.012 | | |
| $\boldsymbol{\Delta}$ Price$_{t-3}$ | 0.030*** | 0.010 | 0.020* | 0.012 | | |
| $\boldsymbol{\Delta}$ Price$_{t-4}$ | 0.371*** | 0.011 | 0.285*** | 0.016 | 0.450*** | 0.035 |
| Price$_t^{DA}$ | -1.22*** | 0.042 | | | | |
| Price$_{t-1}^{ID3}$ | 1.063*** | 0.043 | -0.102*** | 0.014 | -0.306*** | 0.041 |
| $\boldsymbol{\Delta}$ Residual load$_{t-3}(\boldsymbol{Act.-ID})$ | 0.037*** | 0.009 | -0.205*** | 0.054 | 0.128*** | 0.030 |
| $\boldsymbol{\Delta}$ Cloudiness$_{t-3}(\boldsymbol{Act.-ID})$ | 0.002** | 0.001 | 0.002** | 0.001 | | |
| Daily cycle | 0.317*** | 0.014 | -0.09*** | 0.018 | 0.259*** | 0.018 |
| Weekends | 0.222** | 0.111 | -0.230* | 0.152 | 0.421*** | 0.155 |
| Daily cycle x weekends | -0.046** | 0.022 | 0.045* | 0.030 | -0.085*** | 0.031 |
| Adjusted R-squared | 0.603 | | 0.745 | | 0.584 | |
| S.E. of regression | 0.032 | | 0.057 | | 0.052 | |
| Durbin-Watson stat | 1.639 | | 1.831 | | 1.643 | |
| Mean dependent var | -0.001 | | -0.009 | | 0.003 | |
| S.D. dependent var | 0.051 | | 0.112 | | 0.081 | |
| Sum squared resid | 6.075 | | 27.87 | | 23.96 | |

## A.3 Scenario trees

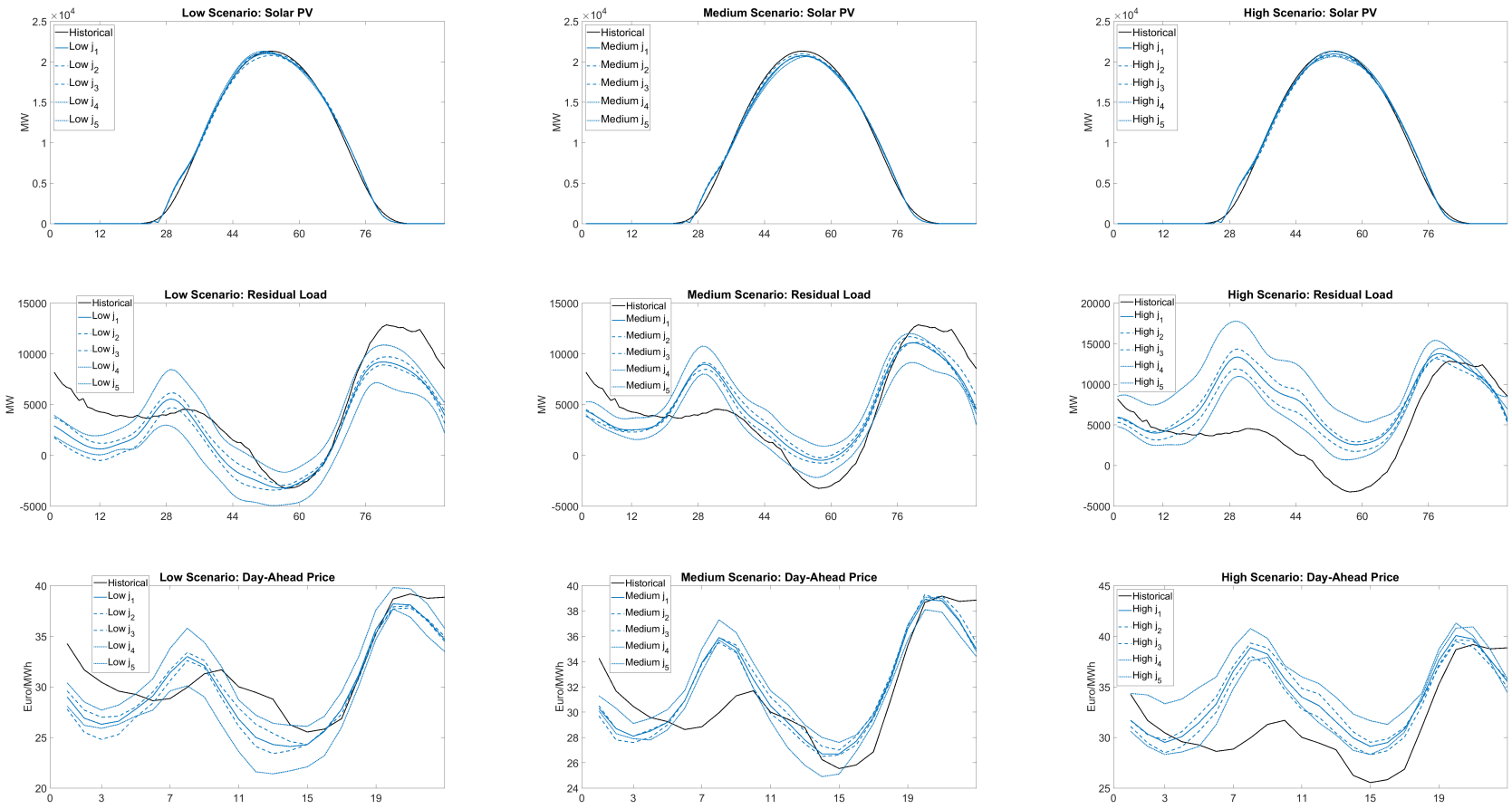


Figure 18: Historical and simulated day-ahead series: Summer weekend day

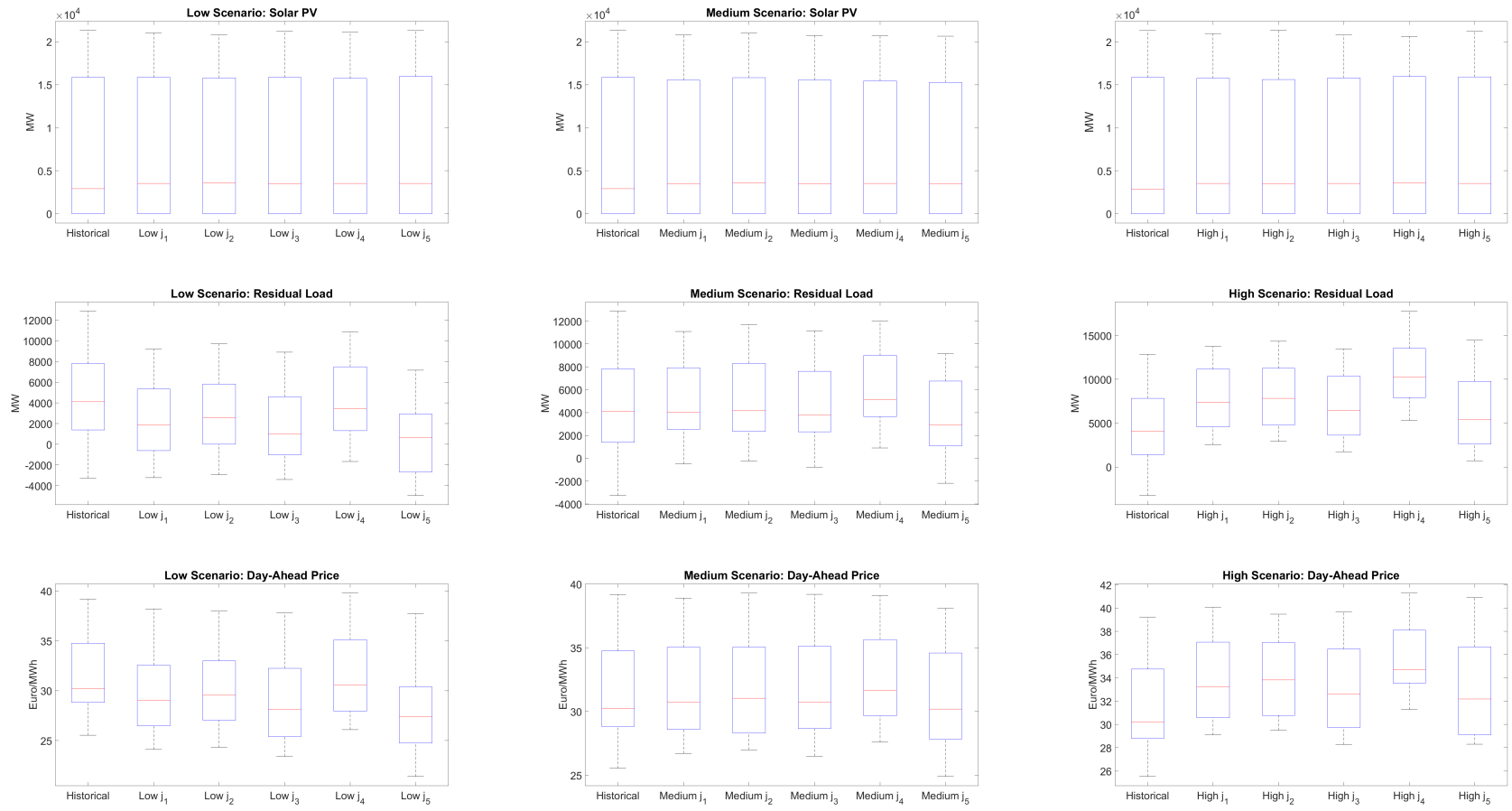


Figure 19: Distribution of the historical and simulated day-ahead series: Summer weekend day

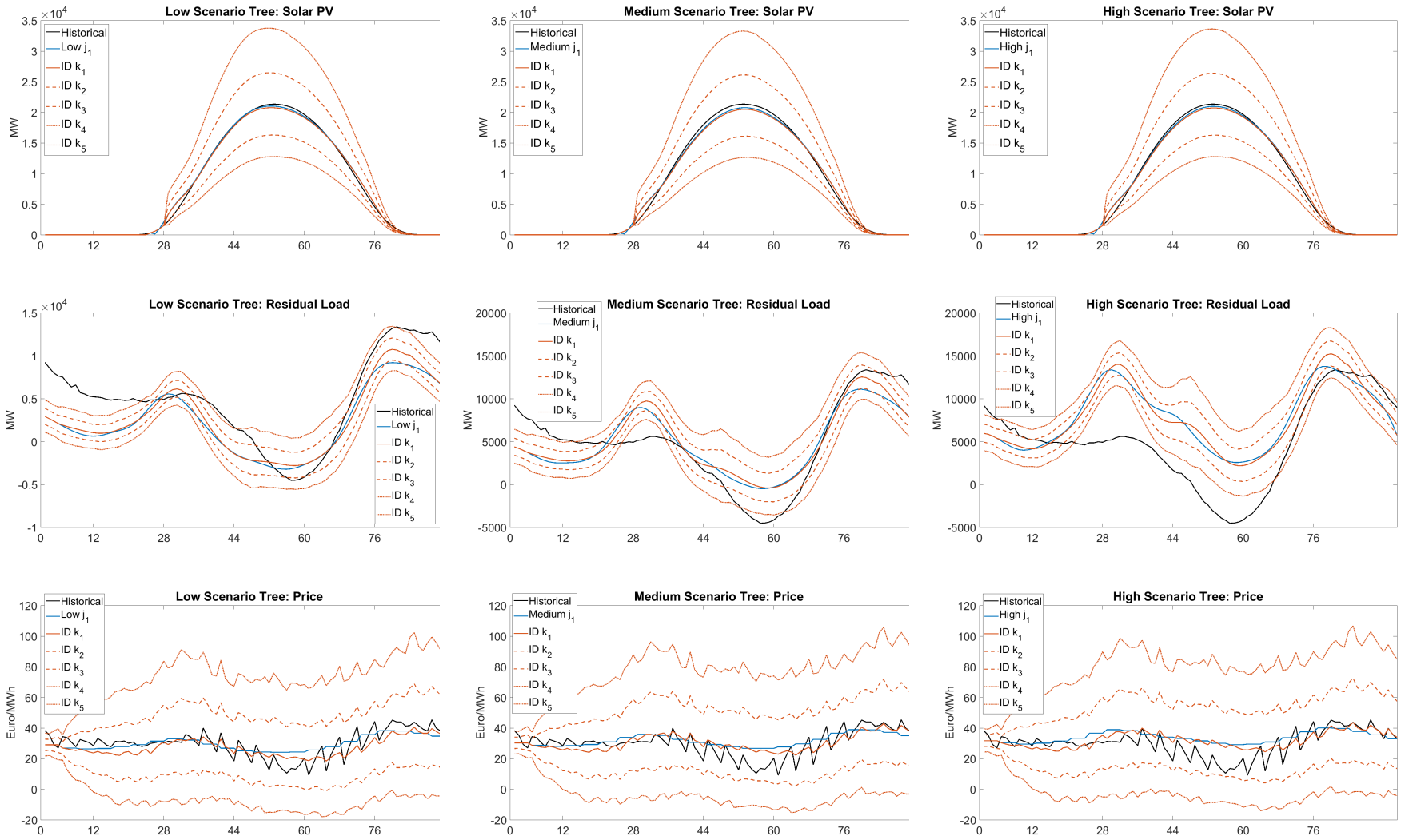


Figure 20: Scenario trees for the representative day-ahead node $\boldsymbol{j_1}$ and its intraday realizations $\boldsymbol{k}$: Summer weekend day

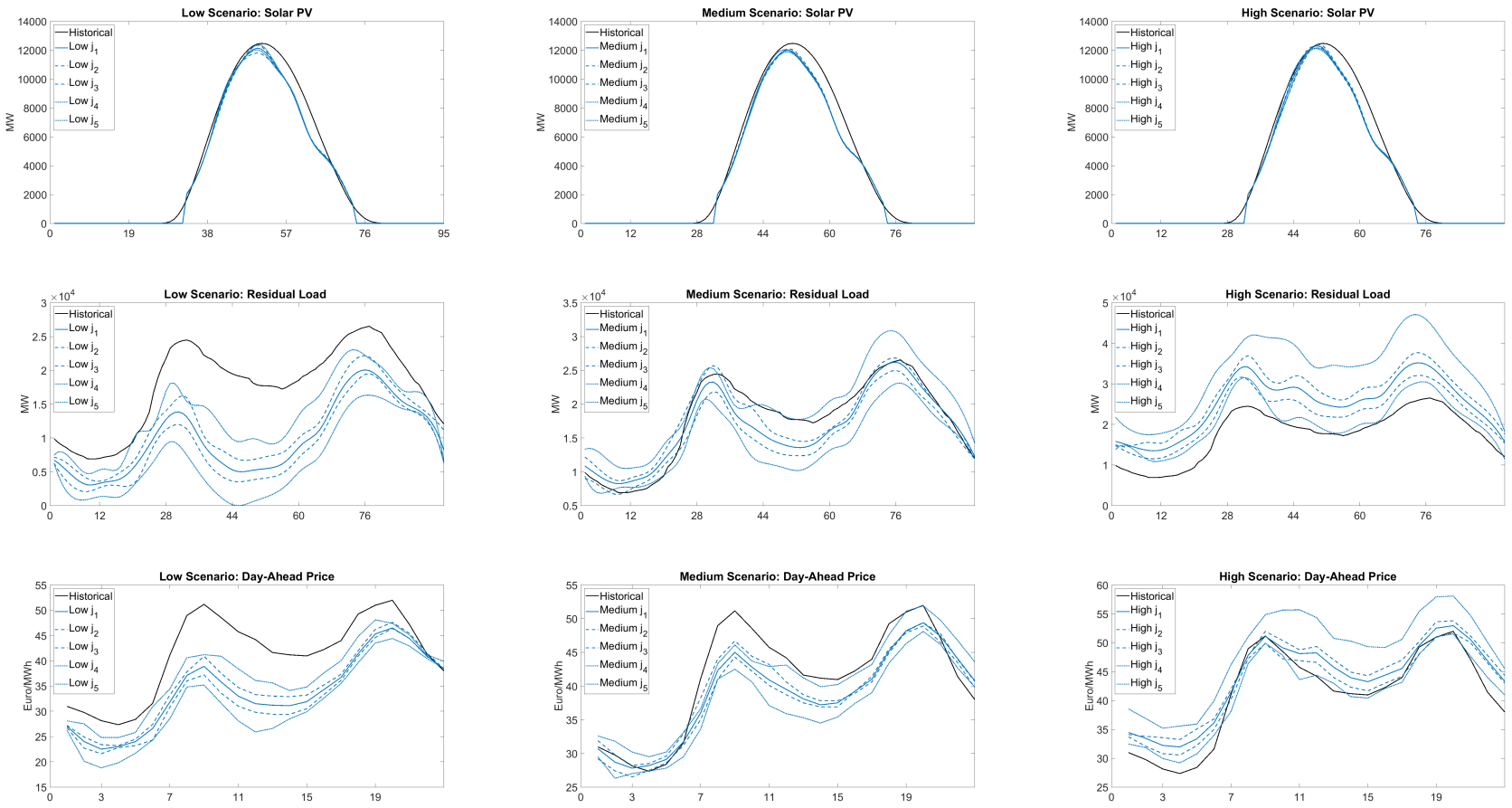


Figure 21: Historical and simulated day-ahead series: Transition season working day

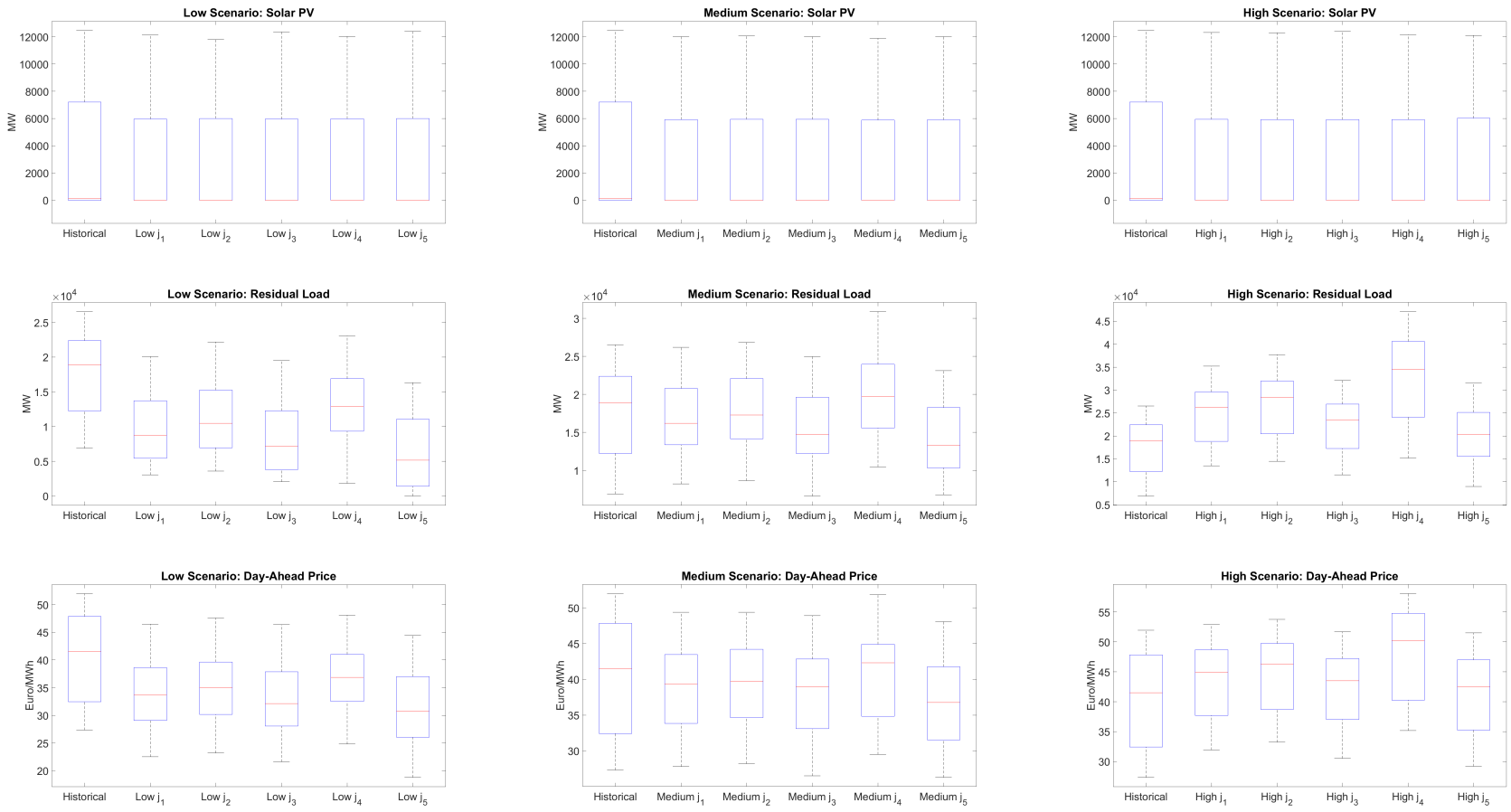


Figure 22: Distribution of the historical and simulated day-ahead series: Transition season working day

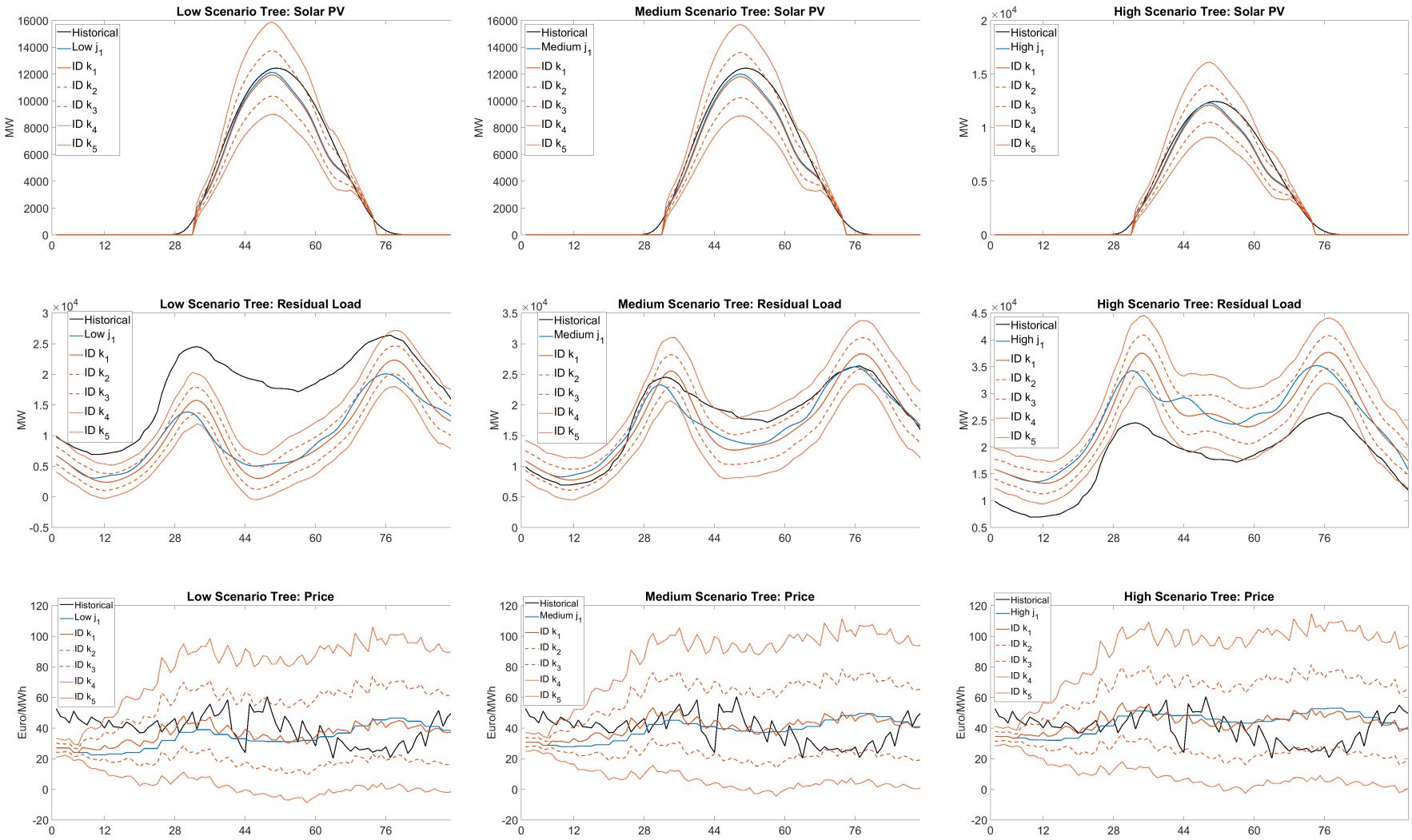


Figure 23: Scenario trees for the representative day-ahead node $\boldsymbol{j_1}$ and its intraday realizations $\boldsymbol{k}$: Transition season working day

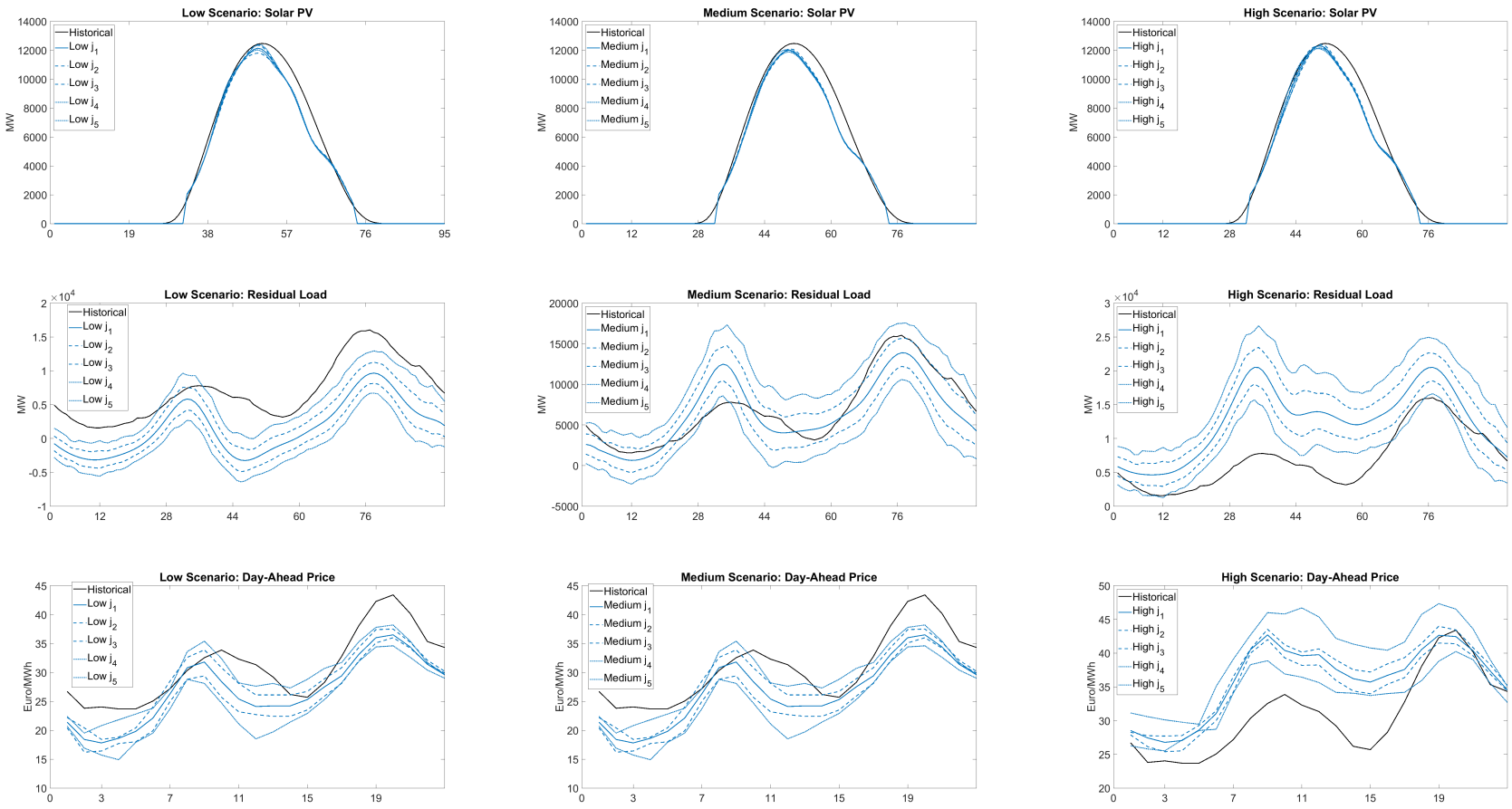


Figure 24: Historical and simulated day-ahead series: Transition season weekend day

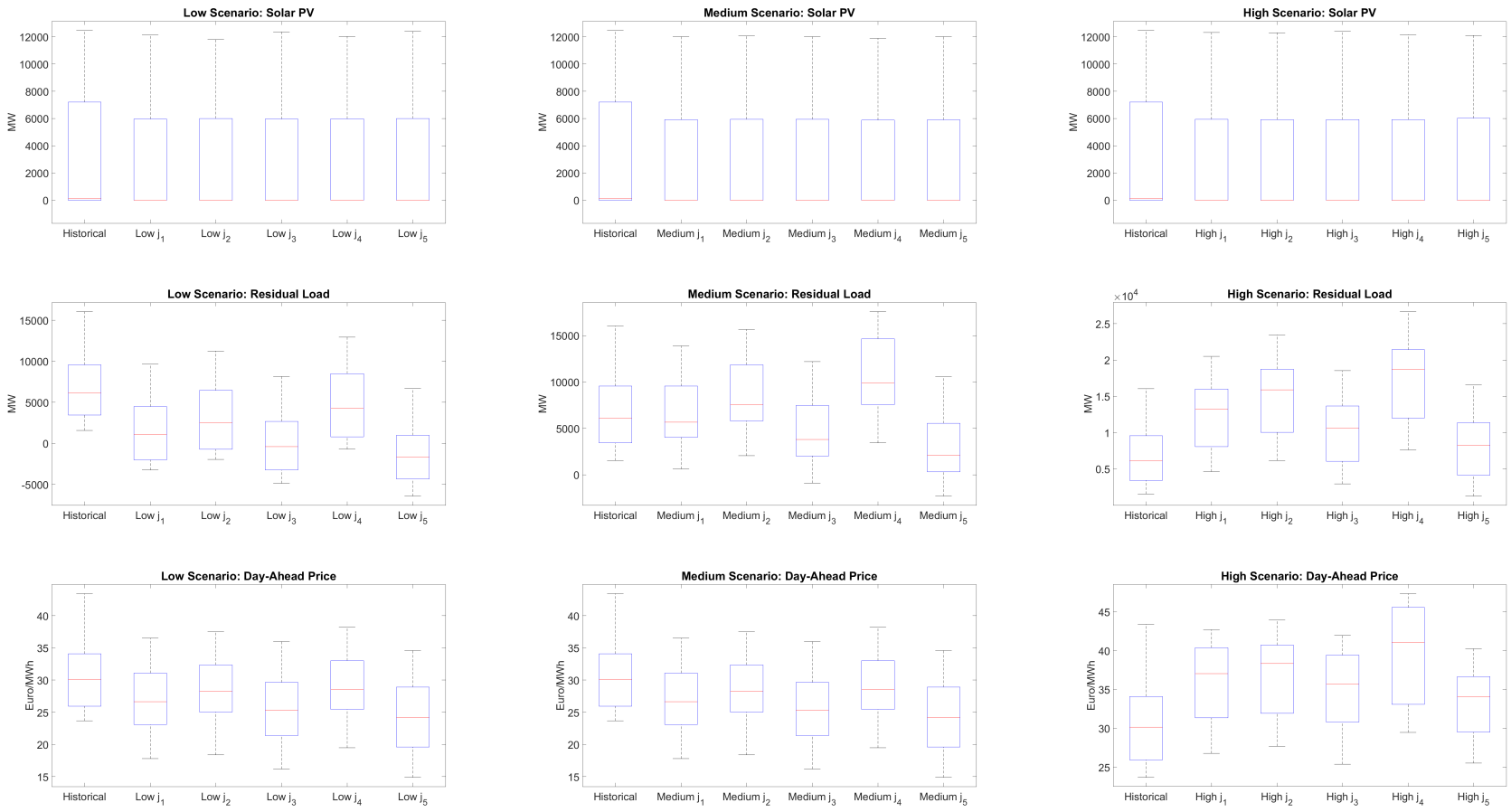


Figure 25: Distribution of the historical and simulated day-ahead series: Transition season weekend day

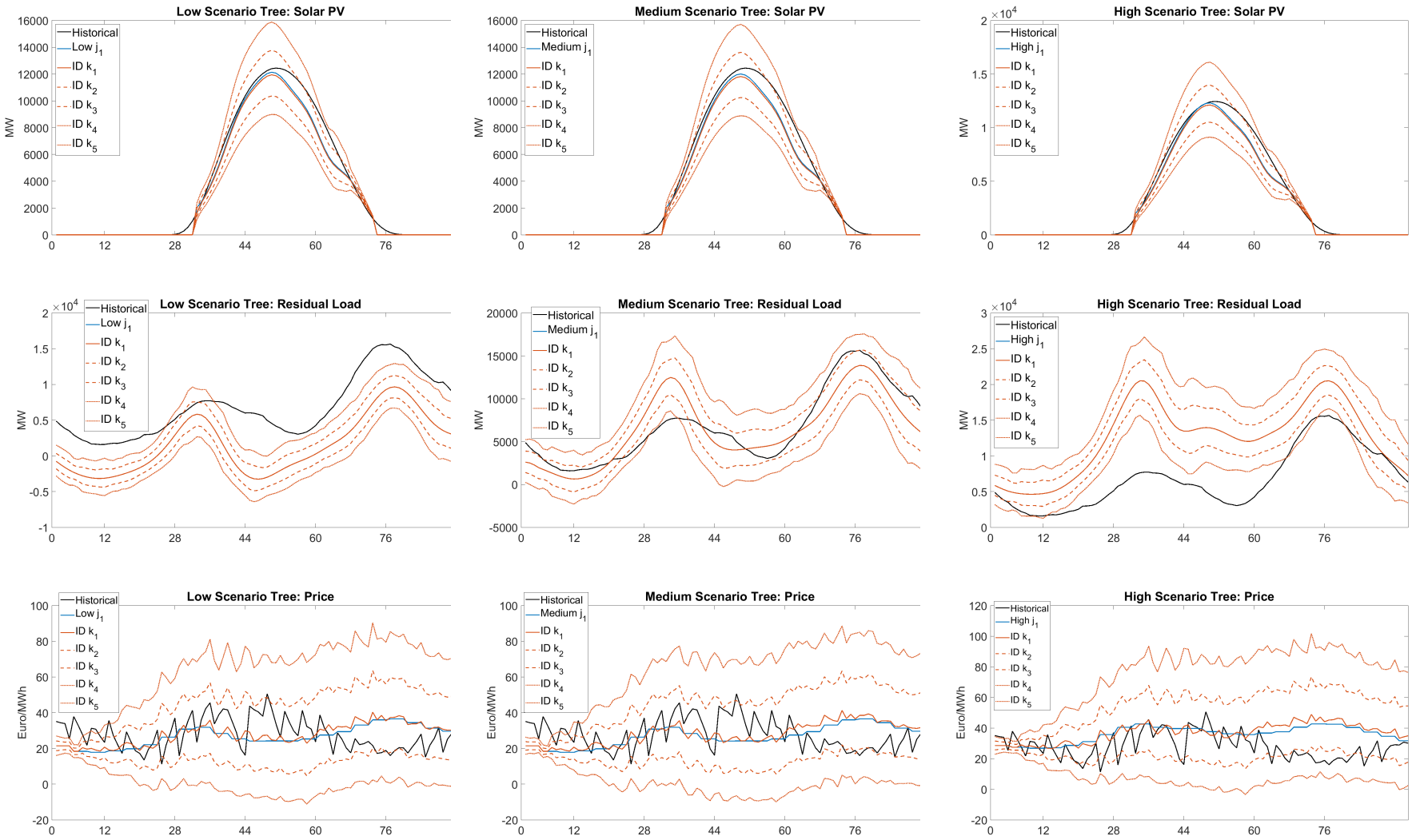


Figure 26: Scenario trees for the representative day-ahead node $j_1$ and its intraday realizations $k$: Transition season weekend day

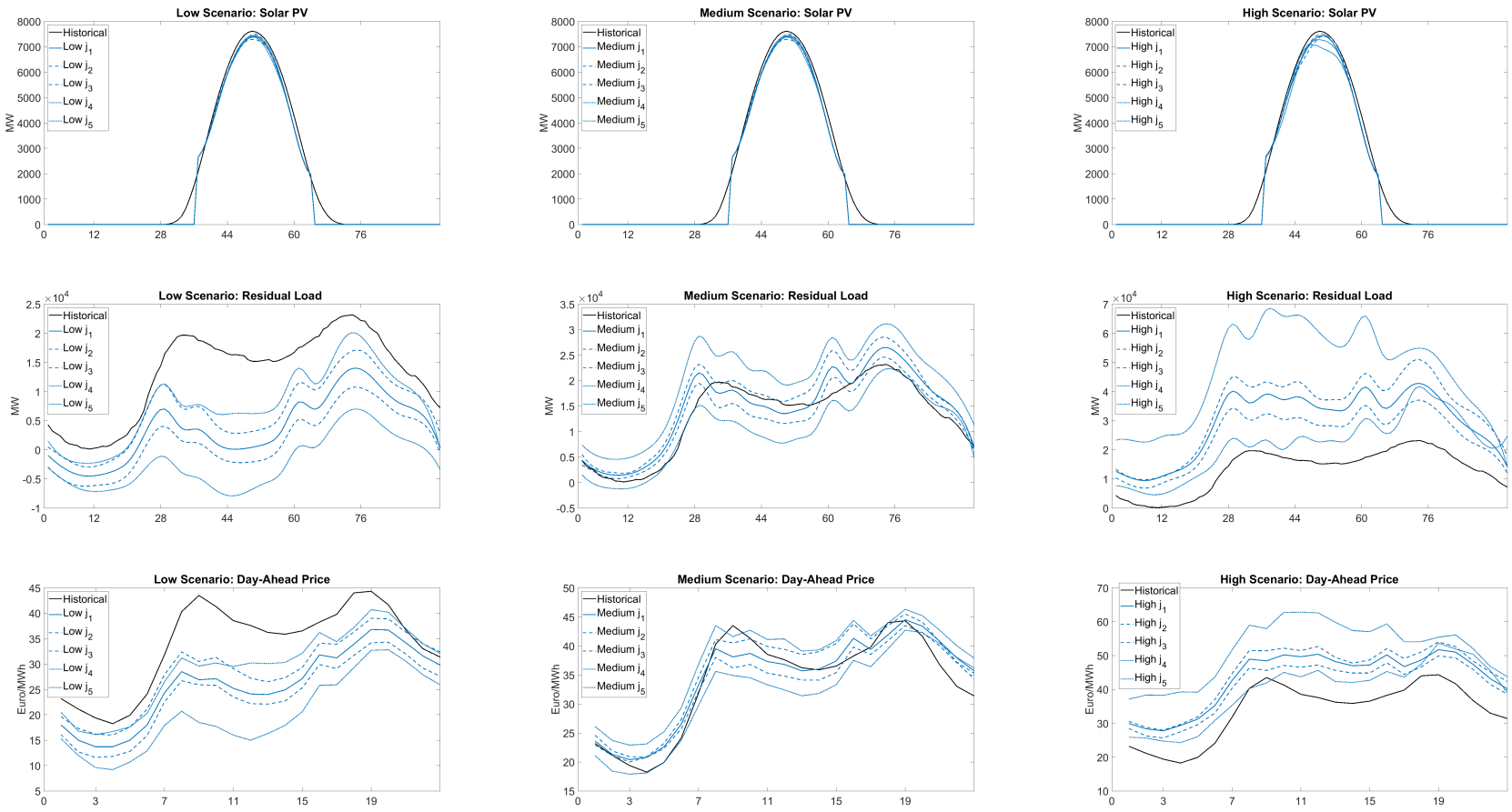


Figure 27: Historical and simulated day-ahead series: Winter working day

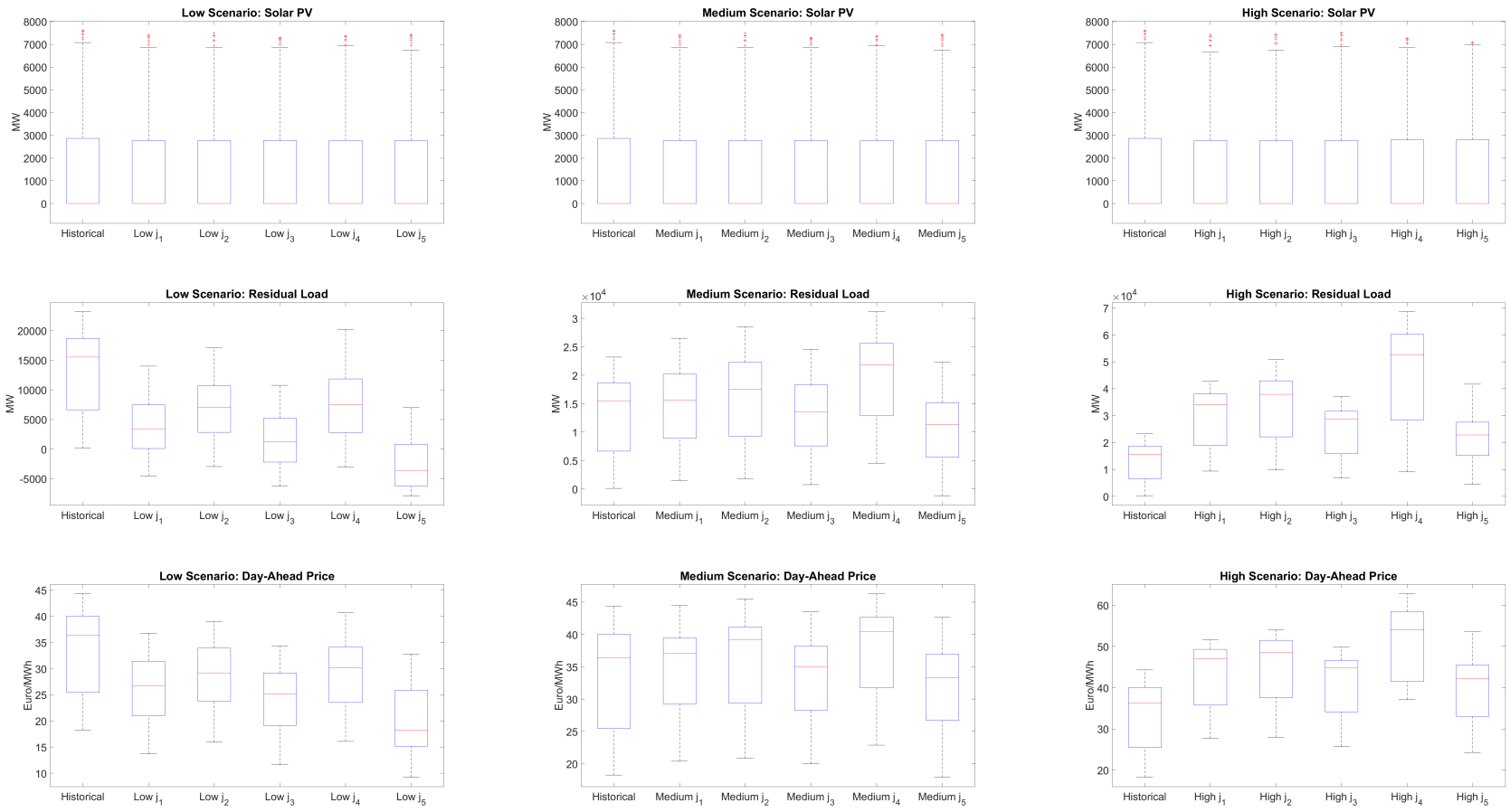


Figure 28: Distribution of the historical and simulated day-ahead series: Winter working day

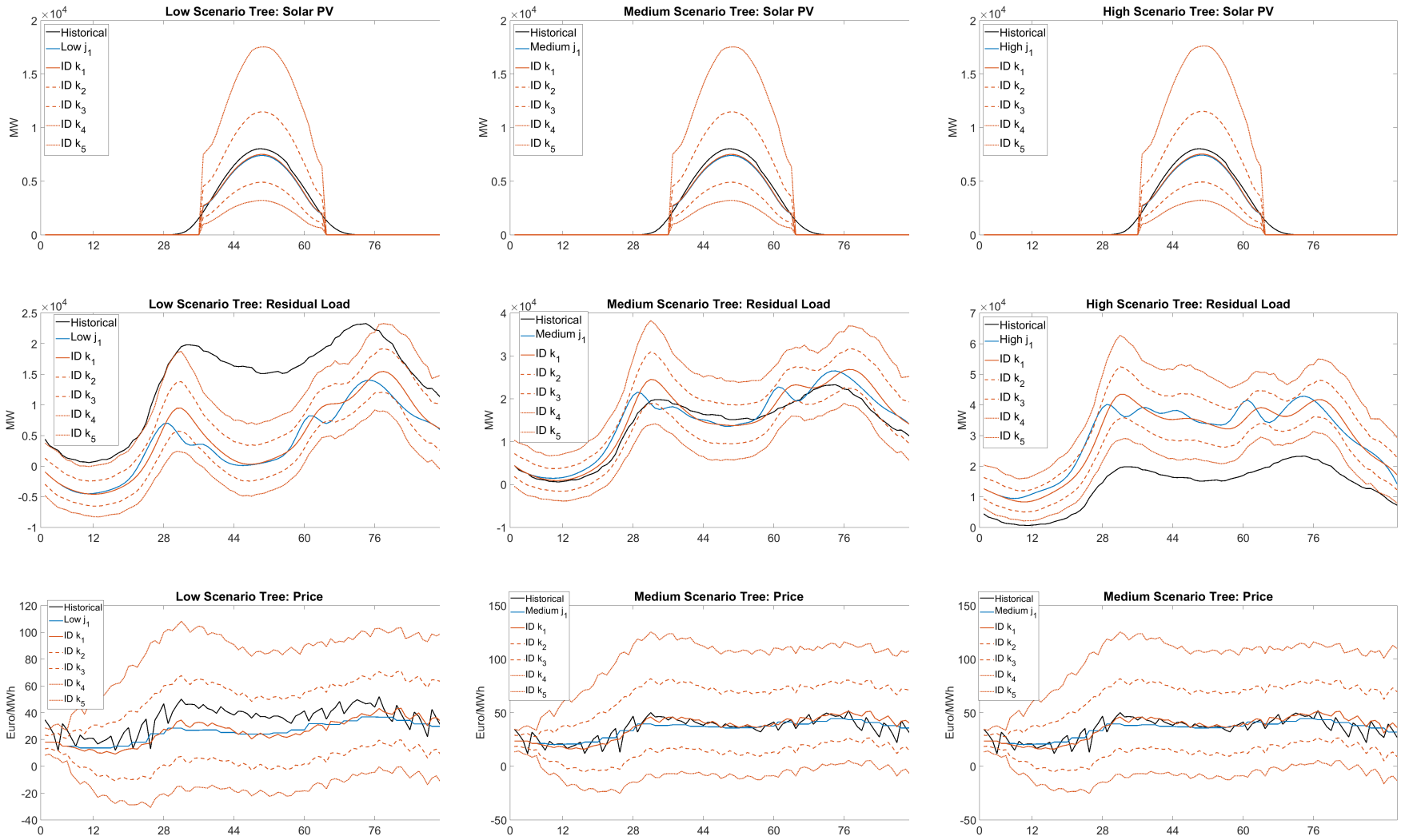


Figure 29: Scenario trees for the representative day-ahead node $\boldsymbol{j_1}$ and its intraday realizations $\boldsymbol{k}$: Winter working day

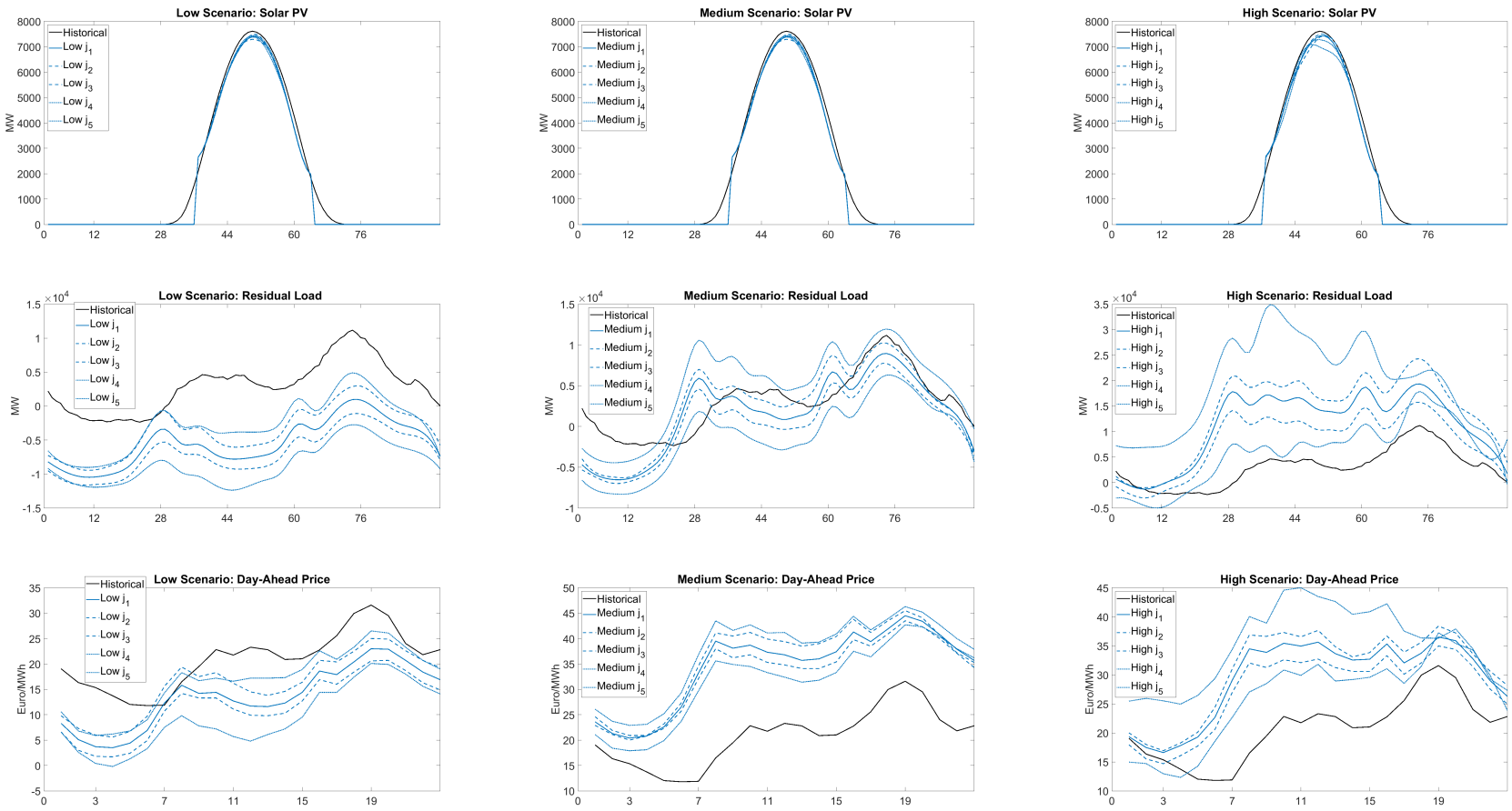


Figure 30: Historical and simulated day-ahead series: Winter weekend day

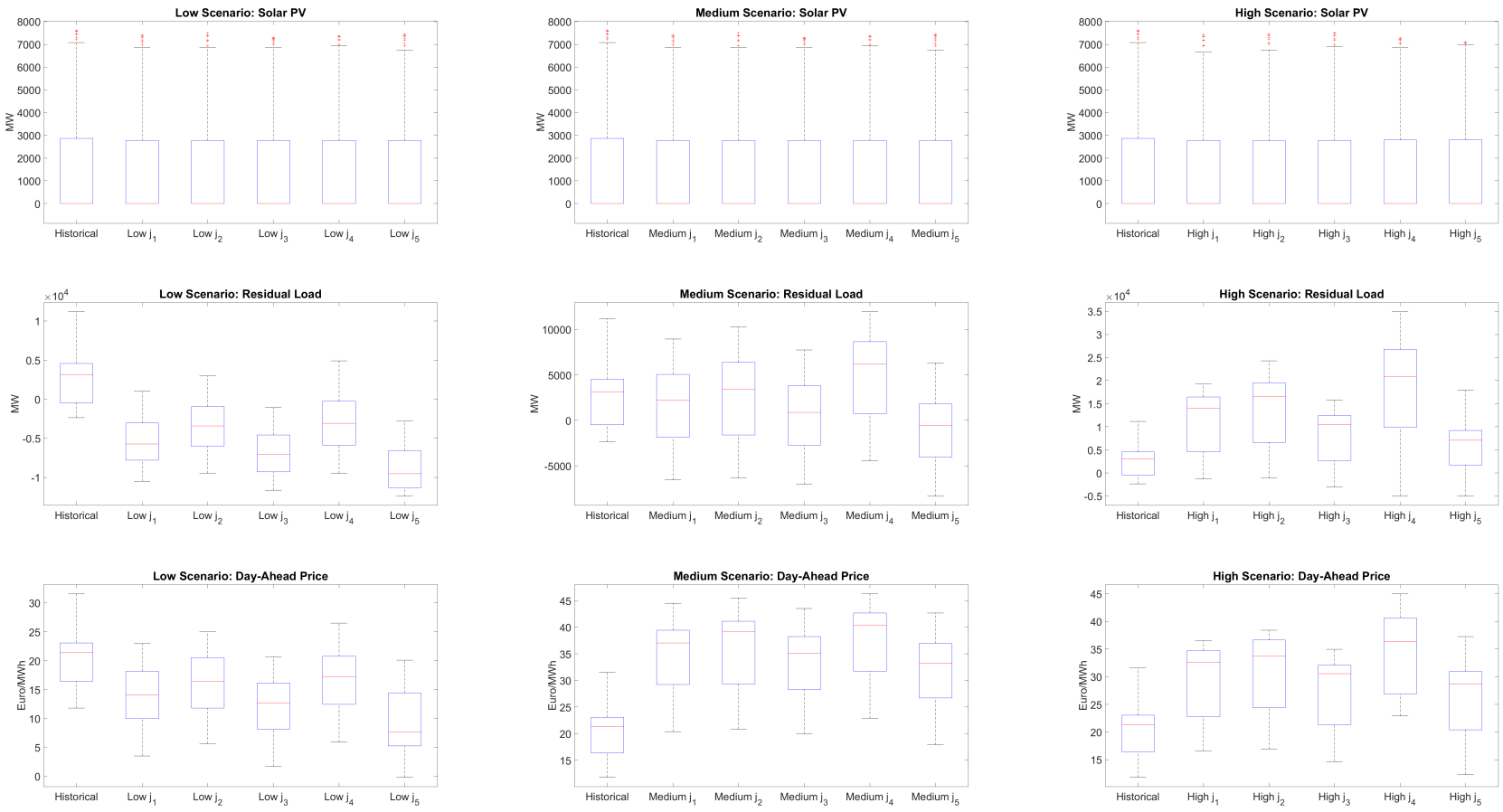


Figure 31: Distribution of the historical and simulated day-ahead series: Winter weekend day

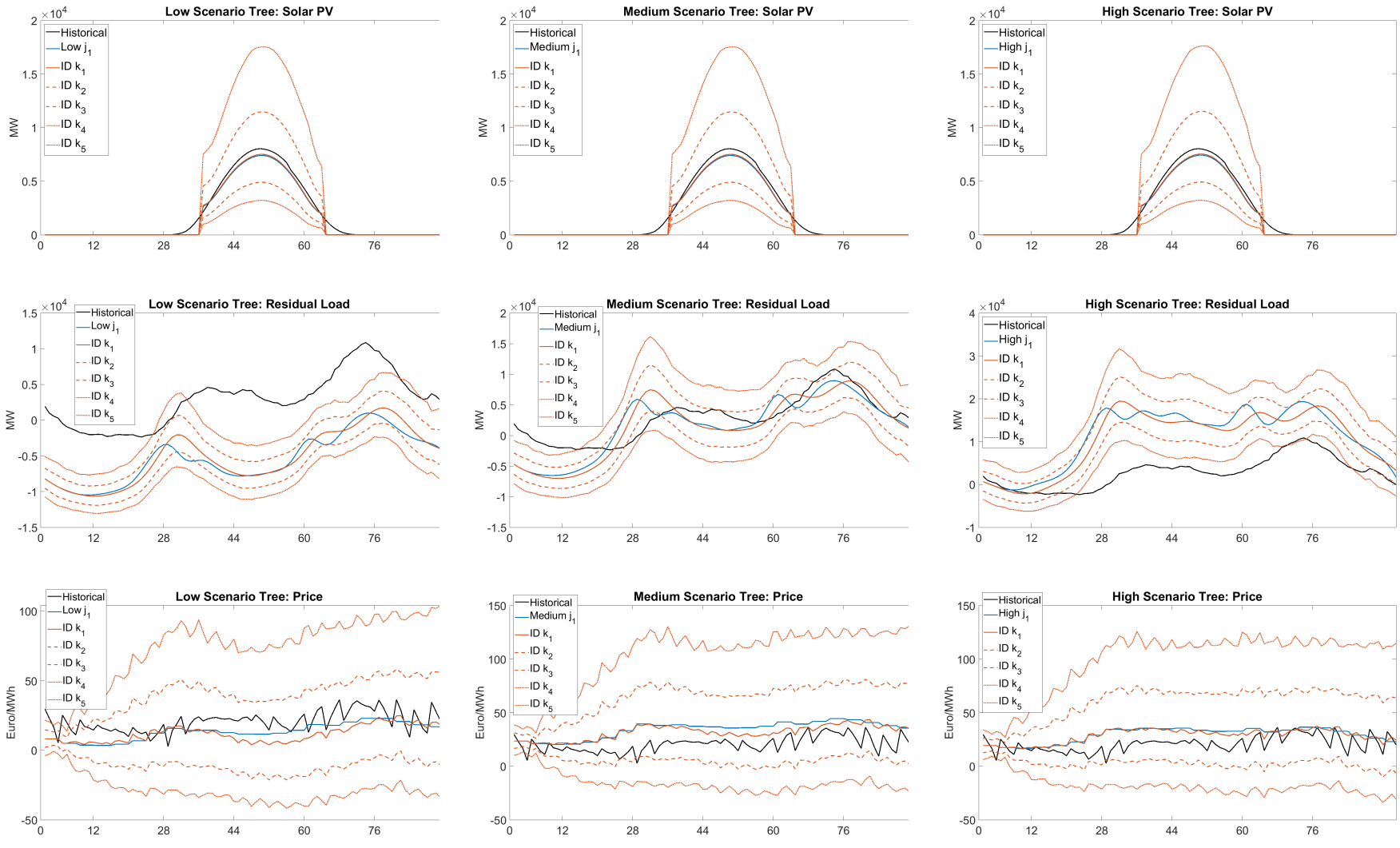


Figure 32: Scenario trees for the representative day-ahead node $j_1$ and its intraday realizations $k$: Winter weekend day

## A.4 Retailer's trading strategies with increasing solar PV self-generation

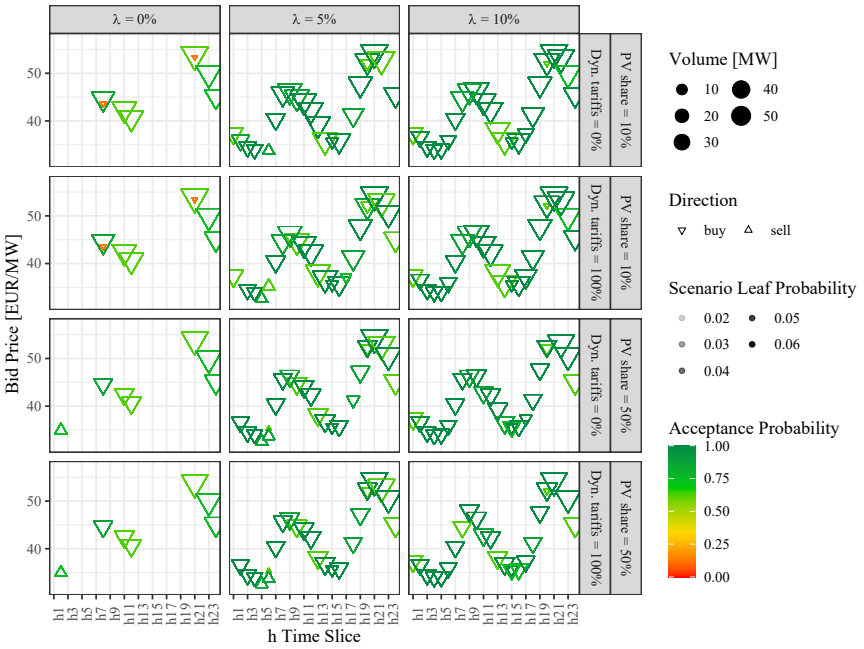


Figure 33: Retailer's day-ahead trading strategy in the summer working day: Medium scenario

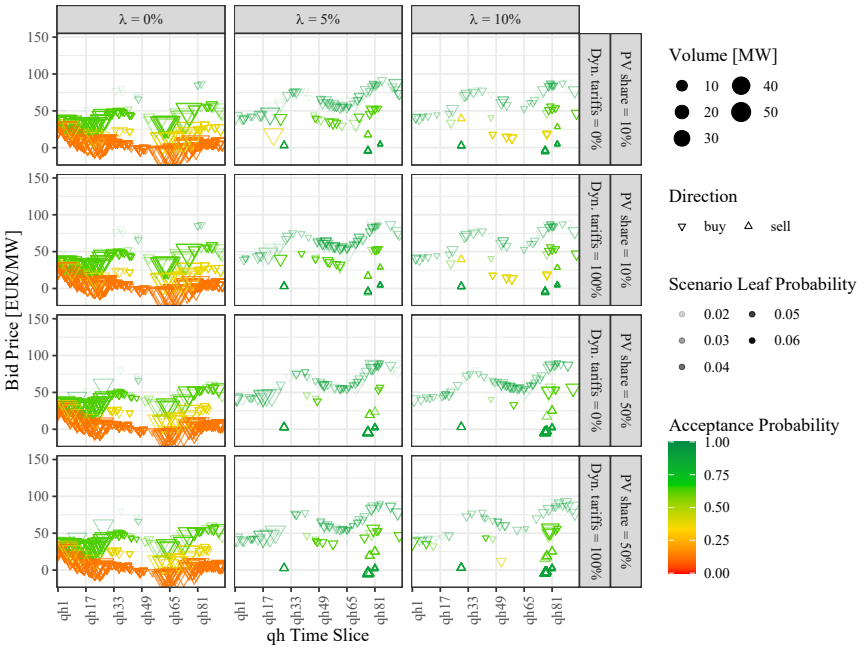


Figure 34: Retailer's intraday trading strategy in the summer working day: Medium scenario

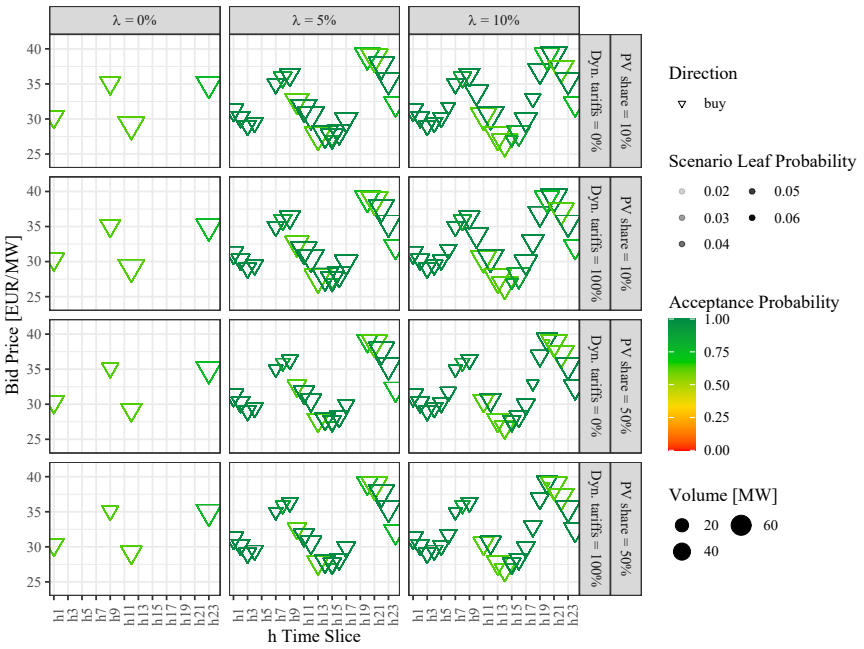


Figure 35: Retailer's day-ahead trading strategy in the summer weekend day: Medium scenario

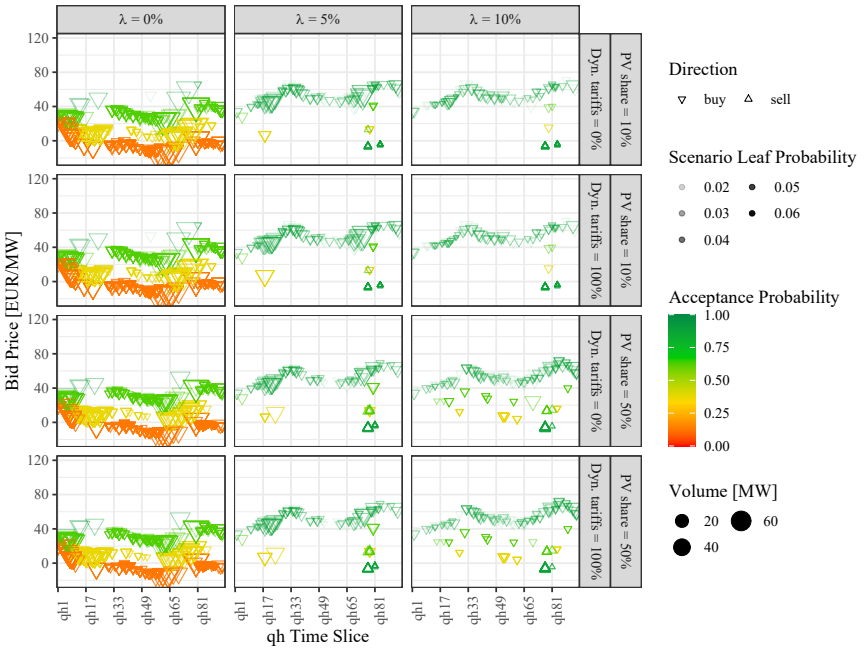


Figure 36: Retailer's intraday trading strategy in the summer weekend day: Medium scenario

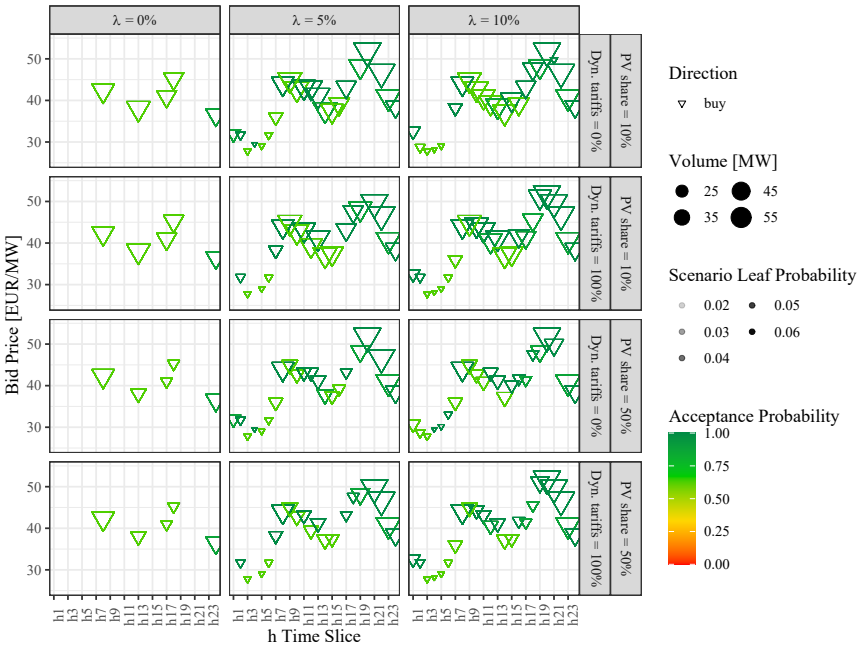


Figure 37: Retailer's day-ahead trading strategy in the transition season working day: Medium scenario

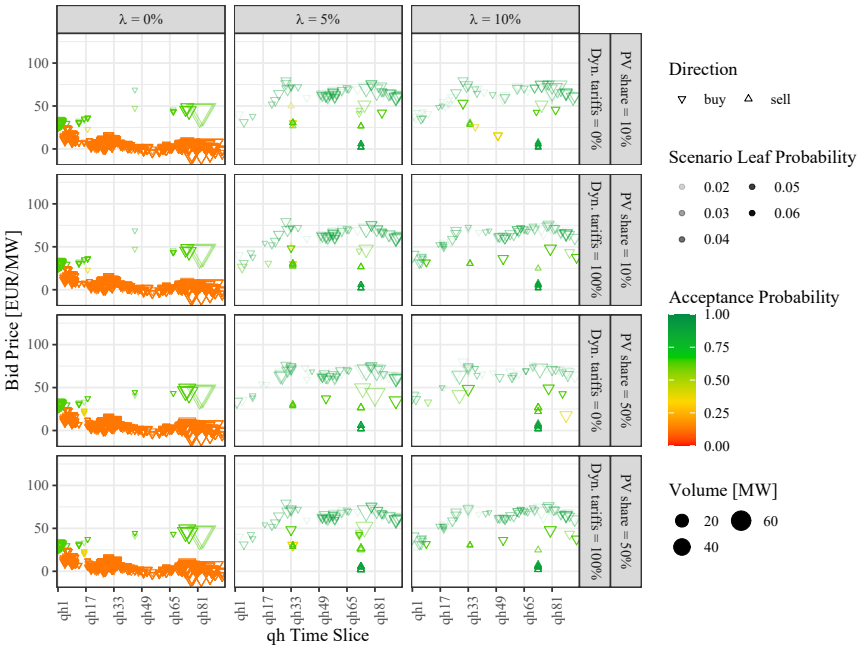


Figure 38: Retailer's intraday trading strategy in the transition season working day: Medium scenario

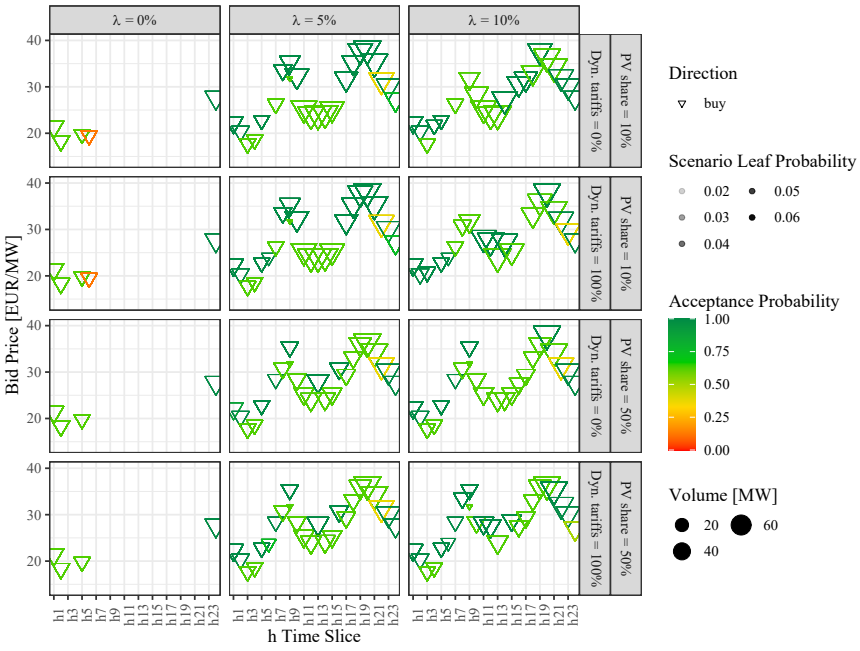


Figure 39: Retailer's day-ahead trading strategy in the transition season weekend day: Medium scenario

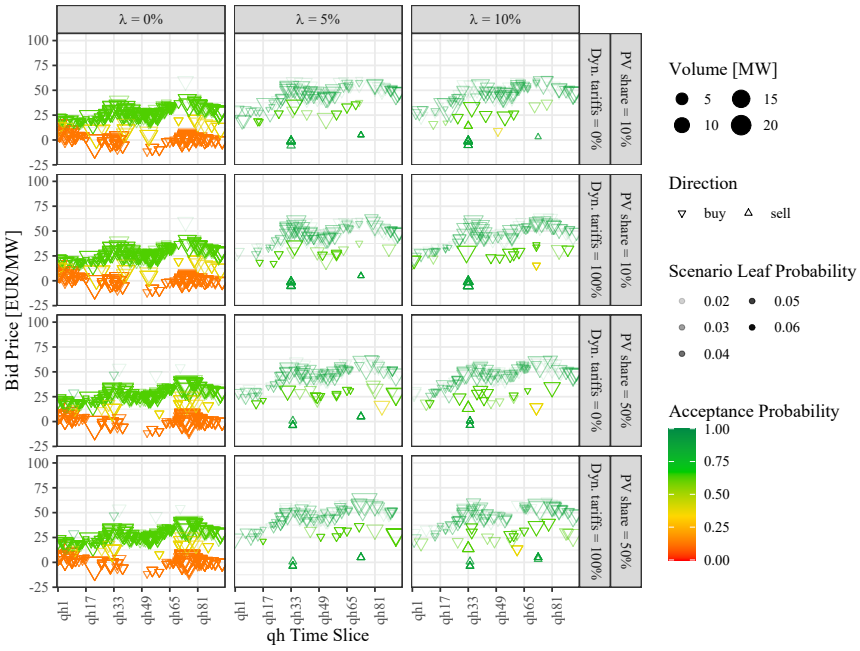


Figure 40: Retailer's intraday trading strategy in the transition season weekend day: Medium scenario

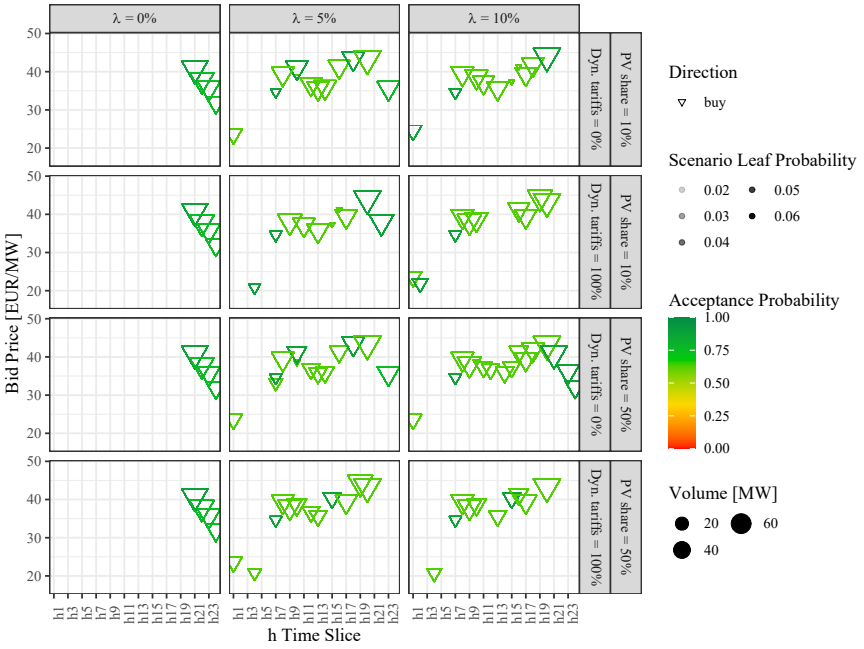


Figure 41: Retailer's day-ahead trading strategy in the winter season working day: Medium scenario

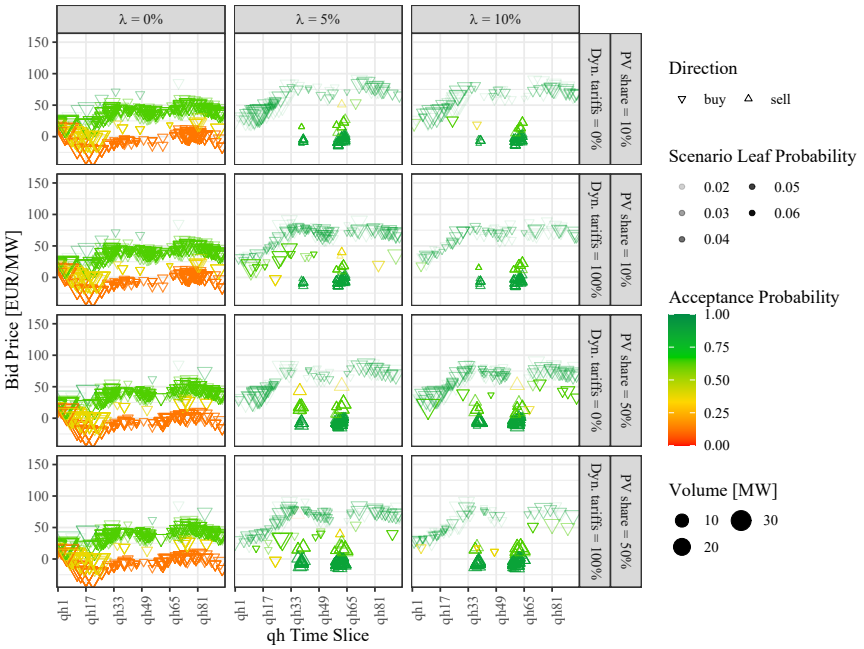


Figure 42: Retailer's intraday trading strategy in the winter season working day: Medium scenario

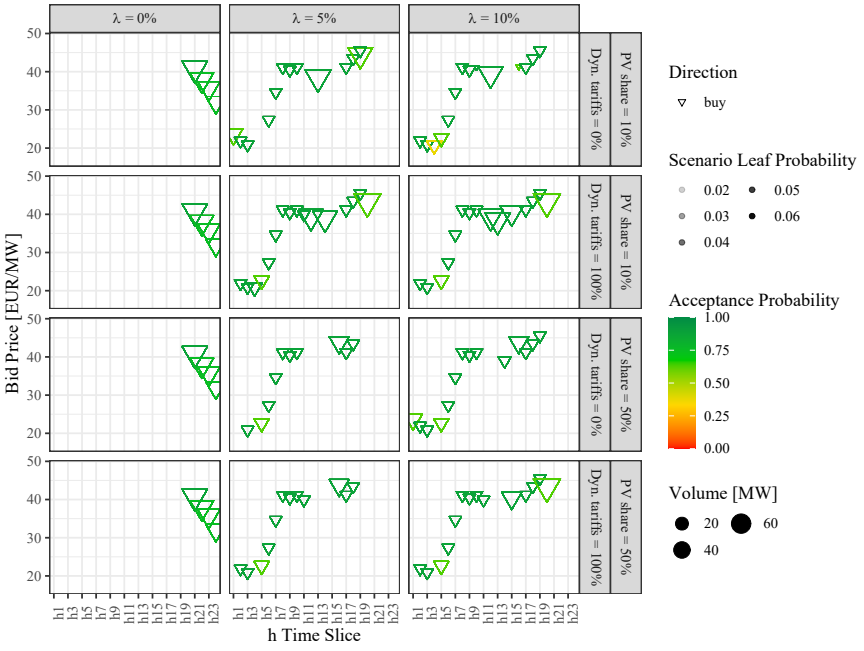


Figure 43: Retailer's day-ahead trading strategy in the winter season weekend day: Medium scenario

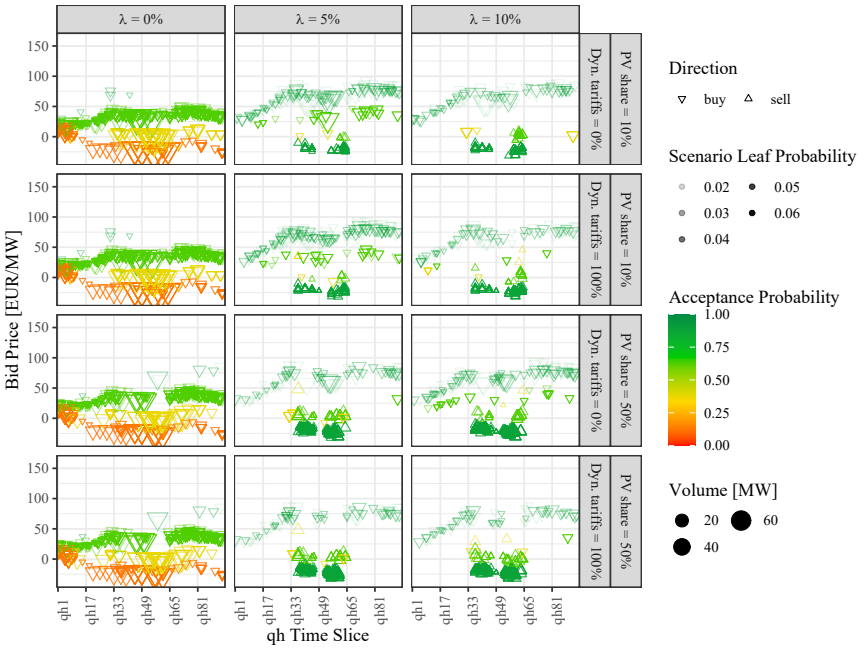


Figure 44: Retailer's intraday trading strategy in the Winter season working day: Medium scenario

## A.5 Retailer's portfolio risk management with increasing solar PV self-generation

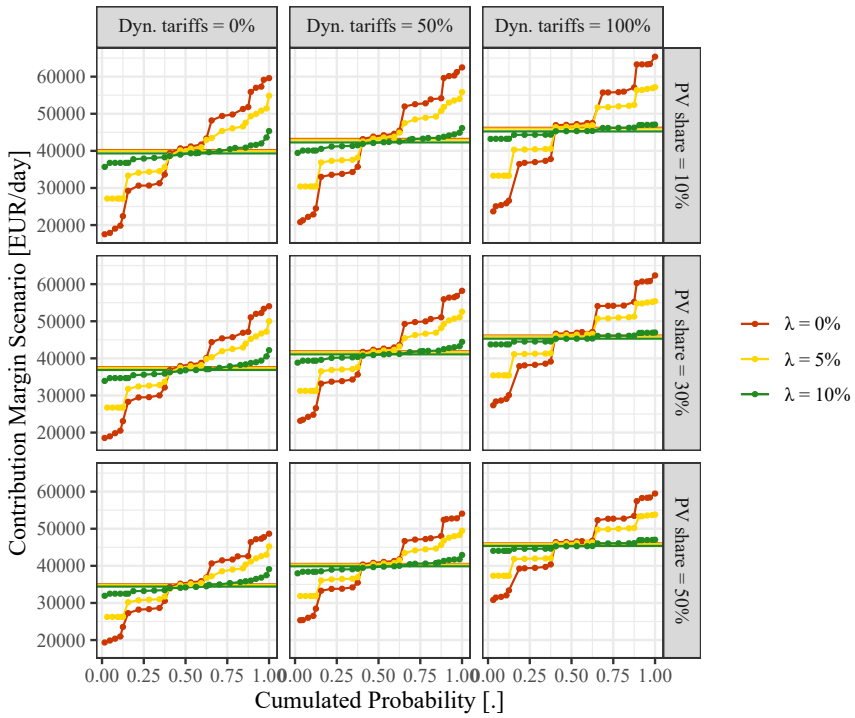


Figure 45: Empirical cumulative distribution functions of contribution margins for the Summer working day: Low scenario

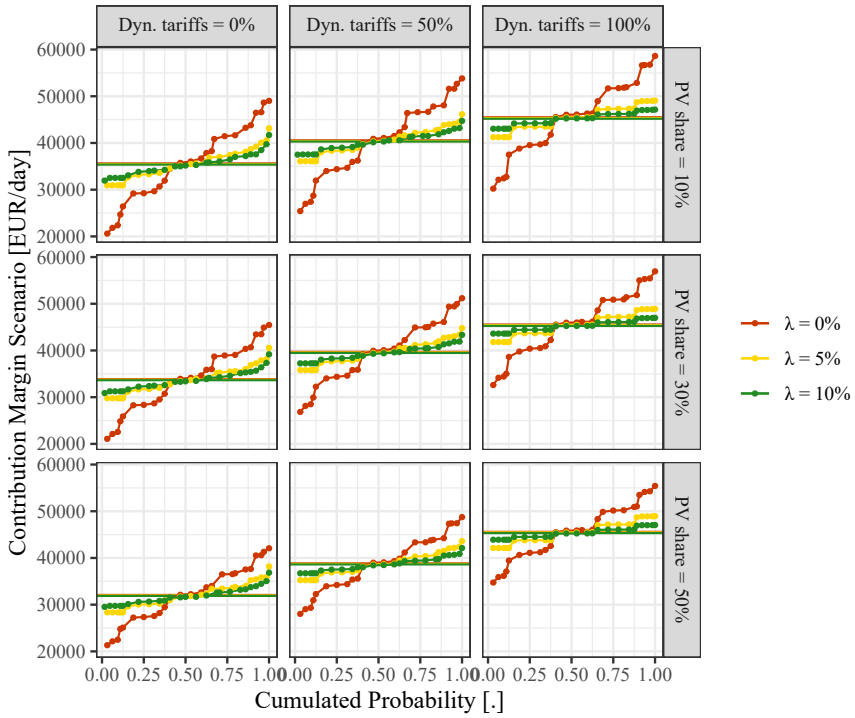


Figure 46: Empirical cumulative distribution functions of contribution margins for the Summer working day: High scenario

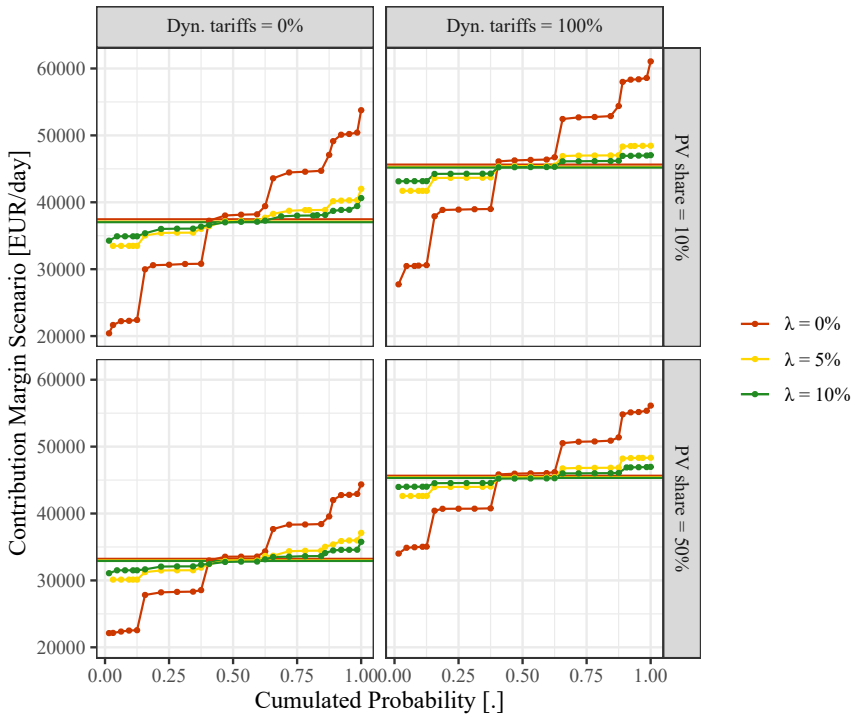


Figure 47: Empirical cumulative distribution functions of contribution margins for the Summer working day: Medium scenario

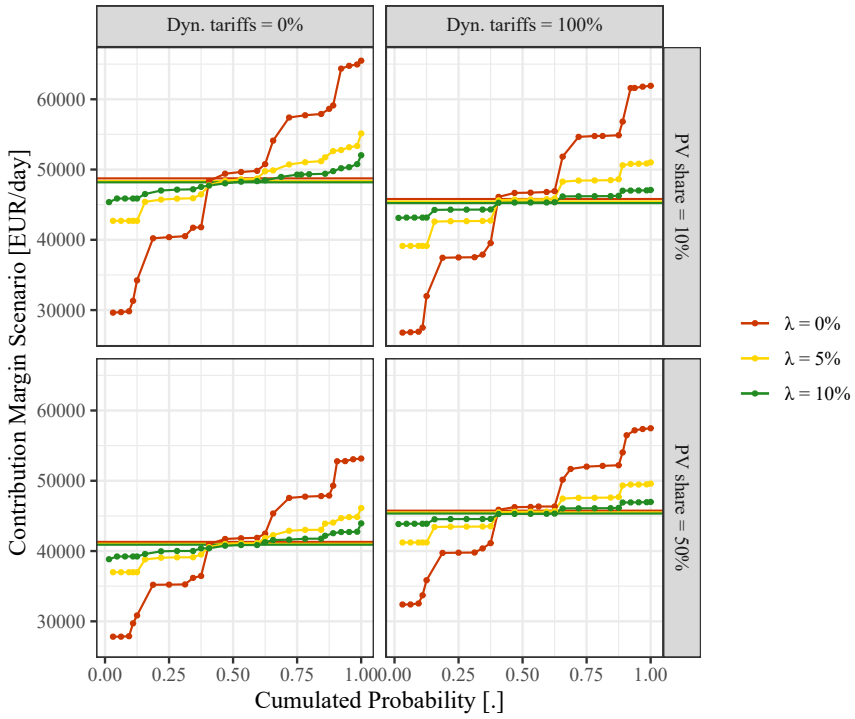


Figure 48: Empirical cumulative distribution functions of contribution margins for the summer weekend day: Medium scenario

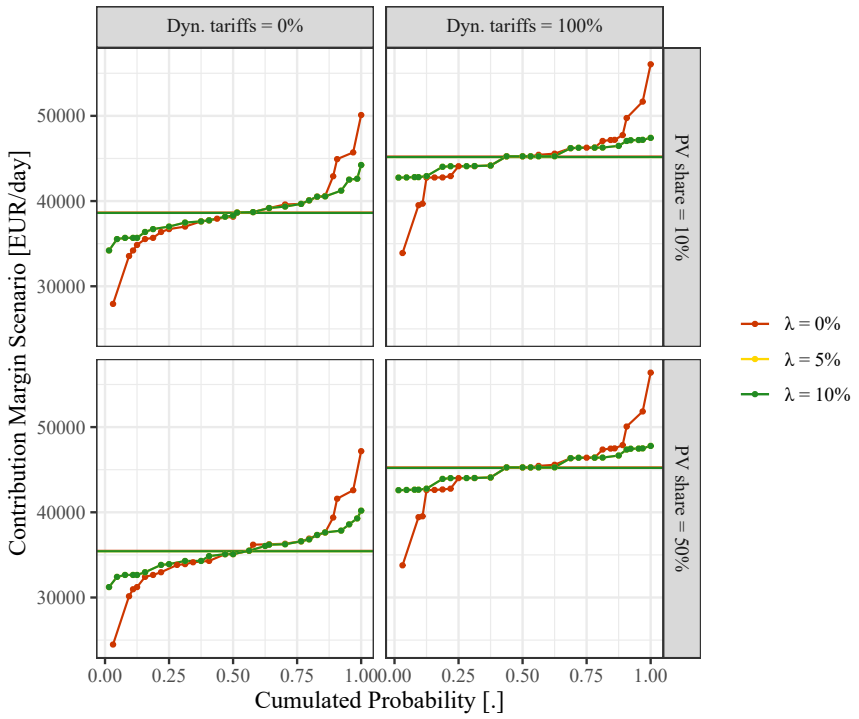


Figure 49: Empirical cumulative distribution functions of contribution margins for the transition season working day: Medium scenario

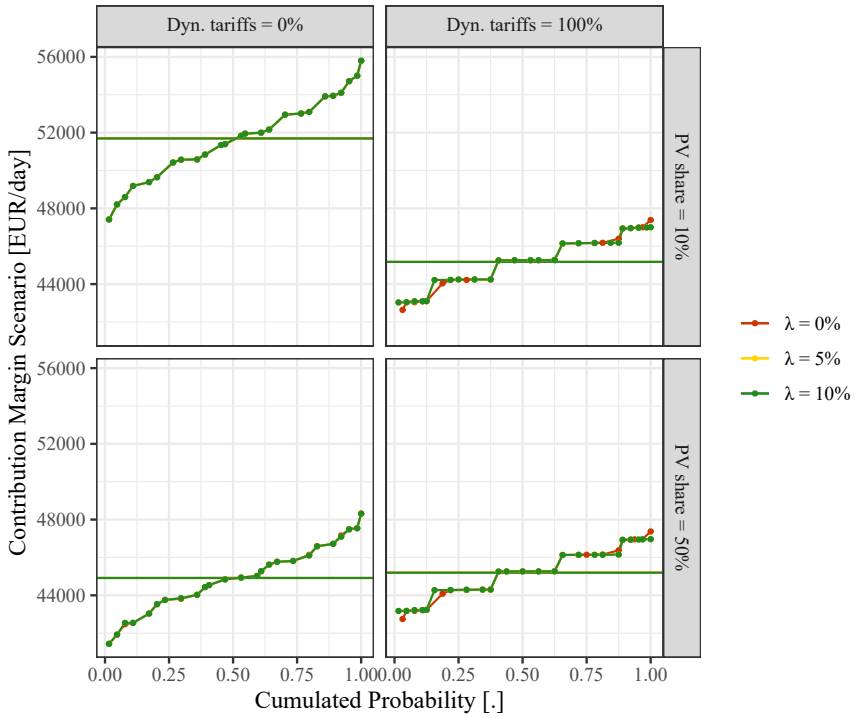


Figure 50: Empirical cumulative distribution functions of contribution margins for the transition season weekend day: Medium scenario

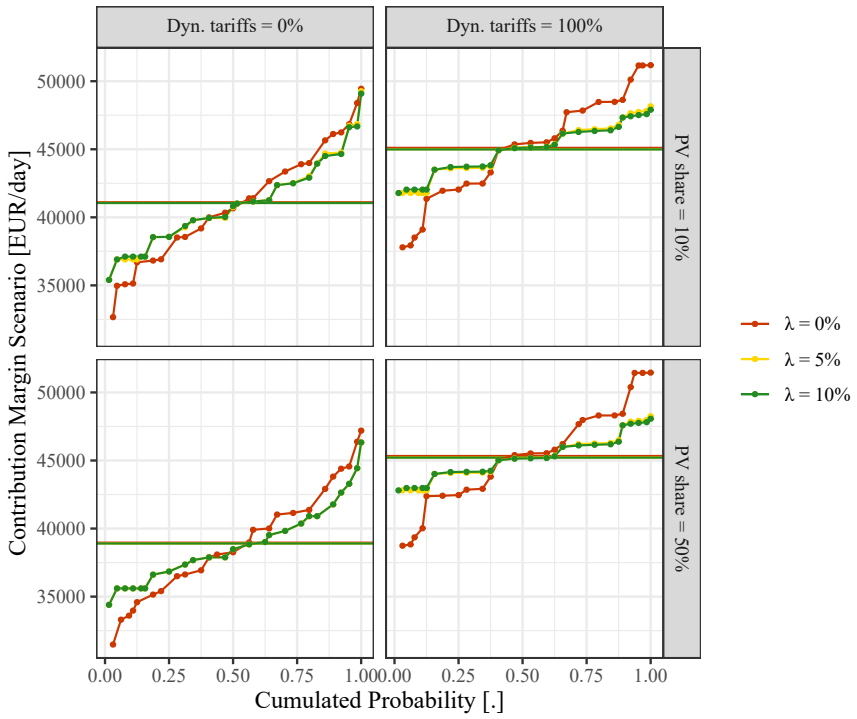


Figure 51: Empirical cumulative distribution functions of contribution margins for the winter working day: Medium scenario

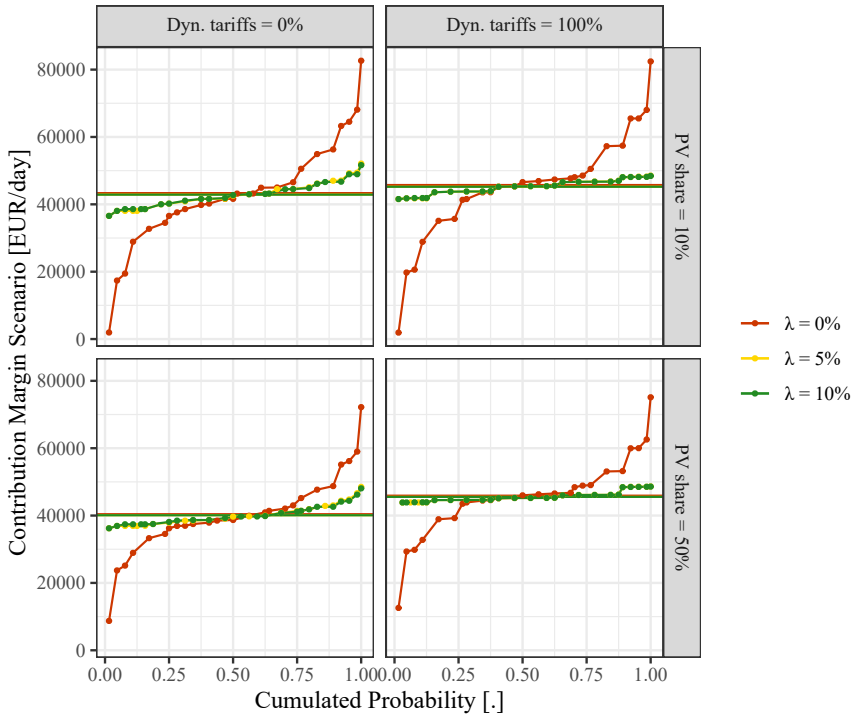


Figure 52: Empirical cumulative distribution functions of contribution margins for the winter weekend day: Medium scenario

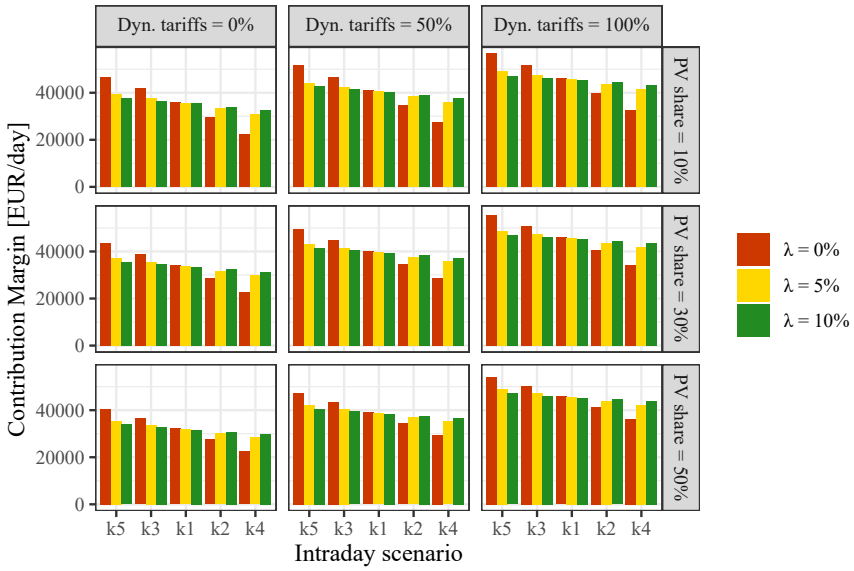


Figure 53: Retailer's contribution margin variability in the intraday market for a summer working day: Low scenario

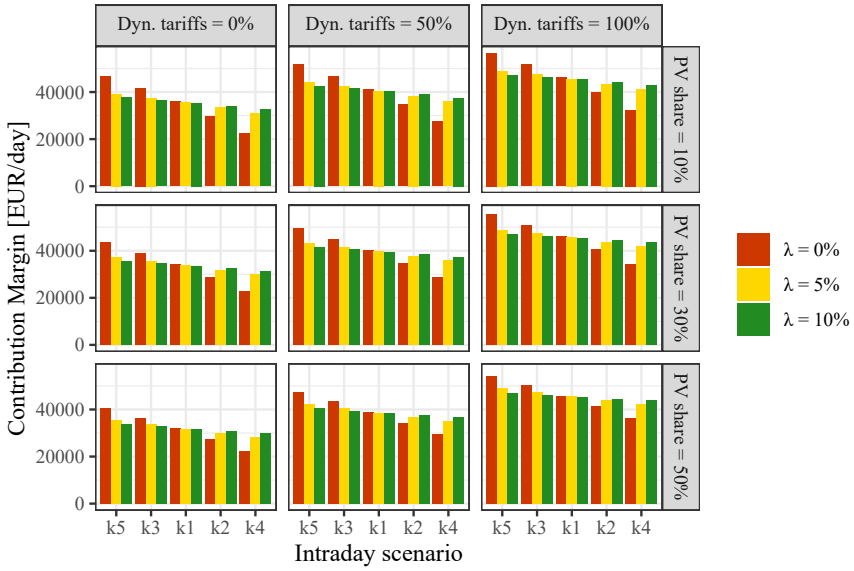


Figure 54: Retailer's contribution margin variability in the intraday market for a summer working day: High scenario

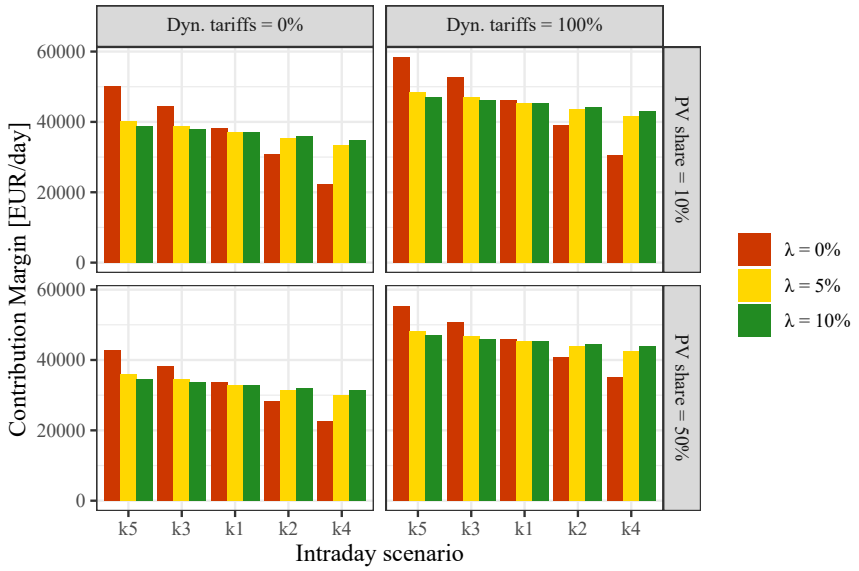


Figure 55: Retailer's contribution margin variability in the intraday market for a summer working day: Medium scenario

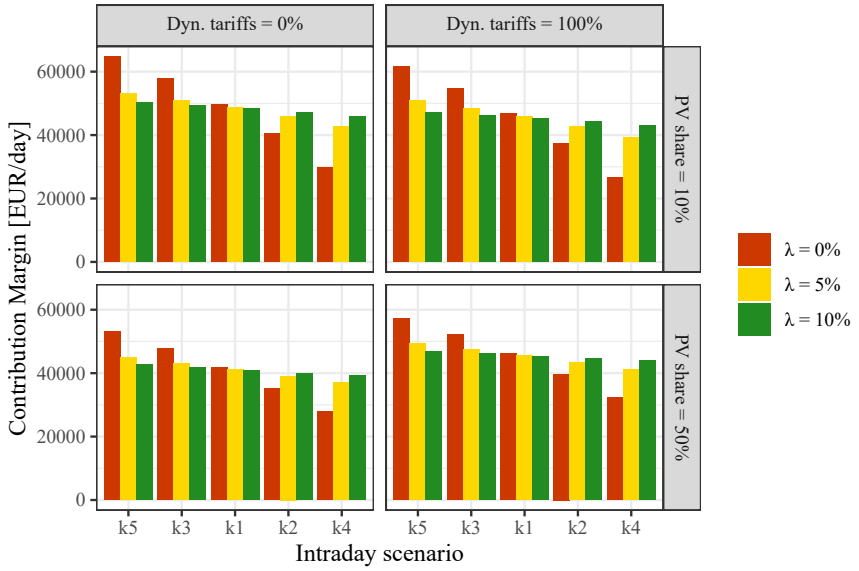


Figure 56: Retailer's contribution margin variability in the intraday market for a summer weekend day: Medium scenario

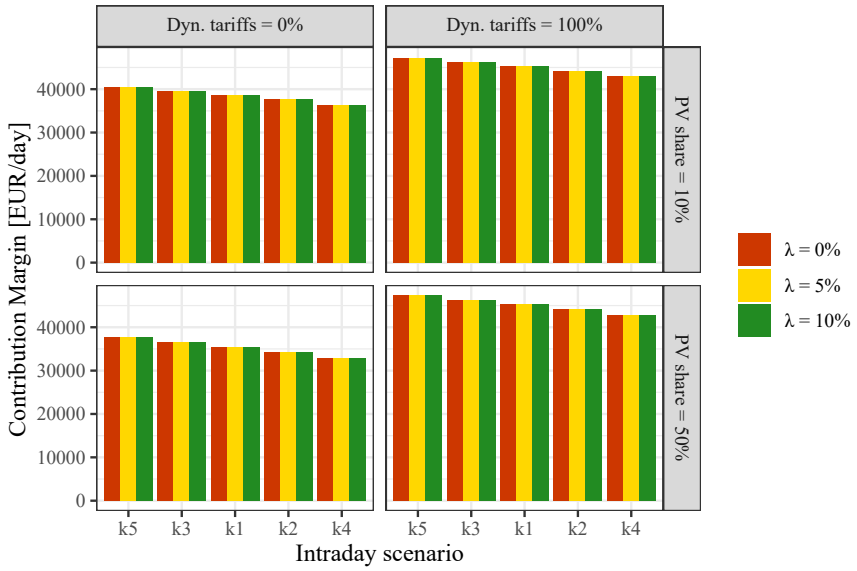


Figure 57: Retailer's contribution margin variability in the intraday market for a transition season working day: Medium scenario

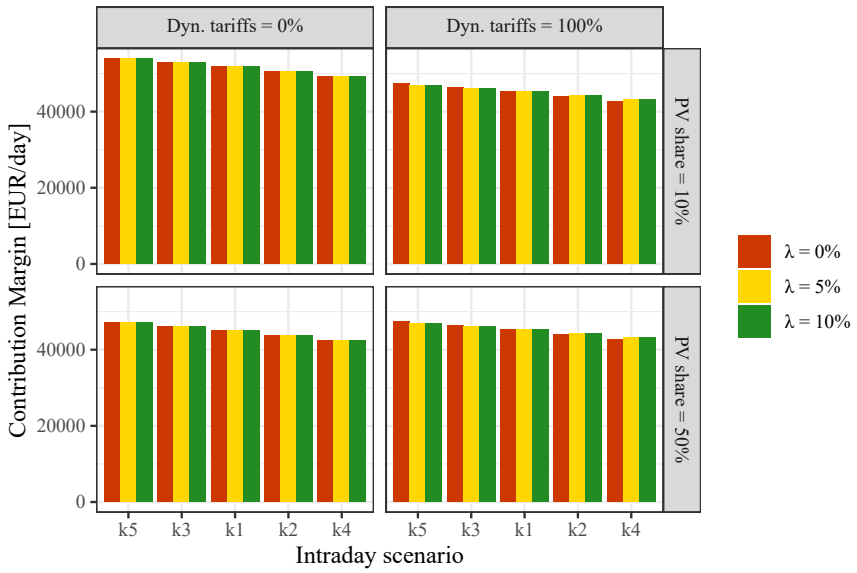


Figure 58: Retailer's contribution margin variability in the intraday market for a transition season weekend day: Medium scenario

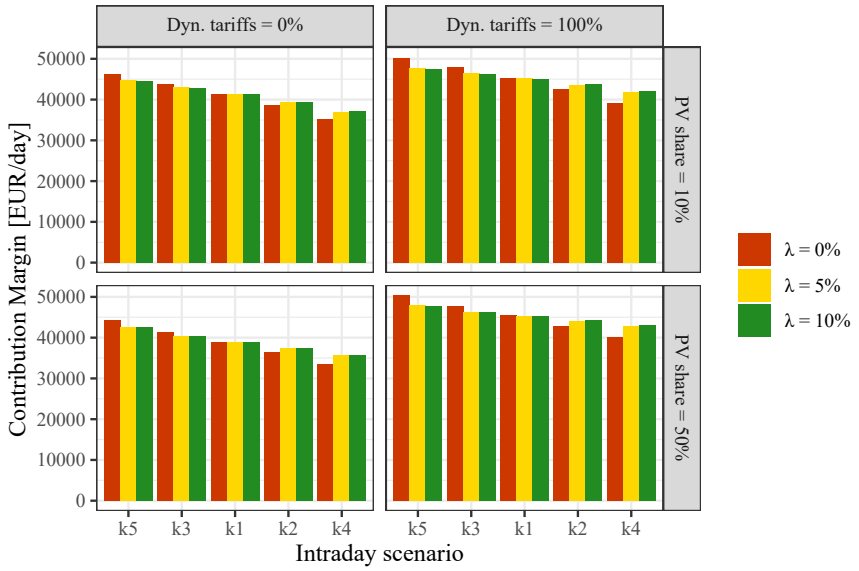


Figure 59: Retailer's contribution margin variability in the intraday market for a winter working day: Medium scenario

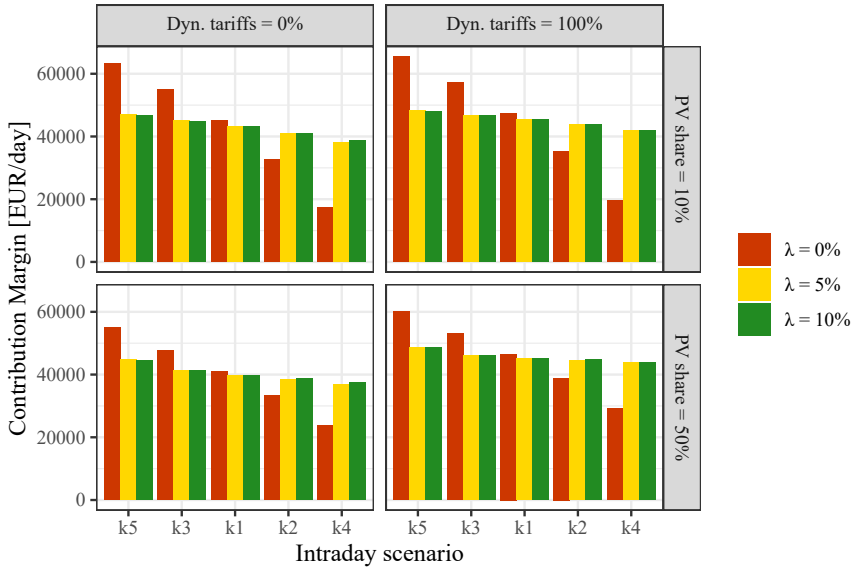


Figure 60: Retailer's contribution margin variability in the intraday market for a winter weekend day: Medium scenario

# Working Paper Series in Production and Energy

recent issues

**No. 56** Anthony Britto, Joris Dehler-Holland, Wolf Fichtner: Optimal Investment in Energy Efficiency as a Problem of Growth-Rate Maximisation

**No. 55** Daniel Fett, Christoph Fraunholz, Dogan Keles: Diffusion and System Impact of Residential Battery Storage under Different Regulatory Settings

**No. 54** Joris Dehler-Holland, Marvin Okoh, Dogan Keles: The Legitimacy of Wind Power in Germany

**No. 53** Florian Diehlmann, Markus Lüttenberg, Lotte Verdonck, Marcus Wiens, Alexander Zienau, Frank Schultmann: Public-Private Collaborations in Emergency Logistics: A Framework based on Logistical and Game-Theoretical Concepts

**No. 52** Florian Diehlmann, Patrick S. Hiemsch, Marcus Wiens, Markus Lüttenberg, and Frank Schultmann: A Novel Approach to Include Social Costs in Humanitarian Objective Functions

**No. 51** Florian Diehlmann, Miriam Klein, Marcus Wiens, Markus Lüttenberg, and Frank Schultmann: On the Value of Accurate Demand Information in Public-Private Emergency Collaborations

**No. 50** Maximilian Schücking, Patrick Jochem: Two-Stage Stochastic Program Optimizing the Total Cost of Ownership of Electric Vehicles in Commercial Fleets

**No. 49** Max Kleinebrahm, Jacopo Torriti, Russell McKenna, Armin Ardone, Wolf Fichtner: Using neural networks to model long-term dependencies in occupancy behavior

**No. 48** Nico Lehmann, Jonathan Müller, Armin Ardone, Katharina Karner, Wolf Fichtner: Regionalität aus Sicht von Energieversorgungsunternehmen - Eine qualitative Inhaltsanalyse zu Regionalstrom in Deutschland

**No. 47** Marcus Wiens, Farnaz Mahdavian, Stephen Platt, Frank Schultmann: Optimal Evacuation-Decisions Facing the Trade-Off between Early-Warning Precision, Evacuation-Cost and Trust – the Warning Compliance Model (WCM)

**No. 46** Phuong Khuong, Fabian Scheller, Russell McKenna, Dogan Keles, Wolf Fichtner: Willingness to pay for residential PV: reconciling gaps between acceptance and adoption

**No. 45** Christoph Fraunholz, Emil Kraft, Dogan Keles, Wolf Fichtner: The Merge of Two Worlds: Integrating Artificial Neural Networks into Agent-Based Electricity Market Simulation

**Impressum**

Karlsruher Institut für Technologie

Institut für Industriebetriebslehre und Industrielle Produktion (IIP)
Deutsch-Französisches Institut für Umweltforschung (DFIU)

Hertzstr. 16
D-76187 Karlsruhe

KIT – Universität des Landes Baden-Württemberg und
nationales Forschungszentrum in der Helmholtz-Gemeinschaft

Working Paper Series in Production and Energy
**No. 57**, June 2021

ISSN 2196-7296

www.iip.kit.edu